Disruption of Gut Homeostasis by Opioids in the Early Stages of HIV Infection

A Dissertation
SUBMITTED TO THE FACULTY OF
UNIVERSITY OF MINNESOTA
BY

Gregory Michael Sindberg

IN PARTIAL FULFILLMENT OF THE REQUIREMENTS
FOR THE DEGREE OF
DOCTOR OF PHILOSOPHY

Advisors: Dr. Sabita Roy and Dr. Thomas Molitor

December 2014

troubleshooting techniques as well as guiding each other through milestones in graduate school. Fuyuan Wang worked with me on initial experiments to establish the microbiome project. Current lab members Dr. Jing Ma, Dr. Raini Dutta, Dr. Shamudeen Moidunny, Anuj Saluja, and past members Dr. Vidhu Anand, Dr. Lisa Koodie, Dr. Jana Ninkovic, Rick Charboneau, Yuxiu, Liu, and Haidong Yu all provided great support to me.

My co-advisor Dr. Thomas Molitor played a role similar to Dr. Roy in guiding me through adversity. I appreciated his kind words, support, and especially for introducing me to the PharmacoNeuroImmunology (PNI) training grant. I am grateful for the financial support on the training grant, which was kindly provided by NIDA at the NIH. Yorie Smart provided essential support for the training grant, and I enjoyed working with her on the seminar committee. I appreciated feedback received from the PNI trainees, especially at our spring semester Monday meet-ups.

I would also like to acknowledge my original primary advisor, Dr. Pratima Bansal-Pakala. I was passionate about diabetes research and she accepted me into the lab without question, and offered me support and developed me as a scientist. She did everything possible to ensure that I had a smooth transition to a new lab, and relentlessly advocated for me even as the sky was falling around us. I also have a large appreciation for Dr. Timothy O'Brien, who served as my co-advisor during this time. I greatly enjoyed our collaboration and support, and

especially appreciated his continued pathology support no matter if I had questions for work or personal (cat) reasons. Anil Pahuja and Beth Lindborg worked very closely with me on the projects while in Dr. Pakala's lab and made it easy to succeed. Anil in particular has been a continued source of support and friendship.

I would like to express gratitude to my three committee members, who provided invaluable feedback and helped to guide me through this process. Dr. Michael Murtaugh was a consistent resource and advocate as the chair of my committee when I was in Dr. Pakala's lab as well as Dr. Roy's lab. Dr. David Brown has provided countless amounts of sage advice both in regards to my project as well as my development towards finding my career path. Finally, a large appreciation to Dr. Sundaram Ramakrishnan for joining the committee relatively late in the game but getting onboard quickly and providing feedback on the project.

A large thanks to Dr. David Volsky at Mount Sinai for collaborating with the Roy lab and providing the EcoHIV virus construct to use. This project relied heavily on that model, and I am appreciative as it gave much more power to the study than the transgenic animals (Tat86) alone.

The microbiome work presented would not have been possible without the support of Dr. Timothy Johnson. He provided support in how to design the experiments and analyze the data at a time when our lab previously had no

Barry and Sarah Summerbell who have made it easy and enjoyable to be a student in the program. I feel fortunate to have met and interacted with many of the students in the CMB graduate program over my tenure, many of whom worked hard to improve the community of the students as well as the quality of the program.

The Basic and Translational Research (BTR) division of the Department of Surgery provided a collaborative environment when help was needed outside from the lab. The combined resources of the PIs in the division, Dr. Ashok Saluja, Dr. Sabita Roy, Dr. Masato Yamamoto, and Dr. Subree Subramanian, provided a good working environment and shared equipment which was essential to this work. Thanks to all the scientists, postdocs, and graduate students on the floor who provided help when needed, as well as Jennie Walker and Erin Brudvik for their assistance and support over the years.

A special appreciation to Elaine O'Brien, who has been a close colleague and friend since I started working in research following my undergraduate degree. Her continued support and willingness to listen made my graduate journey much easier than it could have been. I am very grateful to Dr. Brad Segura for hiring her and bringing her next door to the Roy lab, and I am happy that we are now both moving forward to new projects together.

I was first hired following my undergraduate education by Dr. Laura Mauro, who has continued to be a valuable mentor to me. I greatly appreciate

that she took a chance on me as a scientist, and encouraged me to better myself with graduate school. I likely wouldn't' be here without her support.

A large gratitude to Bob and the group for listening and providing the opportunity to reflect. I made valuable connections and am thankful I decided to join. The support everyone provided is immeasurable, and I wish everyone the best with their future endeavors.

Finally, I would like to acknowledge the abundance of family and friends who have supported me through this process.

A special credit goes to my parents, Michael and Anne Sindberg, for their love and support throughout the years. They provided a strong foundation for my education, and I was always able to proceed with confidence knowing that I was capable. My younger sister, Allison, has also been a large part in this process as we grew up together. I look forward to sharing the wonderful milestones she will accomplish in the near future.

I have a large sense of gratitude for my wife's parents, Greg and Diane Schmidt, for their love and support. They welcomed me into the family unconditionally, and made me feel like one of their own. I feel very fortunate to have married into such a wonderful family.

And last but certainly not least, a big acknowledgement to my wife, Lesley, and daughter, Lyla. My education was a huge sacrifice that Lesley encouraged me to pursue without second thought. I know that it has not always been easy

on her, but I greatly appreciate her willingness to come along on the ride. I thought I was the luckiest man in the world to have found her…until we made Lyla. <u>Now</u> I am the luckiest man in the world. I look forward to our next five year plan. Lyla came late to the graduate school party, but was amazing motivation to persevere and finish my degree. I have gratitutde for her unconditional love with constant smiles and laughter to cheer me up. Watching her grow has been the greatest joy of my life, and I look forward to our future together.

Dedication

To my beautiful daughter, Lyla, and loving wife, Lesley:

You are the reason that this degree, and myself, are complete.

i carry your heart with me (i carry it in
my heart) i am never without it (anywhere
i go you go, my dear; and whatever is done
by only me is your doing, my darling)

i fear
no fate (for you are my fate, my sweet) i want
no world (for beautiful you are my world, my true)
and it's you are whatever a moon has always meant
and whatever a sun will always sing is you

here is the deepest secret nobody knows
(here is the root of the root and the bud of the bud
and the sky of the sky of a tree called life; which grows
higher than soul can hope or mind can hide)
and this is the wonder that's keeping the stars apart

i carry your heart (i carry it in my heart)
~E.E. Cummings

Abstract

Opioids are a common comorbidity with HIV, with the use of opioids being present in up to 40% of the HIV infected population in some countries[1]. Opioids have been shown to worsen HIV pathogenesis, including increased viral replication and faster progression to AIDS[2].

HIV pathogenesis has been shown to be important in the gastrointestinal tract, where early loss of CD4+ T-cells has been observed in SIV infection and infection with either HIV or SIV show evidence of systemic bacterial translocation which is believed to drive HIV replication.[3] Opioids are believed to worsen this effect and have been shown to increase bacterial translocation in HIV patients.[4] The second chapter study was performed to understand the underlying disruption of gut homeostasis that contributes to bacterial translocation. HIV models were validated to show bacterial translocation, and then look at gut morphology, tight junction localization on gut epithelium, and immune function within the gut at early time points of exposure to HIV infection. Overall, based on the measures examined, opioids enhanced the pathogenesis of HIV in the gut at early infection which likely contributes to the greater replication and faster development of AIDS.

While the loss of gut homeostasis is strongly believed to occur at least in part through changes in the host defenses in the gut, namely on immune populations and epithelial barrier integrity, recent evidence suggests that the

microbiome of late stage HIV infected individuals is altered and may contribute to the observed disruption.[5–7] The third chapter investigated the microbiome in early HIV infection to see if dysbiosis occurs, and whether opioids are associated with earlier changes. Using two animals models of infectious HIV, microbial dysbiosis was not observed at early time points of infection in either model. However, this study shows for the first time that morphine induced strong changes in the microbiome, which likely occurs via a combination of constipation and immune mediated effects. Altogether, these findings suggests another mechanism for morphine influencing HIV pathogenesis at early stages of disease.

Combined, these studies show the wide ranging effects that opioids and HIV have on gut defenses, including epithelial barrier, immune function, and dysbiosis from the normal microbiome. While mostly descriptive in nature, the results give potential therapeutic opportunities, including potential oral administration of TLR2 and TLR4 antagonists, opioid antagonist naloxone, and bile acids in order to supplement deficiencies in metabolites observed.

Table of Contents

List of Tables

List of Figures

Chapter 2

Chapter 3

Chapter 1. Background & Literature Review

1.1. Protection by Mucosal surfaces

Exposure of external surfaces of organism to pathogenic elements increases risk of infection and invasion by pathogens. Skin and mucosal surfaces are charged with the important task of guarding the host organism from these threats as the first line of defense. The mucosal surfaces, named due to the secretion of mucous as a lining of protection, include the respiratory, urogenital, and gastrointestinal (GI) tracts. These surfaces combine to make up an enormous surface area, estimated at greater than 400m^2 in an adult human.

Given the ever-present threats at these surfaces, organisms have evolved specialized ways of protecting them. Epithelial cells line the surface and provide an impermeable barrier to the external environment with the help of secreted mucous. Immune cells, including innate cells like dendritic cells and macrophages as well as adaptive T- and B-cells, play a key role in monitoring these surfaces for potential pathogens and responding if a breach in the epithelial cells is found. Externally, organisms have acquired a symbiotic relationship with commensal bacteria, which are not pathogenic at mucosal surfaces. The host benefits from the exchange of nutrients from both the host diet and secreted factors and act to outcompete potential pathogens. Together, these three factors act to protect the mucosal surfaces from negative influences, namely infections, from the outside world. For the remainder of this thesis, the focus will be on the GI tract.

1.1.1. GI homeostasis

The GI tract is the largest mucosal surface and is integral to the host as this is where food is broken down into nutrients and absorbed while keeping large amounts of resident bacteria from the GI tract out. The host has evolved specialized cell types and structures to facilitate this complex interchange. Homeostasis in a healthy GI tract is when conditions favor barrier maintenance and allows for the host to exchange nutrients as needed.

Similar to other mucosal sites, the GI mucosal surface is maintained by epithelial cells, immune cells, and commensal bacteria with each playing a key role in the defense. However, there are unique features in the gut: specialized epithelial cells, specialized lymphoid tissues, and commensal bacteria in greater quantity and diversity than other mucosal surfaces. Each of these will be discussed in detail within the subsequent sections.

1.1.1.1. Physical barrier by epithelial cells

Epithelial cells provide an impermeable barrier to external factors like bacteria in the gut, but also need to allow small molecules, either beneficial nutrients or host-derived waste products, to cross in either direction. Due to the complexity of these functions, epithelial cells in the gut have evolved into multiple types of specialized cells. Epithelial cells differentiate as they travel from the crypt of Lieberkühn, where multipotent-stem cells reside, to the tip of the lamina propria and ultimately get sloughed off into the lumen of the intestine.[8,9] This

happens on a continual basis, where it is estimated 10^{10} epithelial cells are

sloughed into the lumen per day, leading to a complete turnover of the gut in 5-

10 days for many species.[10]

Enterocytes are the most prolific type of epithelial cells and are charged

with absorbing nutrients in the gut.[11,12] They also play an important role in

maintaining the homeostasis within the gut, both by maintaining tight junctions

between cells to keep out potential invaders as well as having innate immune

sensors such as Toll-like receptors (TLRs) which aid in detecting disturbances to

the barrier.[13–15]

Tight junctions, or zonula occludens, mediate cell to cell adhesion and

forms a paracellular barrier by extending from the cytoskeletal proteins of one

cell into the extracellular matrix, finally joining with the tight junction proteins of

another cell.[16] The complex of proteins form semipermeable barriers which

prevents hydrophilic solutes, or potential pathogens, from crossing the epithelium

without active transport.[17] The first tight junction protein discovered was Zonula

Occludens-1 (ZO1) in 1986,[18] which associated with the tight junction but

remained entirely intracellular. It was understood that transmembrane proteins

would be required to maintain the gap, and occludin was another integral tight

junction protein that was discovered to have that functionality.[19] ZO-1 acts as a

link between the actin cytoskeleton and other tight junction proteins such as

occludin.[20] Thus, it makes sense that tight junction are remodeled by changes in

4

the cytoskeleton.[21] Tight junctions need to be remodeled upon injury or

pathologic infection, which allow the barrier to be maintained.[22] However,

disruption of tight junctions have been shown to cause immune activation due to

bacteria being able to cross into the normally sterile body cavity,[23] likely by

activating TLRs.

TLRs are conserved receptors which recognize motifs from potential

pathogens and serve to activate an immune response named due to their

similarity to the Toll receptor from Drosophila.[24] These receptors have been

identified on immune cells from both the classical innate and adaptive lineages,

but also other cells including neurons,[25] endothelial,[26] and importantly epithelial

cells.[27] There have been at least 13 TLRs identified thus far, which can be

placed into two groups based on their localization. Within a cell in the endosomal

compartment lies TLR3, TLR7, TLR8, TLR9, and TLR13 which tend to recognize

nucleic acid motifs. Others, including TLR1, TLR2, TLR4, TLR5, and TLR6 are

found on the cell membrane and recognize macromolecules.[28]

Regulation of TLRs play an important role in the GI tract where there is a

large amount of interaction with both commensal and potential pathogenic

bacteria. The GI tract has evolved to have a compartmentalization of TLRs to

avoid chronic stimulation.[29] Epithelial cells have been shown to have expression

of numerous TLRs including TLR1, TLR2, TLR3, TLR4, TLR5, and TLR9.[15]

Given the vast amount of potential agonists in the lumen of the gut, it makes

sense that the expression of these receptors is very well regulated and sequestered based on location starting at birth.[30] External receptors like TLR2 and TLR4, which recognize cell wall components from gram positive and gram negative bacteria, are relegated primarily to the basolateral side of the tight junction.[31] This enables the epithelial cells to detect a breech quickly but without unnecessary activation.

Using TLRs and other innate receptors as a sensing mechanism, the epithelial cells are capable of orchestrating an immune response at the mucosal surface.[32] However, epithelial cells also secrete many immune factors important for dampening the immune response when one is not needed.[33–35] Thus, epithelial cells play a key role for maintaining homeostasis both as a barrier and in modulating the immune response in order to maintain homeostasis in the GI tract.

1.1.1.2.   Gut Associated Lymphoid Tissue (GALT)

Due to the vast quantities of potentially inflammatory antigens in the GI tract, the immune response in the gut must be controlled very tightly to maintain homeostasis. A cohort of immune cells reside within the GI tissues beneath the epithelial layer and act as both defense against epithelial breeches as well as monitoring and proactively influencing the microbiota within the lumen of the GI tract.

6

The control of immune responses begins at the regulation of antigen-presenting cells (APC), which are the most important cell for instigating an inflammatory response. While epithelial cells maintain a barrier from these pathogen associated molecular patterns (PAMPs), dendritic cells have been shown to sample the lumen of the gut by extending dendrites between epithelial cells.[36,37] To ensure that the constant sampling of commensal bacteria does not incur inflammation, dendritic cells in the GI tract have been shown to be programmed to favor an anti-inflammatory response compared with cells from spleen tissue.[38] Depending on the condition, dendritic cells are able to induce an inflammatory response to control damage when necessary.[39] Macrophages are another important APC within the gut, and specialize in the phagocytosis and debris within tissues.[40,41] Interestingly, macrophages and dendritic cells seem to induce different responses to activation within the gut by increasing different sets of CD4+ T-helper cells.[42]

The GI tract has a unique follicular structure which organize immune cells and assist in the complex relationship of managing nutrient absorption and allowing a commensal population of bacteria to grow within the lumen while still being able to mount a swift attack against potential pathogens. Peyer's patches, along with the smaller lymphoid follicles, are the best studied of these structures. Peyer's patches are found in the small intestine and characterized by having multiple B-cell follicles, which are separated areas containing T-cells and

dendritic cells. At these sites, T-cells interact with plasma B-cells which produce vast quantities of secreted Immunoglobulin A (IgA), estimated at 40-60 mg/kg/day, into the lumen of the gut.[43,44] IgA is secreted in greater quantities than other Ig combined due to its importance in shaping the gut microbiome, which will be discussed in a later section.

Adaptive cells are a major component of gut immunity, and B-cells, secreting IgA as mentioned above, and T-cells play an important role in mediating homeostasis due to their antigen specificity. The specificity of these cells helps to control against unwanted microbiota in the lumen, however they can also control against unwanted inflammatory responses as has been reviewed in FoxP3+ T regulatory cells (Tregs).[45] Other CD4+ also play an important role within the GI tract, especially Th17 cells, which are typically in balance with Tregs, have been suggested to play an extremely important role in mediating homeostasis in the gut.[46]

Together, both the adaptive and innate immune responses are collectively important for maintaining homeostasis within the GI tract. Disruption of any one cell has the potential to set off a chain of events that would render the host susceptible to infections, resulting in an overactive response that has systemic effects and may result in death from complications.

1.1.1.3. GI tract microbiome

Interestingly, germ-free mice which lack microbial colonization have a deficiency in the adaptive immunity discussed above, including in IgA secreting B-cells,[47] inflammatory CD4+ T-helper cells,[48] as well as Tregs.[49] Commensal bacteria are also able to influence many factors of host function including epithelial cells.[50,51] This begins to reveal the important role of microbes in the GI tract: the immune cells are not only there to control the microbes but the microbes actually help to stimulate the development and education of adaptive immunity. Through these and other studies, it has become apparent that the microbes within the gut lumen are an important component of gut homeostasis.

Vast quantities of bacteria reside with the GI tract, estimated at 10^{13} bacterial cells or 10 times more than host cells in humans.[47] Many of the bacteria in the gut are unculturable, which limited appreciation of the composition of the bacteria until recently when DNA sequencing of the 16S gene of ribosomal DNA has allowed for speciation and quantitative analysis.[52] High-throughput sequencing technologies, such as 454 or Illumina, have vastly increased in efficiency and subsequently lowered the cost of studying microbiomes of many environments, but especially in the GI tract where so many bacteria reside.[53,54]

The GI tract microbiome is very diverse, containing hundreds if not thousands of species, and is shaped by numerous factors including environment, diet, and the host organism immune responses. The environment determines

9

which microorganisms a host is exposed to with the potential for colonization, diet determines which microbes can grow with the proper nutrients, and the immune response determines which bacteria are allowed to grow and remain in the lumen. This is grossly evident in studies that have examined microbiome changes in human populations from different ages and locations where differences due to both factors are apparent.[55]

Commensal bacteria are important to the host as they break down food nutrients that the host cannot produce such as vitamins from the food, and support immune host immune development as mentioned above. Resulting metabolites play an important role for host function, and likely are a major reason that commensal bacteria co-evolved with organisms.[56] These bacteria also play a direct role in maintaining homeostasis by competing with potential pathogens for both space and nutrients. Pathogenic bacteria expend lots of energy to colonize and invade hosts, and over the course of infection must down-regulate virulence genes in order to survive and compete metabolically with commensal bacteria.[57] This selective pressure likely explains how bacteria evolved to lose virulence genes and establish mutualism with the host.

The composition of the microbiome varies greatly between individuals, however with an individual the microbiome shifts somewhat from birth to adolescence but stabilizes in adulthood. Deviation from this stable microbiome is

termed dysbiosis, which can have many negative consequences that will be discussed in a later section.[58]

Dysbiosis is generally prevented by a normal and balanced immune response. The host secretes peptides which can act directly in shaping the microbiome. The quantity of IgA response from B-cells is important for maintaining homeostasis in the gut microbiome, and is most favorable in a regulated, rather than inflammatory, environment.[59] Additionally, other antimicrobial peptides are produced by enterocytes or specialized epithelial-derived Paneth cells including alpha-defensins, lysozyme, and RegIIIγ.[60] The host is also able to limit contact between epithelial cells by secreting mucous, which prevents an overactive immune response against commensal bacteria.[61] Pathogens have factors which allow them to invade and colonize beyond the mucous membrane on epithelial cells thus inciting a greater immune response.

Overall, the microbiome in the GI tract plays a very important role in mediating homeostasis, both by contributing to the development of the immune system and by directly competing with potential pathogens. If the microbiome enters dysbiosis, either due to a colonized pathogens or overactive immune response targeting normally commensal bacteria, a negative cycle can develop which prevents homeostasis from returning.

1.1.2. Consequences of disrupting gut homeostasis

As highlighted above, each of the defenses provided by epithelial cells, immune cells, and microbiota are unique and essential to maintaining homeostasis within the GI tract. All of the systems work in conjunction, which is why loss of function of any of the components weighs heavily on the others and can result in failure at the barrier which can have systemic consequences.

One of the most common symptoms of a failure of GI tract homeostasis is when bacteria is observed in the normally sterile body cavity, which is termed bacterial translocation. Translocation can include live pathogens, live commensals, or microbial components such as cell wall proteins.[62,63] Translocation has been observed in many conditions including metabolic diseases obesity and diabetes,[64] inflammatory diseases like Crohn's disease,[65] as well as immunosuppression induced chemically or due to mental or physiological stress such as hemorrhagic shock.[66–69] Translocation from these and other states can lead to local inflammation and tissue damage as in Crohn's disease flare ups, systemic low level inflammation which likely contributes to metabolic disease, or in bad cases can lead to detrimental chronic inflammation known as sepsis.

The direct cause of bacterial translocation varies, however it is clear that disruption of gut homeostasis is the root of the problem. Mechanistic studies have found many areas capable of inducing translocation upon disruption. In

epithelial cells, disrupting TLR signaling can contribute to bacterial translocation which impairs the innate sensing mechism.[70] Similarly, disruption of epithelial pathways connecting to NFκB signaling are closely linked to many translocation disease states.[33,34] As discussed above, immune suppression has been linked with bacterial translocation. Depletion of Th17 cells have been linked to translocation,[71] as have depletion of Tregs,[72] again highlighting the importance of maintaining a balanced immune response in the GI tract. Another defense mechanism that invading bacteria have to overcome, once across the epithelial layer, is clearance by macrophage-mediated phagocytosis. Indeed, studies have shown high levels of bacterial translocation when macrophages are depleted from the gut.[73,74] Immune cells are typically very connected in their responses, which is why immune suppression or over-activation of any cell type in the GI tract would likely lead to bacterial translocation to some degree. It is more difficult to examine the direct effects of dysbiosis on bacterial translocation, as dysbiosis may influence the epithelial or immune response, however many studies have looked at the connection between dysbiosis and translocation in various disease states.[75–77]

Interestingly, opioid drugs have been linked with sepsis,[78] and also have systemic immune modulation which may influence the gut microenvironment.[79] These observations make it imperative to understand the mechanisms that contribute to sepsis.   These studies will be discussed in greater detail in the

upcoming section. Similarly, Human Immunodeficiency Virus (HIV) has been linked to inducing translocation and disrupting gut homeostasis,[63,80] which will also be discussed in later sections along with the potential links between HIV and opioids.

1.2. Opioid abuse and GI symptoms

1.2.1. Uses and distribution of opioids

Opioid class drugs have recently garnered much attention as a class of drugs with major public health concerns. Broadly, opioid abusers generate much higher annual direct health care costs at roughly 8.7 times higher than non-abusers.[81] Due to changes in abuse patterns, opioid drugs have recently been observed as two groups of abusers: illicit opioid drugs, including heroin, as well as prescription opioids, which include morphine and codeine.

The United Nations Office on Drugs and Crime (UNODC) estimated in 2009 that between 12 and 21 million people used illicit opioids at least once, which is a prevalence of between 0.3% and 0.5% of the worldwide population aged 15-64.[82] In the class of illicit drugs, heroin has traditionally been recognized as very problematic, and has maintained a relatively high level of abuse including roughly three quarters of the users cited above. The usage varies regionally, with illicit opioids being mostly consumed in Asia, followed by Europe and Africa. While heroin is the most commonly consumed form of this drug, pure opium consumption is also a problem in producing countries, particularly China and

Afghanistan. In the United States, heroin abuse is considered relatively low, but has remained steady over the past 15 years, including averaging around 250,000 admissions per year to substance abuse facilities,[82] as well as around 2500 heroin overdose deaths per year.[83]

A burgeoning problem worldwide has been the expanded availability and subsequent abuse of prescription opioids, which have primarily designed as pain killers. Since 1991, the number of opioid prescriptions dispensed by retail pharmacies in the United States has nearly tripled, from 76 million to 219 prescriptions filled.[84] Over a similar time course, the overdose deaths from opioid analgesics increased from around 4000 in 1999 to 16000 in 2010, which outnumbers the deaths from heroin and cocaine combined.[83] The death rates are trending upwards highest among people aged 25-64, with the highest being in the 45-54 age group.[83] Those aged 15-24 have seen increases in the past 10 years, but not nearly as much as those mentioned above, and those aged 65 and over have remained relatively stagnant. Patients who are particularly susceptible to abuse are those already taking high doses of prescription opioids for pain due to the development of tolerance. These drugs can be acquired due to their abundant prescriptions: adults are prone to "doctor shop" where they will visit different doctors and tell them that they need more or still have pain whereas younger abusers are more susceptible to steal them from parents or buy them from classmates.[85]

Treatments for opioid abuse are currently limited to psychological counseling and a few pharmacotherapy strategies designed for intervention. One of the earliest strategies following the discovery of opioid receptors was to design antagonists, which offer an attractive way to combat the ability of opioids to act. This would potentially provide a tool with the ability to overcome withdrawal symptoms as well as precipitate overdose patients. Naltrexone, a pure opioid receptor antagonist, received FDA approval for use in 1984.[86] While it is successfully used on overdose patients, its application for blocking withdrawal is limited due to the withdrawal effects being so undesirable that patient-mediated treatment with naltrexone often fails.

This has led to the development of drug replacement pharmacotherapies specifically to ease symptoms of withdrawal. There have been multiple pharmacotherapies developed with the goal of overcome the high levels of relapse in addicted patients, especially since the discovery of opioid receptors. The most established is methadone, in use as early as 1964,[87] which is a mu opioid agonist, similar to heroin and morphine, but has a activation profile; it results in a long, sustained binding to receptors but, when taken appropriately, does not activate the receptors in a way which results in the euphoric high associated with drug abuse.[88] While methadone has been successfully implemented in controlled clinic settings, it has many limitations for widespread use. It is susceptible to abuse itself, and can have side effects and symptoms of

16

withdrawal, similar to other opioid drugs. Thus, to implement this treatment
under proper supervision it has primarily been used in clinical detoxification
facilities. This has led to many patients relapsing when they leave the clinic and
return to their home environment which have associated cues to drug use.[89]
Clinics for detoxification are also stigmatized societally, which deters many
people from attending despite the recognized need or desire.

New treatments will be needed in the future which are able to be
prescribed to patients for home use which a treatment regimen that promotes
adherence. One such medication that has been gaining popularity is
Buprenorphine, which received FDA approval in 2002.[90] The advantage of
buprenorphine is that, while it is able to prevent relapse as effectively as
methadone, it has a lower risk of overdose and abuse, and thus is deemed safe
for home use. A novel formulation of the drug, named suboxone, goes one step
further and combines buprenorphine with the opioid antagonist naloxone.[91] This
allows the drug to be effective orally, but if injected to try and generate euphoria
via a higher dose then the naloxone antagonizes opioid receptors. Hopefully this
drug, along with new drug formulations, will allow patients to avoid the stigma
associated with detoxification clinics and maintain their treatments to become
drug independent.

There is a need to erase stigma which is associated with opioid abuse.
Due to existing stigma, drug use is believed to be underreported which makes it

difficult to fully assess and treat the problem.[91] Opioid abuse will not disappear,

and opioid drugs will continue to be prescribed in large amounts due to the

limited alternatives for pain relief. Addressing the problem of opioid abuse is

important due to rising public health costs, as well as the burgeoning public

health issue of diseases spread in the high risk drug-using populations, such as

hepatitis and HIV. Being able to treat as high of a percentage of opioid users as

possible would result in vast improvements of global health.

1.2.2. Systemic effects of opioids

Opioid abuse has many deleterious consequences in both acute and

chronic forms of use and is potentially fatal. In fact, heroin users are 7 to 10

times more likely to die at any given time when compared to age matched

controls.[92] Overdose is relatively common in both illicit drug and prescription

drug abuse, as discussed above. Side effects while on the drug can include

rapid heartbeat, skewed judgment, slurred speech, restlessness, hyperactivity,

diminished coordination, and difficulty concentrating.[93] Drug abuse can cause

many mental changes, including mood swings and behavior modifications due to

the highs and lows associated with drug use and withdrawal. One can imagine

that this can have deleterious consequences in their lives, including maintaining

personal relationships as well as jobs.

Aside from changes in the neurological systems associated with behavior

changes, research has also shown that opioids can cause drastic changes on

other bodily functions. In terms of death, a common cause is respiratory depression in response to high doses of drug.[93] Many cell types have been shown to express opioid receptors, including immune cells. Modulation of opioid receptors on immune cells lead to attenuation of immune function thus contributing to immunosuppression making opioid abusers more susceptible to disease.[79]

Another major and common side effect of opioid use is constipation. Discomfort from constipation is enough to drive many patients who were prescribed opioids off of their drug course. Smooth muscle in the gut expresses constitutive levels of the Mu-opioid receptor which maintains consistent levels in humans even after chronic exposure. Aside from discomfort, constipation induced by opioids can obviously contribute to changes in the GI tract. Recently, diet-induced constipation has been shown to alter the gut microbiome.[94]

1.2.3. Opioid-mediated disruption of gut homeostasis

Due to the constipation induced by opioids in the GI tract and the known effects of opioid drugs on the cells of the immune system[79], it would follow that homeostasis is likely interrupted while the host is using or abusing opioids. In support of this theory, it has been observed in animal models that morphine increases the incidence of sepsis, implying that translocation is occurring.[78]

Consequences of losing GI tract homeostasis are also worsened with morphine. Morphine has been shown to alter the immune response to gram

19

negative bacterial cell-wall lipopolysaccharide (LPS) and worsen the outcome to the host.[95] Similarly, morphine can accelerate the development of septic shock from LPS.[96] The source of LPS in these studies is likely translocation from the gut.

More recently, it has been shown that morphine can directly alter epithelial tight junctions through a TLR4 mechanism which leads to bacterial translocation.[97] A further consequence of the translocation is that the resulting immune response is prolonged, implying that morphine disrupts tolerance that typically occurs to prevent over-activation and damage within the gut.[98] Thus far, no studies have examined the consequences of the immune response on the global microbiome, although studies have shown that morphine can directly increase the virulence and potency of enteric bacteria.[99,100]

1.3. HIV and GI symptoms

1.3.1. HIV history and epidemiology

The HIV epidemic was first brought to attention in the early 1980s with the discovery of uncharacteristic opportunistic infections in homosexual males in New York and California due to immune suppression.[101] The viral cause of the immune suppression was described in 1983, which was identified to be a double stranded RNA retrovirus that has an envelope coated with glycoproteins that makes infection host specific for humans.[102,103] It likely evolved from Simian

Immunodeficiency Virus (SIV), which is endemic in primates in Africa, to be able to infect humans.[104]

Since the virus has been identified, the number of people infected has burgeoned to an alarming 35 million people worldwide.[105] Despite awareness of how to prevent the disease, namely by using condoms during sex in the case of sexual transmission or by not sharing needles between drug abusers, the disease is still commonly transmitted. This is likely in part due to the long-term unawareness of infected patients, with up to 10 years after infection without symptoms, which will be discussed more in detail below.

The immune suppression resulting from HIV is very fatal if left untreated. Beginning in 1990s antiretroviral drugs were developed that could lower the viral replication of HIV and allow the immune system of patients to recover.[106] These drugs have allowed patients to live longer, which has contributed to the increasing number of infected people living with HIV simply by preventing deaths. However, the drugs are not a cure for the disease and despite being controlled many patients still experience detrimental effects of both infection and the drugs themselves.[106,107] Access to the drugs is also an issue in populations where the disease is rampant, including Sub-Saharan Africa due to drug cost, as well as drug abusing populations in more developed nations who typically have poor access to healthcare but are at high risk for disease due to needle sharing. Ultimately, a cure for the disease would be ideal but unfortunately, despite being

aware of the genetic code of HIV for nearly 30 years,[108] the field still lacks a sufficient understanding of the disease and pathogenesis for a cure.

1.3.2. HIV pathogenesis

HIV has a relatively long pathogenesis compared to other infections, with mortality in untreated patients happening 8-10 years after infection. The disease is transmitted via body fluids, namely blood, semen/vaginal fluids, or breast milk.[109] Once inside the host, the glycoproteins on the virus target specific immune cells with coexpression of CD4 and either CCR5 or CXCR4 which are generally helper T-cells or macrophages.[103,110] HIV infection can be viewed as having three phases: acute, asymptomatic but progressive, and Aquired Immunodeficiency Syndrom (AIDS).[3]

The early phase of HIV is characterized by high viremia and a dip in CD4+ T-cells. The GI tract is rich with CD4+ T-cells cells so it is no surprise that HIV has been found at this site in early pathogenesis.[111] Interestingly, infected cells have been shown preferentially locate to the Peyer's patches of infected SIV rhesus macaques.[112] As a consequence of this, HIV infection induces the loss of CD4+ T-cells in the GI tract earlier than is typically associated with systemic immunosuppression.[80,113] Despite this loss, systemic CD4+ T-cells do not reach a low enough number to cause opportunistic infections, which is why many patients do not realize they have contracted HIV until the AIDS stage of disease when these infections present. By the end of the acute phase, systemic T-cells

levels mostly recover, although remain depleted in the GI tract, and adaptive immunity develops in the form of cytotoxic CD8+ T-cells (CTL) and HIV antibodies.[3] Inflammation during the acute stage drives the development of these adaptive immune responses, and can lead to generic symptoms such as fever or rashes.[114] These symptoms are difficult to link definitely to HIV which is why early diagnosis is uncommon unless exposure is known.

The asymptomatic but progressive phase has lower levels of virus in circulation and a sustained level of HIV-specific CTL and antibodies.[3] Despite low levels of inflammation, there are still no direct symptoms to identify that a patient is infected with HIV. This phase can last 5-10 years if left untreated (World Health Organization), and culminates in the adaptive responses, including systemic CD4+ T-cells, diminishing due to exhaustion of long term activation. This causes fibrosis of lymphoid tissues, which will impair the recovery of the immune system if the virus is eventually suppressed with antiretroviral therapy.[115]

Once the CD4+ T-cells are depleted, the patient is susceptible to opportunistic infections and is considered in the AIDS phase of disease. In the early stages of the HIV epidemic, identification of HIV infection, as well as the cause of mortality, was often associated with opportunistic infections such as *Pneumocystis carinii* Pneumonia and Kaposi's Sarcoma.[101]

1.3.3. HIV-mediated disruption of gut homeostasis

The early loss of CD4+ T-cells in the gut in HIV infection discussed above contributes to a disruption in normal homeostasis within the intestine that results in systemic translocation of bacterial products.[63,4] HIV replication is driven by activation of infected cells, the process of which has been reviewed to play an intimate role with bacterial translocation in the course of disease.[116] Specifically, CD4+ Th17 cells seem to play an important role in mediating this process, as studies comparing pathogenic and nonpathogenic SIV infection have shown a preferential loss of these cells in pathogenic infections.[117–119] As discussed earlier, Th17 cells have been shown to be important in homeostasis and the loss can result in bacterial translocation.[71,120]

HIV has also been shown to modulate the tight junctions between both endothelial and epithelial cells.[121–123] As discussed above, the tight junctions in the GI tract play a key role in maintaining a sterile barrier between the lumen of the intestine and the host. Systemically, this is also important due to the modulation of the blood brain barrier, as HIV can establish reservoirs in the brain and long term has many consequential neurocognitive effects.[4,124] Modulation of tight junctions may occur indirectly by HIV disrupting CD4+ T-cells which typically support the maintenance of tight junctions. However, studies have also shown that HIV proteins such as Tat (transactivator of transcription) can directly disrupt tight junctions on epithelial cells in culture.[125,126] This may be a mechanism in

early pathogenesis for how bacterial translocation gets initiated to start a vicious cycle of immune activation and infection in the GI tract.

In addition to the loss of barrier integrity, it has also been suggested that HIV infection reduces the ability of the host to clear bacterial products,[127,128] which would explain how bacterial products such as the TLR4 agonist LPS has been identified in the serum of HIV patients rather than being contained after translocation.[63]

More recently, evidence suggests that HIV pathogenesis induces dysbiosis in the microbiome of infected patients at multiple sites.   In areas where opportunistic infections take place, such as the lingual cavity, the microbiome has been suggested to become more pathogenic.[129] Within the GI tract, microbial populations such as *proteobacteria* species, *Prevotella*, and *Enterobacteriaceae* have been shown to be correlated with increase immune activation and increased in abundance in HIV patients.[7,6] Interestingly, species of *Proteobacteria* have been identified in the brains of HIV-infected patients,[130] which is likely a cumulative result of microbial dysbiosis and disruption of tight junctions especially in the blood brain barrier as discussed above. Certain strains have also been correlated with better health in HIV patients. For instance, high abundance of *Lactobacillales* have been shown to be protective of CD4+ T-cell loss and microbial translocation.[131] Metabolic changes have also been correlated to microbial dysbiosis.[132] These changes are likely a result of

prolonged immune activation characteristic of HIV patients and exacerbate
dysfunction within the GI tract.

1.3.4. Models of HIV

As HIV is a human-only infection, modeling the infectious disease has
been relatively challenging. Human case studies were originally the only means
of studying the disease, however this greatly limits the questions that can be
ethically studied. Aside from this, the stages of diagnosis for humans are
generally very late making it difficult to study early stages of disease.

One way to overcome this would be to study HIV using *in vitro* models.
For instance, human-derived CD4+ cells can be infected *in vitro* with HIV and
functionally assessed.[124,133] Additionally, HIV proteins, such as Tat, can be
produced and the effects on cells, especially bystander cells which do not get
infected but may be exposed to these proteins, can be examined *in vitro*. Tat in
particular has been shown to alter many normal cell functions in culture, such as
astrocytes, neurons, and even epithelial cells.[125,134–138] However, the
applications of this are relatively limited since many of the negative effects of HIV
are likely due to a chain of systemic events in an organism. Thus, it became a
priority of the field to develop animal models of HIV infection to study the
systemic effects of HIV infection.

As mentioned in earlier sections, SIV is the most straightforward model
that existed in nature. SIV is endemic in African monkeys such as African Green

Monkeys or Sooty Mangabeys but, despite high levels of viremia, causes no appreciable disease symptoms and no development of AIDS.[139] Conversely in Rhesus Macaques, who have not been exposed to SIV infection in the wild, full pathogenesis of SIV to AIDS develops.[140,141] This has provided a useful model for comparison to study which symptoms of SIV (or HIV) at early stages of disease may contribute to the development of AIDS.[118,142] However, cost and the lack of molecular research tools such as genetic models still limit the accessibility and depth of questions that can be asked with nonhuman primate models.

More recently, transgenic mouse models of HIV have been developed to take advantage of the diverse research tools and lower cost compared to nonhuman primate models. As there is no natural virus that would infect mice to compare with as in nonhuman primates, strategies have been employed to modify either the host or HIV to be receptive to infection. One major strength of mouse models is that they can be manipulated genetically, which can be used either to directly express HIV proteins or to express human co-receptors to allow HIV to infect mouse cells. For example one early model, Tg26 mice, has a germ line insertion which expresses most HIV genes with the exception of gag and pol; interestingly, this model has been published primarily to study HIV-associated renal disease.[143,144] Another useful mouse model singularly expresses the Tat protein constitutively and has provided interesting insights of what the protein can do systemically.[145,146] Both of these models express the transgenic genes from

27

birth, which is a major weakness in that it is difficult to control the temporal effects in a study. Groups have attempted to improve on transgenic mice by making them inducible in order to control the duration of exposure.[147] These models are still very limited in that they do not actually model infection of HIV. An alternate approach to HIV transgenic mice has been to express human receptors for HIV co-receptors CD4 and CCR5 to allow infection of HIV into mice cells.[148] Unfortunately, these models have been shown to have limitations which have been difficult to overcome including altered immune cell trafficking and depletion even when HIV is absent.[149–151]

In place of expressing human receptors in mice, chimeric mice have been developed with humanized immune systems. HIV is able to actively infect and replicate in the human immune cells as if the cells were in their natural hosts, causing immunopathogenesis in models independent of the source of human immune cells.[152,153] These models have been valuable for studying HIV replication in a system of immune cells, but having a chimeric humanized mouse makes it difficult to interpret the interactions between human immune cells and other mouse cells. Especially in the GI tract, as discussed above, this becomes complicated due to the intimate relationship immune and epithelial cells typically share. They are also limited in that mice need to be immunocompromised to be receptive to the human cells, which eliminates the use of genetic models such as knockouts which can be important in mechanistic studies.

In addition to modifying the mice to suit HIV infection, another approach employed has been to modify the HIV virus to infect mice cells. One version of this, termed EcoHIV, the genome of HIV is altered to produce glycoprotein GP80 from Murine Leukemia Virus (MLV) in place of gp120.[154] Gp120 is the protein that binds to human CD4 as a first step to cell entry. Thus, replacing it with gp80, which binds murine MCAT1 receptor, allows HIV to enter mouse cells and not human cells.[155] While this alters the exact pathogenesis of HIV (infected cells with MCAT1 receptor include T-cells, macrophages, and B-cells), it does allow an infectious model in mice. Because of this, EcoHIV has an advantage over humanized mice for studies that wish to use genetic knockout mice as well as study the effect of HIV infection on bystander cells.

1.4. HIV and opioid interactions

1.4.1. Epidemiology of HIV and opioid abuse

Chronic opioid abuse is of particular public health concern for the spread of infectious diseases, especially in the context of the HIV epidemic. In certain regions, up to 40% of HIV infected individuals are believed to abuse opioids.[105] A large contributor to this is thought to be the widespread use of unsterile needles in heroin abusers. Rather than focus on eliminating drug use, which is practically impossible in the high risk populations, one public health strategy has been the focus of some programs to distribute clean needles to drug users.[156] However, it is also believed that opioid abuse can directly lead to higher overall

infection rates, including HIV, by altering immune responses as reviewed and discussed above.[79] Opioid users also suffer from a faster progression of infection to AIDS, as well as severe long term consequences such as neurocognitive defects in both humans and nonhuman primate models studied.[157–159] Thus, it is no surprise that recently opioid substitution therapies have been shown to reduce HIV transmissions and care of HIV-infected patients.[160,161] Despite awareness of the problem that opioids create in the HIV community, there is still a great need for research to understand the mechanisms of HIV infection pathogenesis and opioid interactions in patients such that effective treatment strategies can be developed.

1.4.2. Opioid effects on HIV pathogenesis

Once HIV is able to infect the host, there is evidence that opioids alter disease pathogenesis. Opioids can increase the infectivity of cells and viremia, which is blocked by the mu-opioid receptor antagonist methylnaltrexone.[161]

Many studies have focused on late disease effects of drug use on HIV as these patients acquire side effects of HIV infection earlier and more severely than non-drug users as discussed above. Non-drug users experience some neurocognitive effects like HIV-Associated Neurocognitive Disorders (HAND), however they rarely reach the severity that opioid users experience which includes HIV-associated dimensia.[162–164] Studies in models of HIV have validated that opioid drugs increase inflammation and neurotoxicity in the

brain.[138,147,165] Thus, neurocognitive defects in drug abusers are likely associated with higher levels of systemic inflammation than is typically observed in HIV patients as discussed above.

Interestingly, as in non-users of drugs of abuse, the genesis of this inflammation is likely translocation of bacterial products from the GI tract. Indeed, humans infected with HIV who use heroin have been shown to have greater amounts of LPS in their serum compared with non-users.[4] This implies that disruption of homeostasis within the gut is more severe in drug using HIV patients. Morphine has been implicated to disrupt populations of Tregs and Th17 cells, including the homing of T-cells to the GI tract, in SIV infection.[166]

1.4.3. Hypothesis/Study AIMS

Our study aims to resolve the lack of understanding on how HIV and opioid drugs interact in disrupting gut homeostasis. Unfortunately, the body of evidence studying HIV and opioids in the GI tract is lacking. Early pathogenesis is difficult to study in human populations, and thus far animal models have made studies either cost prohibitive (SIV) or limited to interpret systemic effects (humanized mice).

As discussed above, morphine and HIV have both been shown to have effects within the GI tract. Anecdotal evidence from translocation in HIV-infected opioid abusing populations suggests that translocation is more severe than in

HIV alone,[4] however to our knowledge no systematic study has been done to examine them together.

Our hypothesis is that HIV and opioid drugs will disrupt gut homeostasis in epithelial cells, immune cells, and microbiome more severely than HIV or opioids alone. Homeostasis in the gut will be examined in both the effects on the host epithelial and immune cells within the GI tract (Chapter 2), as well as the effects on the gut microbiome (Chapter 3).

Chapter 2.   **Effects of opioids on early HIV pathogenesis in the gut**

33

2.1.   Chapter Summary

Opioids are a common comorbidity with HIV, with the use of opioids being present in up to 40% of the HIV infected population in some countries.[1] Opioids have been shown to worsen HIV pathogenesis, including increased viral replication and faster progression to AIDS.[2] HIV pathogenesis has been shown to be important in the gastrointestinal tract, where early loss of CD4+ T-cells has been observed in SIV infection and infection with either HIV or SIV show evidence of systemic bacterial translocation which is believed to drive HIV replication.[3] Opioids are believed to worsen this effect and have been shown to increase bacterial translocation in HIV patients.[4] This study was performed to understand the underlying disruption of gut homeostasis that contributes to bacterial translocation. HIV models were validated to show bacterial translocation, and then look at gut morphology, tight junction localization on gut epithelium, and immune function within the gut at early time points of exposure to HIV infection. Overall, based on the measures examined, opioids enhanced the pathogenesis of HIV in the gut at early infection which likely contributes to the greater replication and faster development of AIDS.

2.2.   Introduction

HIV infection is highly prevalent in injection drug users (IDU) with upwards of 40% in various regions globally.[167] While IDU was recognized early in the history of HIV as a potential means of transmitting the disease by sharing needles with blood remnants, IDU has also been observed to correlate with a more severe HIV pathogenesis than non-users including a much faster development of AIDS and higher rates of neurocognitive deficiencies.[157,168] The mechanism for this is currently unknown, however it likely occurs via a combination of the ability of the drugs to modulate systemic changes in the patient along with decreased access to adequate healthcare.[169]

Clinically, it is nearly impossible to delineate how IDU may enhance HIV due to poly-drug use which is estimated to occur in over 70% of IDU patients.[170] Opioids, the most common IDU agent in HIV cases, have been reviewed to have drastic systemic effects including the immune system[79]. Given that opioid-mediated immune deficiencies are in many cell types, including cells infected by HIV such as CD4+ T-cells and macrophages, there are likely interactions between HIV and opioid use in the immune compartment. The consequence of altering the immune response with opioids could lead to deregulated immune function, including greater inflammation and lack of tolerance, and ultimately hamper the ability of the host to control HIV[2]. Thus, understanding the interactions between HIV and opioids is important, especially at the early stages

of disease, in order to develop interventions and prevent the severity of HIV pathogenesis observed in IDU-using infected patients.

Early stages of pathogenesis in HIV infection has been difficult to study in clinical populations since the disease does not make itself obvious until years later when opportunistic infections develop. Nonhuman primates infected with Simian Immunodeficiency Virus (SIV) have been an invaluable tool to overcome this limitation, especially since there are different species of NHP which experience pathogenic and nonpathogenic progression of SIV, which allows for differences between the two to be mapped.[171,172] Initial stages of HIV pathogenesis are now strongly believed to be reliant on microbial translocation from the gut which drives the systemic inflammation needed for HIV/SIV.[63,126] Despite these findings, studies of mechanisms in nonhuman primates, as in humans, are still very restricted by the lack of genetic tools and increased cost compared to small animal models like mice.

Developing HIV models for mice has been limited by the host specificity of HIV. Mice can be made transgenic to express HIV proteins in varying combinations, from all of the proteins except gag and pol (Tg26) to specific proteins such as the Tat protein.[143,145] Most infectious models have focused on "humanizing" the mice either by creating transgenic mice with human HIV co-receptors or generating chimeric mice with human

immune cell grafts.[152,153] The latter method has shown a remarkable ability to recapitulate HIV pathogenesis in the human immune cells within a mouse.[153] However, studies using chimeric mice cannot adequately make conclusions about physiological effects of HIV infection on non-immune cells, such as neurons or epithelial cells, because the interactions between human and mouse cells are likely not conserved. Humanized mice are also susceptible to Graft Versus Host Disease, which can further complicate interpretation of results.[173] For this reason, Potash et al created the EcoHIV model, which is a genetically modified chimeric HIV virus which uses murine leukemia virus gp80 for cell entry in place of gp120 from HIV-1.[154]

With the goal to study gut homeostasis as a system between immune and epithelial cells, humanized mice were ruled out due to the complicated interpretation of human cells communicating with mice cells. HIV was hypothesized to disrupt epithelial cells both directly with HIV proteins and indirectly through inflammation. To study this, the following studies utilized an infectious EcoHIV model in addition to transgenic mice to Tg26[143] and Tat proteins[174].

2.3.   Methods

Mice

All studies using mice in Dr. Roy's laboratory were approved by the University of Minnesota Animal Care and Use Committee and were conducted in full compliance with NIH guidelines. Male or female C57Bl/6 and BALB/c mice were purchased from the Jackson Laboratory, while Tat86, Tg26, Mu Opioid Receptor Knock Out (MORKO) and Toll-Like Receptor 4 Knock Out (TLR4KO) mice were bred in house. All animals were between 10-16 weeks of age at the beginning of each experiment.

Morphine treatment

Mice were implanted with either a placebo or 25mg slow-release morphine pellet. Pellets have been shown previously to achieve a steady state dosing quickly and maintain serum levels of morphine up to 384 hr post-implantation, albeit with diminishing doses following 72 hr.[175] In EcoHIV infection, implantation occurred at 24 hr prior to infection. Timing of implantation with transgenic mice were listed in each experiment. Pellets were generously provided by NIH/NIDA.

EcoHIV infection

The EcoHIV constructs used in the present work were EcoHIV/NL4-3 which was constructed on the backbone of HIV-1/NL4-3[154] and EcoHIV/NL4-3-GFP which

expresses enhanced green fluorescence protein (EGFP) as a marker protein (He-14). For brevity, the viruses are called EcoHIV and EcoHIV-GFP. The viruses were propagated in HEK293TN cells as previously described.[154] Mice were injected in the intraperitoneal cavity with 1mL of either saline or 1×10^6 pg of p24 of EcoHIV as measured by p24 ELISA following manufacturer's instructions (ZeptoMetrix Corporation). *In vitro* work performed in macrophage cell lines (J774 or RAW) were treated with 1×10^3 pg of p24 of EcoHIV per 1×10^6 cells.

Bacterial Translocation

Tissues were harvested and homogenized in sterile PBS with 100μM cell strainers (BD) following aseptic techniques. Homogenized tissue was then plated on blood agar plates and incubated at 37°C overnight. Colonies were counted and normalized for varying protein concentrations in the tissue homogenate.

RNA isolation and processing

RNA isolation was performed on homogenized tissue using the Qiagen RNeasy prep and cDNA was generated using the Promega Reverse Transcription System, each according to the manufacturer's protocol. RT-PCR was run and quantified with Sybr Green (Roche) for 40 cycles on an Applied Biosystems 7500 machine. Samples which crossed the threshold above 32 Ct were considered to

be non-specific amplification and discarded. Primers are listed in Table 2.1.

Mouse Innate & Adapative Immune Responses PCR RNA array (SABiosciences)

was run using purified RNA, pooled together from mice of each treatment group,

following manufacturer's directions.

Table 2. 1 Primers for RNA quantification

Primer	Forward (5' to 3')	Reverse (5' to 3')
LTR-gag	TCTCTAGCAGTGGCGCCCGAACA	TCTCCTTCTAGCCTCCGCTAGTC
18S	TTGACGGAAGGGCACCACCAG	CTCCTTAATGTCACGCACGATTTC
Beclin-1	GCTGAGAGACTGGATCAGGA	ATTGTGCCAAACTGTCCACT
EGFR	TTGGCCTATTCATGCGAAGAC	GAGGTTCCACGAGCTCTCTCT
Lysozyme2	GCACACTGTCAAAACCGAGA	GCCCTGTTTCTGCTGAAGTC
TLR2	CGCCTAAGAGCAGGATCAAC	GGAGACTCTGGAAGCAGGTG
TLR4	TCCAGTGTGCAGAATTCCAA	GGCTCACCTTCCATCACTCT

Immunofluorescence

For occludin, distal small intestine (Ileum) and large intestine (colon) tissues were

flushed with PBS and frozen in TFM tissue freezing medium (TBS, Durham, NC).

Sections were cut on a cryostat at 5uM; At least four sections from each of three

animals for each condition were prepared and analyzed. Sections were fixed

with 1% paraformaldehyde in PBS for 10 min at room temperature. Following

washing in PBS, slides were blocked with 5% bovine serum albumin (BSA) and

then incubated with polyclonal rabbit anti-occludin at 5µg/mL (Invitrogen) for 2 hr

at room temperature. Slides were again washed prior to incubating with with

DyLight 488-conjugated AffiniPure Donkey anti-rabbit IgG for 60 min. Tat86 mice

sections also included rhodamine phalloidin (Invitrogen). Sections were washed

and mounted under coverslips using ProLong Gold antifade reagent with DAPI (Invitrogen). Sections were imaged using a Nikon confocal microscope.

Histology

Intestinal tissues were flushed and preserved in 10% formalin for 24hr and transferred to 70% ethanol. Samples were then embedded in paraffin, sectioned, and stained for H&E or a custom stain including haemotoxylin, alcian blue (at pH 2.5) which stains goblet cells, and saffron stain which stains collagen/connective tissue. Both stains were done by Bionet (UMN). Slides imaged at 20X.

FACS

Lamina propria immune cells were collected from small, cecum, or large instestine following a previously published method.[176] Briefly, intestine was washed with HBSS with 5% FBS and .5M EDTA to remove epithelial cells. Remaining tissue was digested using HBSS with 5% FBS and .4 mg/mL Collagenase (Sigma-Aldrich). Cells were harvested via centrifugation at 500g and fixed in IC fixation buffer (Ebiosciences) for 20 minutes on ice and stained using I-A, I-E (AF488, Biolegend), CD4 (PE, BD), CD8 (APC, eBioscience), CD19 (Alexa 700, BD), CD11B (PE-cy7, Biolegend), CD11C (PE-cy5, Biolegend), and CD45 (V500, BD) and acquired by a FACS Canto II flow cytometer. Analysis was done using Flowjo software (Treestar Inc).

Phagocytosis

Peritoneal macrophages were harvested by putting 1mL sterile saline inside the omentum sac and removing to a sterile tube, which were then cultured for 30 min in serum-free media and washed to select for adherent cells. Peritoneal, RAW, or J774 macrophages were cultured with enriched DMEM with and without 1uM morphine, 10, 000 / well in black 96-well plate or cover slip and incubated with either FITC-dextran or *E. coli* or *S. aureus* opsonized particles (1:20, cell:bacteria/bead ratio) for 30 minutes. Phagocytosis was stopped by addition of trypan blue, which quenches fluorescence of noninternalized particles. Cells were either analyzed by fluorometry in black 96-well plates after staining with DAPI (D9542 Sigma) or fixed for confocal microscopy on sterile glass cover slips, where they were co-stained with rhodamine phalloidin and Prolong Gold with DAPI (Life Technologies) and imaged by confocal microscopy. Fluorescence was recorded at an excitation of 485 nm and an emission of 520 nm for opsonized particles (FITC) and an excitation of 355 nm and an emission of 460 nm for DAPI. Phagocytosis per cell was quantified as phagocytic Index = FITC/DAPI [both given in relative fluorescence units (RFUs)], indicative of particle fluorescence per cell.

ELISA

Liver and lung homogenates were prepared as described in bacterial translocation experiments. TNFα, IL17A, and IL-6 Ready-Set-Go kits (Ebiosciences) were performed following the manufacturer's instructions and plates were read on an absorbance plate reader at 435nM/495nM (background). A standard curve was generated for each kit and values were calculated using the linear fit of the standard curve data points.

ECIS

Caco2 or IEC-6 cells were plated at 1.5×10^5 cells per well in an 8-well Electrode Cell Impedance System 8W10E+ plate (Applied Biophysics). Once confluence was reached in the wells, 1µM morphine was added to appropriate wells. The following day, the plates were placed in the ECIS ZΦ machine for 2 hr to gather a baseline. 100ng/mL Tat or gp120 was added to media of appropriate wells and again monitored by ECIS for 7hr. Lipotechoic acid (LTA, Sigma) was then added to the wells and monitored by ECIS for at least 12 hr. Results were normalized to control wells.

Statistics

Statistical significance was calculated by two-way ANOVA using Bonferroni post-tests to compare each treatment with the others using Prism software (Graphpad Inc).

2.4.   Results

Model: EcoHIV

The goal of these studies was to examine whether an infectious HIV model, utilizing EcoHIV, can mimic symptoms of gut pathology observed in HIV patients. While previous studies with EcoHIV predominantly characterized the brain compartment in response to infection,[177,178] initial experiments examined the capacity of EcoHIV to recapitulate early consequences of HIV-1 at the systemic level, such as bacterial translocation, and inquired whether combination of infection with opiates would worsen these effects. Knowing that EcoHIV can infect CD4+ and macrophages in mice,[154] the next step was to verify the systemic nature of infection, including whether morphine influences the amplitude of infection. EcoHIV infection of macrophage cell lines was validated *in vitro* by examining the RNA expression of LTR-gag in both J774 and RAW cells. In these cell lines, HIV LTR-gag RNA expression was observed but importantly was not detected in uninfected cells (Fig 2.1A). Infection was validated *in vivo* by observing expression levels of LTR-gag RNA in the spleen of infected mice 2 days, 5 days, and 7 days post-infection, but not in uninfected mice (Fig 2.1B). Using EcoHIV which expresses GFP within infected cells,[178] expression of GFP

was examined in both F4/80+ macrophages and CD4+ lymphocytes isolated from peritoneal lavage and spleen at 5 days post-infection (Fig 2.1C). Male and female animals manifested similar levels of infection in all cell types with the possible exception of CD4+ peritoneal cells. Peritoneal macrophages were also visually examined using confocal microscopy to verify positive GFP expression in EcoHIV infected animals (Fig 2.1D). EcoHIV infection was also measured using systemic p24 levels observed in liver (Fig 2.1E), lung (Fig 2.1F), and brain (Fig 2.1G) on day 5, day 10, and day 21 post infection. There was little difference between mice implanted with either placebo or 25mg pellets of morphine aside from at day 21 in liver (Fig 2.1E). Together, these results established successful infection of EcoHIV of CD4+ T-cells and macrophages in animals when EcoHIV was administered systemically thus recapitulating observations seen in humans with HIV-1 infections.

Translocation of bacterial products have been shown to play a key role in the early pathogenesis of HIV.[63] Similarly, sepsis and bacterial translocation have been observed when animals are implanted with morphine pellets.[78,97] In combination, IDU has been shown to increase the translocation induced by HIV,[4] therefore the next question examined whether bacterial translocation occurs in the EcoHIV-infected animals and will morphine exacerbate the effects. Significantly increased bacterial translocation, as measured by colony forming units (CFU), occurred at day 2 post infection (Fig 2.2A) but not day 5 post

infection (Fig 2.2B). The highest amount of bacterial translocation (CFU) was observed in the liver when compared to the lung and spleen in animals that were infected with EcoHIV and in morphine treated EcoHIV-infected animals. To validate these findings, liver homogenate was incubated with RAW Blue cells to look for the presence of PAMPs such as LPS from gram-negative bacteria or LTA from gram-positive bacteria. Similarly to the CFU translocation observed, day 2 post infection showed significantly higher NFκB activation in morphine, EcoHIV infected, and EcoHIV infected + morphine treated animals compared to placebo (Fig 2.2C), whereas day 5 post infection showed no change (Fig 2.2D). Finally, animals were gavaged with Rhodamine Dextran (Sigma) 4hr prior to Xenogen visualization on day 2 post infection, where noticeable translocation was observed especially in the EcoHIV infected + morphine treated animals (Fig 2.2E). Overall, the induction of bacterial translocation in wild type animals infected with EcoHIV is similar to HIV-1 in humans despite the time point being at very early stages of the disease.

The next set of experiments examined if disruption in tight junction proteins contributed to the bacterial translocation. Indeed, differences were observed in the integrity of the epithelial layer by examining the tight junction protein Occludin, which is an integral transmembrane protein that binds cells.[179] In the small intestine, punctate staining is observed at the boundary of the gut lumen and epithelial cells (Fig 2.3, upper left). As has been shown previously,[97]

morphine treated animals showed a reduction of the punctate staining (Fig 2.3, upper right). Interestingly, EcoHIV also showed a reduction of the punctate staining (Fig 2.3, lower left). Combination of EcoHIV+morphine treatment resulted in the highest amount of bacterial translocation and showed almost no staining at the epithelial boundary (Fig 2.3, lower right), suggesting that tight junctions are disrupted. Conversely to small intestine, large intestinal tissue showed no difference in Occludin staining between placebo and morphine treated mice (Fig 2.4, upper left and right). Both EcoHIV and EcoHIV+morphine show a reduction in punctate staining, again suggesting a breach in barrier function which supports the translocation data. Together, the reduced localization of Occludin at the epithelial boundary suggesting remodeling of tight junction proteins in animals treated with morphine, EcoHIV and most notably in combination with EcoHIV+morphine.

TLRs on enterocytes, especially TLR2 and TLR4, have been shown to play a role in tight junction remodeling and bacterial translocation.[70,97,180] Thus, TLR2 and TLR4 RNA expression and protein levels were examined in isolated gut epithelial cells. Small intestine epithelial cells showed a 2-fold increase in TLR2 mRNA expression and an 80-fold increase in TLR4 mRNA expression in EcoHIV+morphine animals, while morphine and EcoHIV individually showed a 3-fold increase in TLR4 (Fig 2.5A). Similar to tight junction staining, large intestine epithelial cells did not show much change in either TLR expression with EcoHIV

47

infection (Fig 2.5B). EcoHIV+morphine treated animals showing a slight (1.5-2 fold) change in TLR4 mRNA expression (Fig 2.5B). Following this, protein levels were examined in epithelial cells flow cytometry. Unfortunately, with the antibodies available, this method was not sensitive for TLR2 (very low fluorescence in all samples). However, TLR4 showed a significant increase in morphine and EcoHIV+morphine animals compared to placebo (Fig 2.5C). Large intestine again had less variation from placebo, with morphine having significantly higher levels than placebo (Fig 2.5D). Altogether, this data indicates that TLR4 increases significantly in small intestine and large intestine and could be a potential reason for the observed bacterial translocation.

Examining the intestinal tissues histologically, the placebo animals had characteristic smooth and long lamina propria (LP) while treated animals had shorter LP with inversions and perceived gaps in the epithelial cells (highlighted by black arrows, Fig 2.6A). Ratios of small intestine LP length to width and LP length to crypt depth have been used as a measurement of gut health, shown to be reduced in HIV.[181] LP length from tip to beginning of crypt, LP width, and crypt depth from end of LP to smooth muscle were measured. Ratios of LP height:width were significantly reduced in morphine, EcoHIV, and EcoHIV+morphine treatments compared with placebo (Fig 2.6B). LP height:crypt depth showed a similar trend with morphine, EcoHIV, and EcoHIV+morphine all showing significance over placebo (Fig 2.6C). Tissues were stained with Alcian

Blue in order to stain for goblet cells, which produce mucin into the lumen of the gut to provide a buffer from bacteria and defend against invasion and translocation. Goblet cells were counted, revealing a significantly lower count in EcoHIV+morphine treated mice compared with placebo (Fig 2.6D). As this could be a consequence of shorter LP heights, goblet cell count was plotted against LP height and no significant correlation was found implying that goblet cells are reduced independent of LP height (Fig 2.6E). Large intestine histology was also compared but, as in the occludin staining, EcoHIV+morphine was the only group to look different than placebo (Fig 2.7A, upper left and lower right). Large intestine LP depth was measured as a comparison to the height and width measures in the small intestine. As in visual analysis of the histology, LP depth in EcoHIV+morphine was found to be significantly decreased compared to placebo (Fig 2.7B, $p<.05$). Goblet cells were approximated by measuring the blue area within the colon depth. There was a significant difference in the morphine group but not in the EcoHIV+morphine group compared with placebo (Fig 2.7C, $p<.05$). These differences may be accounted for by correlating goblet cells and LP depth, which showed a positive correlation (Fig 2.7D). Thus, EcoHIV+Ms mice had fewer goblet cells due to a decrease in LP depth. Together, the pathology in the gut appears significantly changed in the EcoHIV+morphine treated animals both in morphology in both the small and large intestine. Goblet cells were also reduced in EcoHIV+morphine by count in

49

the small intestine and by area in the large intestine due to LP depth decrease

which likely plays a role in mediated bacterial translocation.

As the morphological changes in the gut were so apparent, the next set of

experiments investigated if stress markers in epithelial cells correlated with

bacterial translocation observed. Beclin-1 is a marker of mitophagy and

autophagy which is often increased with damage.[182] Interestingly, expression of

Beclin-1 is increased in EcoHIV+morphine animals, which corresponds with the

damage observed in morphology. Epithelial cells isolated from the small

intestine (Ileum) showed a 25-30 fold increase in morphine and EcoHIV treated

animals, and a 200-fold increase in EcoHIV+morphine animals (Fig 2.8A). In

epithelial cells from the large intestine (colon), a modest 5-fold increase was

observed with EcoHIV infection, but again a 250-fold change in

EcoHIV+morphine animals (Fig 2.8A). While Beclin-1 is a marker of stress,

EGFR is increased by epithelial cells to promote tissue repair in response to

stress and damage in the gut.[183] EGFR saw a very similar profile to Beclin-1,

with small intestine showing a 5-12-fold increase in morphine, EcoHIV, and

EcoHIV+morphine (Fig 2.8B). Similarly to the profile observed in small intestine,

large intestine epithelial cells had a 15-fold increase in EcoHIV+morphine treated

animals (Fig 2.8B). Combined, this data suggests that the epithelial cells are

undergoing stress and are trying to process it in a healthy way (autophagy vs

necrosis), but that the tissue is undergoing a repair process which may contribute to the lack of translocation by Day 5 post-infection.

To determine if morphine was acting with EcoHIV on disrupting gut homeostasis through the mu-opioid receptor, translocation was examined using the mu-opioid receptor knock out (MORKO) mice at 72 hr after morphine and 48 hr post-infection. No bacterial translocation was observed in the MORKO animals following morphine treatment, but surprisingly very little bacterial translocation was observed in the EcoHIV or EcoHIV+morphine groups as well (Fig 2.9A). Histology of these animals was examined and, as was predicted by the bacterial translocation data, no differences were observed between any of the treatment groups in small intestine (Fig 2.9B) or large intestine (Fig 2.10). Given that protection from the translocation and morphological changes was observed in MORKO animals, this shows that MOR plays an important role in mediating the pathology observed in WT animals.

Due to the increase in epithelial TLR4 observed above and the known interactions of TLR4 in the bacterial translocation process,[70] TLR4 knockout mice were subsequently examined. Similar to MORKO mice, reduced translocation was observed in animals treated singly with morphine or EcoHIV compared with WT (Fig 2.11A). However, animals infected with EcoHIV+morphine were found to have translocation at levels similar to the wildtype genotype with the same treatment, implying that responses are blunted

51

but the combined therapy is able to overcome the threshold for translocation (Fig 2.11A).   Unfortunately, no TLR4KO animals treated with placebo were available for comparison. Compared to wildtype, the morphology of small intestine (Fig 2.11B) and large intestine (Fig 2.12) in TLR4KO mice appear protected compared to the gross morphological changes observed in WT EcoHIV+morphine treated animals. Overall, the induction of bacterial translocation in wild type animals infected with EcoHIV is similar to HIV-1 in humans and is abolished in MORKO and TLR4KO animals, which suggests that both genotypes play a role in the bacterial translocation and the disruption of gut homeostasis within the gut.

Inflammatory pathology likely plays a role in the observed morphological changes, which would be mediated by local immune cells in the gut. To determine whether recruitment to the site contributed to observed pathology, immune cell populations within the gut were examined. Within CD4+ and CD8+ T-cell populations, no changes between treatment groups were observed in the small intestine (Fig 2.13A), cecum (Fig 2.13B), and large intestine (Fig 2.13C). In the large intestine, EcoHIV + morphine treated animals had significantly higher percentages of double positive CD4+CD8+ T-cells (p<.05) which have been shown to be highly activated, cytokine secreting cells within the gut.[184] B-cell percentage, as measured by CD19, was unchanged in the small intestine (Fig 2.13D), cecum (Fig 2.13E), or large intestine (Fig 2.13F). Monocytes populations

were examined in terms of CD11B+, CD11C+, or double positive populations. Similarly to T-cells, monocytes showed no changes in the small intestine (Fig 2.13G) or cecum (Fig 2.13H), but had a higher percentage of CD11B+CD11C+ double positive cells in the large intestine (Fig 2.13I, p<.05), which favors inflammatory cytokines secretion when increased in ratio over CD11B+ CD11C- macrophages.[176] Supporting this environment of pro-activation in the gut, higher levels of monocytes were observed that expressed CCR5, a proinflammatory marker which also is a receptor for HIV entry into cells in gut-isolated cells as well as systemically in blood (Fig 2.13J). At the time points examined, the gross loss of CD4 cells observed in HIV do not appear to occur in EcoHIV and there is no loss of macrophages to account for bacterial translocation. However, changes in CD4+CD8+ T-cells and CD11B+CD11C+ monocytes support a promotion of proinflammatory cytokines which has been shown to drive replication of HIV/EcoHIV.

As shown in Fig 2.13, systemic translocation of bacteria with morphine alone and EcoHIV+morphine occurred despite unchanged levels of macrophages and T cell subpopulations. Given the important role that macrophage phagocytosis plays in preventing systemic bacterial translocation, functional differences in the phagocytic activity of macrophages was examined. Studies have previously shown that morphine alone can cause deficiency in the phagocytic activity of macrophages,[185–187] so changes by EcoHIV and

EcoHIV+morphine were compared. Cells were pretreated overnight and incubated with GFP *E.coli* for 1hr to allow phagocytosis to occur and then were fixed and quenched to remove fluorescence outside of the cells. RAW macrophage cell line showed a noticeable difference in internalized bacteria when cultured with morphine and EcoHIV+morphine (Fig 2.14). Another macrophage cell line, J774, showed consistent results with Morphine, EcoHIV, and EcoHIV+morphine all showing less internalized bacteria as compared to saline treatment (Fig 2.15). This phagocytic deficiency in all three treatment groups was verified in primary peritoneal macrophages via fluorometry and confocal imaging of peritoneal primary macrophages (not shown). Overall, phagocytosis is reduced by morphine and EcoHIV for either *in vitro* or *in vivo* macrophages, which may contribute to lack of bacterial clearance and sustained systemic bacteremia.

Given the observed increase in systemic bacterial translocation combined with increase in activation markers and the lack of phagocytosis, the hypothesis moving forward was that inflammation would be apparent in both the gut and systemic compartments. An RNA array examining global analysis of inflammation was performed on total small intestinal tissue from 5 days post-infection as that is where most of the morphological changes were observed. Surprisingly, very few markers changed overall in morphine (Fig 2.16A) or EcoHIV (Fig 2.16B) when compared with placebo. In EcoHIV+Ms animals, a

greater number of markers changed to be over the 1.5-fold change threshold (Fig 2.16C and Table 2.2). Interestingly, a marker that was consistently reduced in morphine and EcoHIV+Ms was Lysozyme 2 (Fig 2.16D), which is secreted by macrophages and specialized Paneth epithelial cells within the gut to break down bacteria cell walls.[188,189] Next, supernatant from homogenized gut tissue was examined for cytokines levels. Similar to the RNA array, relatively few changes between treatment groups were observed. IL-6 showed no changes in the small intestine between placebo and EcoHIV+morphine (Fig 2.17A), however significant changes in the large intestine (Fig 2.17B). IL-17A showed no changes between placebo and EcoHIV+morphine in either small intestine (Fig 2.17C) or large intestine (Fig 2.17D). TNFα also had no change in the small intestine (Fig 2.17E) or large intestine (Fig 2.17F). Overall, the inflammation within the gut seemed to resolve with the bacterial translocation being gone at 5 days post-infection.

Systemically, at 5 days post infection a significant increase in IL-6 was observed within the liver of EcoHIV and EcoHIV+morphine treated animals, and EcoHIV+morphine animals had a significant increase over EcoHIV alone (Fig 2.18A). TNFα also showed significantly higher levels at this time point in EcoHIV infected and EcoHIV+morphine animals in liver homogenate above placebo treated animals (Fig 2.18B). Lung IL-6 levels trended to be higher but did not reach significance (Fig 2.18C) whereas TNFα levels were significantly higher in

EcoHIV+morphine animals and a significant increase in EcoHIV+morphine compared to EcoHIV infection alone (Fig 2.18D). Supernatant was examined from RAW 264.7 cells infected with EcoHIV as in the phagocytosis assay and found that IL-6 (Fig 2.18E) and TNFα (Fig 2.18F) were both significantly increased in EcoHIV infection and EcoHIV+morphine. Systemic inflammation, with elevated TNFα and IL-6 observed in the EcoHIV and morphine treated animals corroborates with observations demonstrated in HIV and IDU patients. Sustained systemic Inflammation has been shown to correlate with bacterial translocation and systemic replication of EcoHIV. Morphine in conjunction with EcoHIV infection shows higher levels of inflammation in liver and lung than EcoHIV infection alone.

Model: Transgenic models of HIV (Tg26 and Tat86)

To distinguish whether HIV proteins in the absence of infection could induce bacterial translocation, models using expression of HIV proteins were utilized, including transgenic animals for Tg26 (express all HIV genes except gag and pol) and Tat86 (full length Tat) as well as *in vitro* work with Tat. The exposure to HIV proteins in the transgenic animals is not controlled as it was in the infectious model, so morphine was implanted for shorter term (24 or 48hr).

In regards to bacterial translocation, Tg26 background mice showed similar levels of induction by morphine in both Tg26-/- and Tg+/- positive animals, implying that this background did not recapitulate the phenotype observed in

EcoHIV (Fig 2.19). Tat86 mice showed a modest amount of translocation in placebo treated animals, where previous results showed that wildtype placebo saw no detectible translocation (Fig 2.20). When Tat86 animals were given morphine pellets, this induced a large amount of bacterial translocation. Tat has been implicated in both endothelial and epithelial cells to modulate tight junctions at other locations,[123,125] and given the bacterial translocation observed in TAT86 mice subsequent experiments focused primarily on this transgenic model.

Tight junction integrity was examined as with the studies using EcoHIV. As discussed earlier, morphine was observed to cause a disruption of occludin (green) punctate staining at the boundary of the lumen and epithelial cells in the small intestine, shown here as yellow due to co-localization with F-actin (red) (Fig 2.21, upper left and right), which anchors the transmembrane protein occludin to the cell cytoskeleton with other intermediates.[20] In the placebo treated Tat86 background, no reduction in yellow co-localization was observed (Fig 2.21, lower left). However when Tat86 mice were treated with morphine a drastic reduction in yellow co-localization was observed compared with WT untreated animals (Fig 2.21, lower right). In the large intestine, results were again consistent with EcoHIV, with Tat86 background+morphine the only group showing a reduction in yellow co-localization compared with placebo (Fig 2.22, upper left and lower right). Combined, this implies that the Tat protein is likely playing a role in

57

disrupting the integrity of tight junctions which leads to bacterial translocation in both the Tat86 mice and EcoHIV infection.

Next, histology of the gut was visualized to see how Tat86 animals compared with EcoHIV infection. Morphologically, Wt+morphine and Tat86+placebo animals had minor changes in LP structure of the small intestine (Fig 2.23, upper right and lower left). However, Tat86+morphine animals had very severe effects in the small intestine with a phenotype that resembled what was observed in EcoHIV with blunted villi (Fig 2.23 lower right). In the large intestine, little to no change was observed with morphine, Tat86, or Tat86+morphine (Fig 2.24). With the changes observed in Tat86+morphine in the small intestine, this suggests that Tat86 and morphine may amplify each other's effects which may explain the high amounts of translocation observed.

To examine the direct effects of Tat on epithelial cells, a cell culture system was utilized that can measure the permeability between cells via electrical current impedance sensing, or ECIS. A reduction in impedance is correlated with a disruption of the tight junctions between the cells. Caco2 cells were cultured to confluence on ECIS plates and incubated with morphine, Tat, or gp120 which has also been shown to alter tight junctions in the gut.[126] At 7 hr following addition of Tat or gp120 to the cultures, a 10% reduction in barrier integrity was observed by Tat and gp120, and a 15% reduction when Tat and gp120 were combined with morphine (Fig 2.25A). To demonstrate the

importance of TLRs in this process, lipotechoic acid (LTA) was added to the culture, which activates TLR2. In IEC-6 cells, a modest reduction in resistance was observed when LTA alone was given (Fig 2.25B, green). Interestingly, with Tat and morphine together in the culture, LTA lead to a greater disruption (Fig 2.25B, red). While this difference is relatively small, the epithelial cells of the gut are constantly exposed to bacteria with LTA (TLR2 agonist) and LPS (TLR4 agonist) and this effect likely gets amplified over time. Overall, these results show that Tat can have a direct effect on epithelial tight junctions, especially when combined with morphine.

2.5.   Discussion

Altogether, results using both an infectious model and an HIV protein transgenic model imply that HIV can act both indirectly through inflammation as well as directly via secreted proteins to alter integrity of tight junction proteins leading to the observed increase in bacterial translocation. Morphine exacerbates both bacterial translocation and tight junction integrity by increasing the inflammation observed. Additionally, morphine alters the sensitivity of epithelial cells to TLR that play a role in modulating tight junctions as well diminishing macrophage phagocytosis which leads to bacteria accumulating in systemic compartments such as the liver (Fig 2.26).

A combination of EcoHIV infection and morphine leads to an exacerbated inflammatory state compared to EcoHIV infection alone, likely by influencing bacterial translocation and increasing inflammatory cytokines. Bacterial translocation from the gut has been shown to directly correlate with inflammation that drives HIV replication in long term HIV-infected nonprogressors despite lower amounts of LPS in their serum at levels virtually identical to control patients.[63] LPS as a biomarker has also been highlighted as a vital factor in what drives SIV to be pathogenic in Rhesus Macaques as compared to natural hosts who do not develop AIDS.[139]

Given this tight link between bacterial translocation and HIV replication, it should come as no surprise that increasing LPS further would worsen HIV pathogenesis. Previous studies have shown that morphine alone not only disrupts the physical barrier in the gut provided by epithelial cells, but also alters the function of immune cells by reducing the clearance of bacterial products by macrophages,[79,97,187] leading to an overt increase in the amount of systemic bacterial translocation. This effect by opioids has been suggested in limited HIV studies in heroin abusers.[4] While research has long suggested that HIV has a faster progression to AIDS with substance abuse, it has been difficult for epidemiological studies to validate this on a population level.[157] This deficiency highlights the major difficulties with studying drug abuse in a human population, especially among HIV patients, and the lack of animal models to study these

interactions has limited the progression to understanding the interactions between HIV and morphine. Although there have been a number of studies on effects of morphine on SIV infection in macaques,[158,190–193] to our knowledge early pathogenesis within the gut has not been investigated. In order to take advantage of genetic tools and low cost of mice, an infectious model of HIV was advantageous to combine with an established model of opioid abuse in order to overcome limitations in the field.

Translocation occurred in both EcoHIV infected and Tat86 transgenic models of HIV in mice, and each was also amplified by morphine. At 2 days post-infection, EcoHIV+morphine showed the highest amount of bacterial translocation, where 5-days infection did not show translocation. A live CFU assay was utilized along with the RAW blue assay to account for both gram positive and gram negative bacteria, as opposed to serum LPS which only accounts for gram negative bacteria. Translocation occurred highest in the liver, which suggests the bacteria is traversing via the portal circulation following a lack of clearance in the intestine and mesenteric lymph node. MORKO mice treated with morphine, EcoHIV, or EcoHIV+morphine showed a reduced amount of translocation at 2 days post-infection indicating that morphine plays a direct role in exacerbating this pathology. Interestingly, TLR4 knockout mice, which lack a functional receptor that recognizes LPS, also had drastically reduced translocation at 2 days post-infection. This supports the notion that LPS is

playing a direct role in the pathogenesis, likely due to sustained activation in the presence of morphine.[98]

The clearance of bacteria from systemic compartments observed in EcoHIV treated animals at 5 days infection contrasts from HIV and SIV, where LPS is observed in all stages of uncontrolled infection including early, late, and AIDS phases.[63,121,194] However, time points this early in HIV pathogenesis have not been examined which could account for the difference and it is unknown whether disruption of gut homeostasis at early stages happens stably or in phases with the ongoing pathogensis of HIV. Gut CD4 loss has been suggested to contribute to microbial translocation in SIV,[118] which was not observed at the time points examined in this model and could be a reason for this conflict. Given that this model allows us to look at very early stages of disease, EcoHIV is beneficial for studying the mechanisms of early HIV pathogenesis of HIV in the context of drugs of abuse, which has been nearly impossible to study due to the unknown infection status of individuals. This model may also give a resolution to mechanisms at early time points not possible with HIV-infected humans.

While translocation was cleared at 5 days post-infection in the EcoHIV model, gut pathology and inflammation was still apparent which suggests that the translocation had a persistent effect and could play a role in HIV pathogenesis even after it abates. A consistent reduction was observed in punctate staining for the tight junction protein occludin at the boundary of the lumen and epithelial

cells of animals treated with morphine in both EcoHIV and Tat86 mice. This is likely an additive effect of inflammation and HIV proteins in the EcoHIV mice, however that Tat86 mice highlight the ability of HIV Tat to directly disrupt the tight junctions and amplify the effects that morphine has on epithelial cells by increasing TLR expression.

In addition to pathology in the gut, this study proves that EcoHIV and morphine have a negative effect on the ability of peritoneal macrophages to perform phagocytosis, which plays a major role in the clearance of translocated bacteria. This coincides with previous data that showed morphine alone causes a deficiency in phagocytosis.[185–187] A breech in epithelial barrier is not enough for translocation to become systemic, so a decrease in phagocytosis likely contributes to the bacterial translocation observed in the liver.

One major difference between EcoHIV and HIV pathogenesis is the lack of early CD4+ T-cell depletion within the gut which have been observed at acute stages of HIV infection.[80,195] Prolonged time points in this model are needed to resolve this difference, as this study included time points that were very early relative to what has been examined in HIV or SIV studies. Thus, this model provides flexibility to study time points which are unattainable or impractical to study in HIV or SIV infections. Examining CD4 cells at a deeper resolution, depletion of Th17 cells have been suggested to be the predominant cause for the observed microbial translocation following SIV infection in Rhesus Macaques

63

since Th17 cell depletion is not observed in nonprogressors.[118] Recent data from our lab suggests that morphine alone can induce a deficiency in the Th17 response (communicated), which supports the results in this study. Future work will examine the effect of morphine on CD4 skewing in EcoHIV infection with an emphasis on the role of Th17 cell depletion and microbial translocation.

Despite clearance of bacteria, cytokines TNFα and IL-6 were increased to high levels in EcoHIV treated animals in combination with morphine in both liver and lung at day 5 post-infection. This inflammation can act to drive systemic HIV replication and drive HIV into long-lived cellular reservoirs such as macrophages, where it can continue promoting secretion of inflammatory molecules in the absence of further translocation.   HIV and opioid abuse have been shown to cause more severe neurocognitive deficits due to immune dysfunction,[191,196] so morphine treatment was investigated in this model to test for inflammation in the brain. Indeed, higher expression of inflammatory cytokines was observed in the brain tissues of EcoHIV infected mice in combination with morphine 30 days post-infection consistent with inflammation playing a significant role in long-term neurocognitive defects. While neurocognitive defects are commonly observed in IDU HIV patients, it is impossible to study the direct effects of opioids and how they contribute to neurological effects in people. Comorbidities in human IDU, such as nutritional deficiencies, stress, or lack of medical care, make an animal model to study the mechanism leading to neurocognitive defects extremely

desirable.   HIV patients who abuse substances have much lower adherence to medications so, despite reasonable therapeutics being available, they are more susceptible to negative consequences of uncontrolled infection.[197] EcoHIV as an animal model provides a great opportunity to study HIV with drugs of abuse in combination with antiretroviral therapies to finally tease apart the mechanisms of substance abuse with the comorbidities associated with aberrant lifestyles. Future work with EcoHIV will examine whether the inflammation observed in the brain is instigated by the original translocation events observed or is an independent event induced by morphine and EcoHIV infection.

Overall, this study showed that HIV, both directly via proteins and indirectly with infection via inflammation, in combination with morphine disrupts the host gut homeostasis leading to bacterial translocation at early stages in HIV pathogenesis. The experimental design utilized examines a very early time point of HIV pathogenesis that has not been examined with other models; for instance it is not known how early translocation occurs in HIV infection or once translocation is established whether it is constant. Thus, the differences between the HIV infection models may be resolved better with experimental manipulation such as utilizing different lengths of EcoHIV infection. For instance, while bacterial clearance was observed as a difference between HIV infections, this may be resolved by different dosing patterns of morphine such as giving morphine after infection or using a time course which includes withdrawal. The

EcoHIV infection model provides a useful avenue for studying HIV and drugs of abuse where other models have fallen short as it utilizes the mouse as a system and permits the use of genetic knockouts in an infectious model of HIV. Future studies with this model will be used to further elucidate the mechanisms underlying the interactions between HIV and drugs of abuse at early stages of disease and ideally test therapeutics to prevent these side effects.
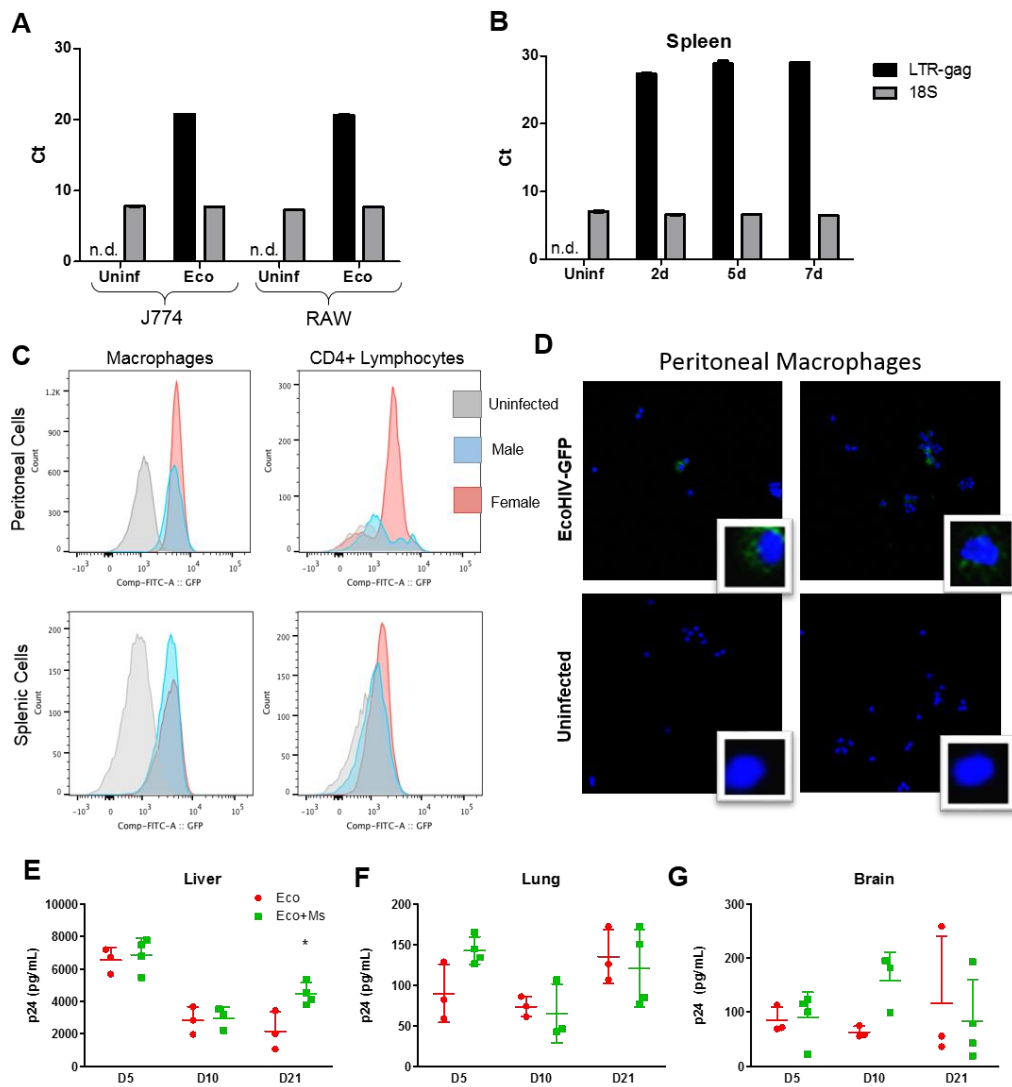
Fig 2. 1 Establishment of Systemic EcoHIV infection in mice

EcoHIV infects both *in vitro and in vivo*, but morphine does not alter viral burden. QPCR was performed on EcoHIV infected RAW/J774 cells (A) or spleens from C57BL/6 mice (B) to look for HIV LTR-gag, where expression was observed except in untreated animals. Peritoneal or spleen cells were harvested from Eco-GFP infected mice and analyzed for infected cells by FACS (C), showing a positive shift in peak from uninfected, or microscopy (D), which show positive green staining in infected cells (Magnification 100X). P24 ELISA was performed on liver (E), lung (F), or brain (G) of infected mice, which show detectible levels at all timepoints and a significant difference between EcoHIV+morphine and EcoHIV at D21 in the liver. *P<.05
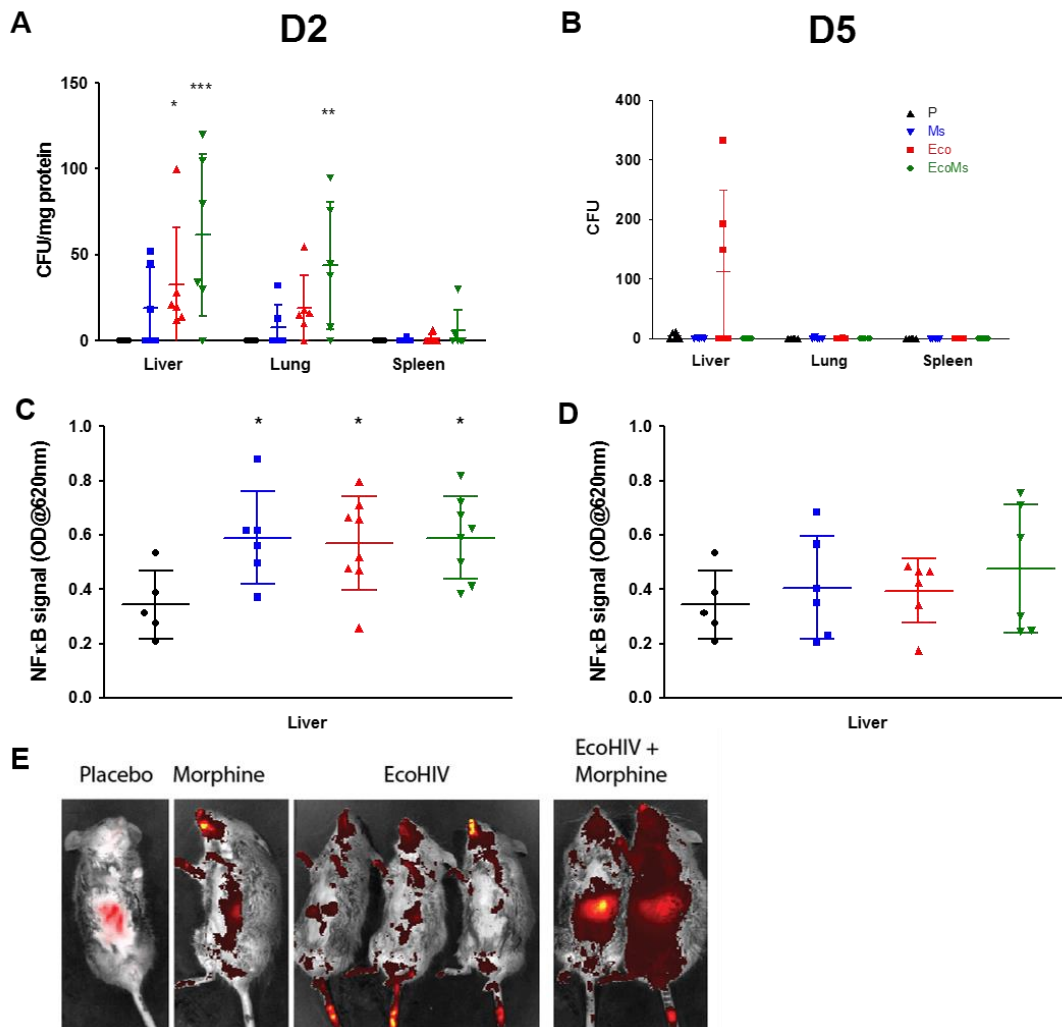
Fig 2. 2 Bacterial translocation occurs early in EcoHIV infection and is exacerbated by morphine.

Liver, lung, or spleen was homogenized and cultured on blood agar plates in aerobic conditions to count live CFUs. Mice were infected either 2 days (A), which showed significant translocation to liver and lung in EcoHIV+ morphine and to liver in EcoHIV, or 5 days (B), which showed no significant translocation. Homogenate from liver was tested, using RAW blue cells (Invitrogen) which express SEAP on NFκB promoter upon stimulation by PAMPs, at 2 days (C) and 5 days (D) which validated the translocation results in (A) and (B) for liver. (E) Mice infected for 2 days were gavaged with Rhodamine-dextran 4 hr prior to Xenogen imaging. *P<.05

Small Intestine - Occludin
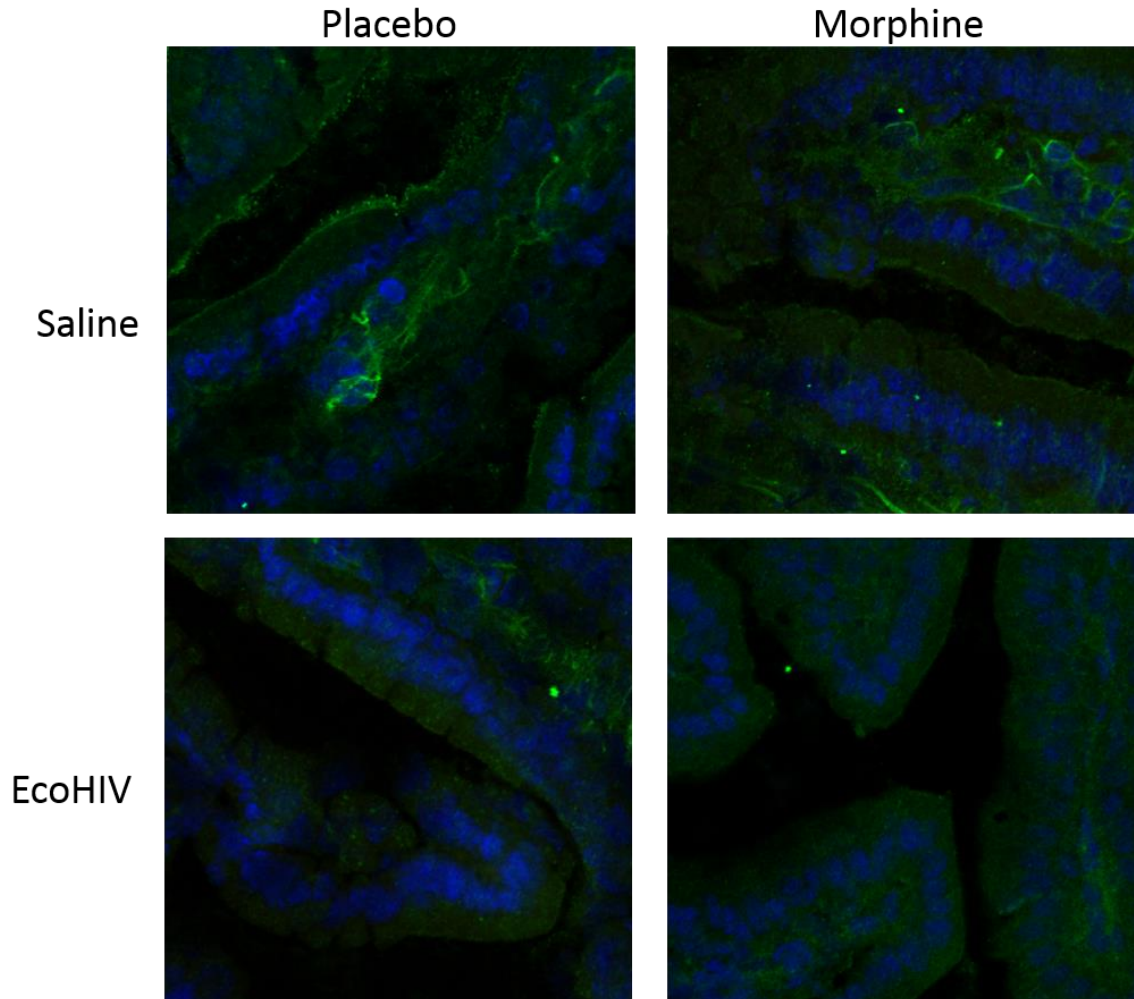
Fig 2. 3 Tight junction protein occludin distribution is disrupted by EcoHIV and morphine in small intestine at 5 days post-infection

Frozen distal small intestine (ileum) was stained with Occludin (green) and dapi (blue, nuclei). EcoHIV (lower left panel) and morphine (upper right panel) each show reduction in the punctate occludin staining between the lumen (black) and the epithelial boundary. EcoHIV+morphine (lower right panel) shows representative picture of drastic reduction in punctate occludin staining. Magnification: 400X

Large Intestine - Occludin
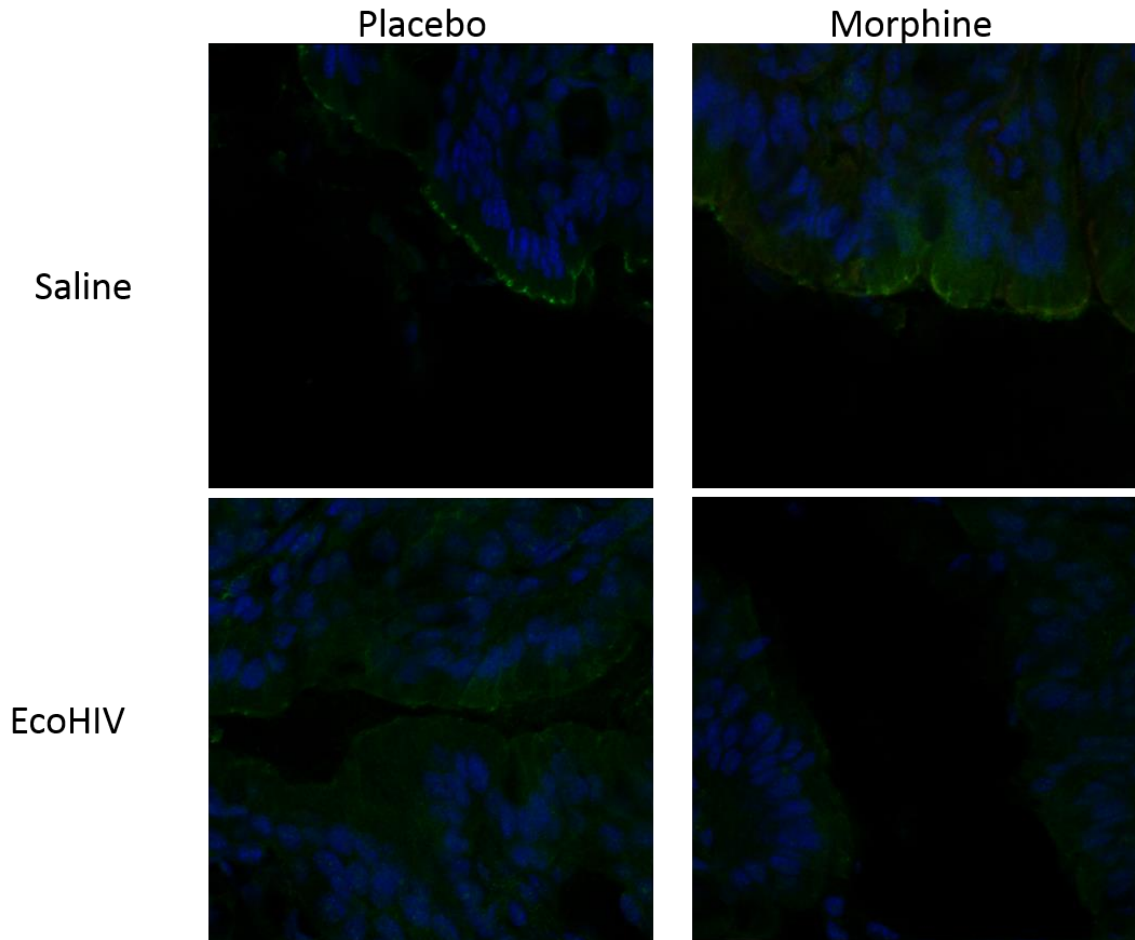
Fig 2. 4 Tight junction protein occludin distribution is disrupted by EcoHIV and morphine in large intestine at 5 days post-infection

Frozen distal small intestine (ileum) was stained with Occludin (green) and dapi (blue, nuclei). EcoHIV and morphine alone did not induce changes, however EcoHIV+morphine (lower right panel) shows representative picture of drastic reduction in punctate occludin staining between the lumen (black) and the epithelial boundary. Magnification: 400X
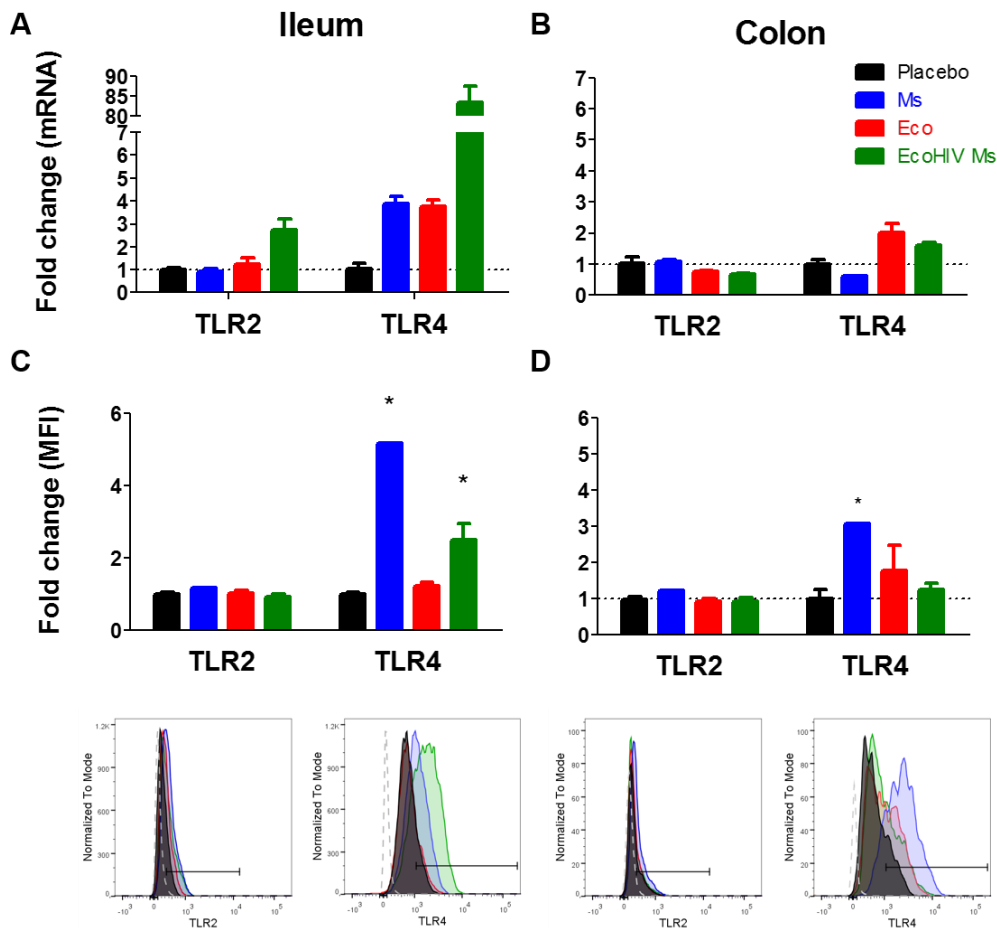
Fig 2. 5 Epithelial expression of TLR2 and 4 increases in both small and large intestine at 5 days post-infection.

Epithelial cells were isolated and either processed for RNA or fixed and stained for TLR2 and TLR4 with conjugated antibodies and detected with flow cytometry. (A) Small intestine showed above a 2-fold increase in TLR2 expression in EcoHIV+morphine and in TLR4 expression in morphine, EcoHIV, and EcoHIV+morphine treatments. (B) Large Intestine showed a 2-fold increase in TLR4 expression in EcoHIV and EcoHIV+morphine treatments. (C) MFI of small intestine TLR2 showed no change while TLR4 had significantly higher levels in morphine and EcoHIV+morphine animals. Lower panel shows representative FACS plots used for MFI calculation of TLR2/4 expression for ileum. (D) MFI of large intestine TLR2 showed no change while TLR4 had significantly higher levels in morphine only. Lower panel shows representative FACS plots used for MFI calculation of TLR2/4 expression for colon. *p<.05

71
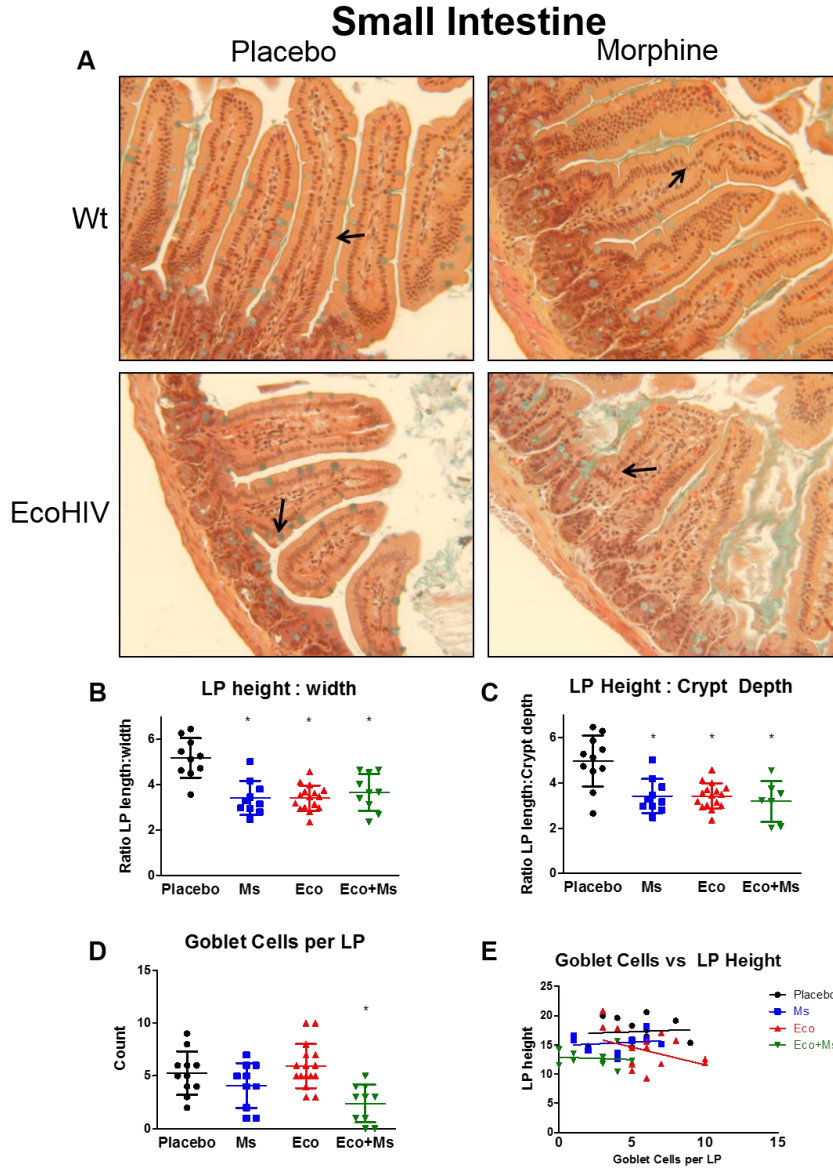
Fig 2. 6 Small intestine shows morphology changes with EcoHIV and morphine alone or in combination at 5 days post-infection

(A)Distal small intestine was stained with Hematoxylin (cell counter stain, brown), Alcian Blue (goblet cells, blue), and Saffron (connective tissue, yellow). Small intestine sections were measured for LP length, LP width, and crypth depth. Morphine, EcoHIV, and EcoHIV+morphine showed a decrease when compared by ratios of LP length:width (B) or LP length:crypt depth (C). Goblet cells showed a decreased count per LP in EcoHIV+morphine (D) and no correlation with count versus LP length was found (E). *p<.05. Magnification: 100X

72

Wildtype - Large Intestine

A

Placebo   Morphine

Wt

EcoHIV

B LP Depth

C Goblet Cells

D Goblet area vs LP depth
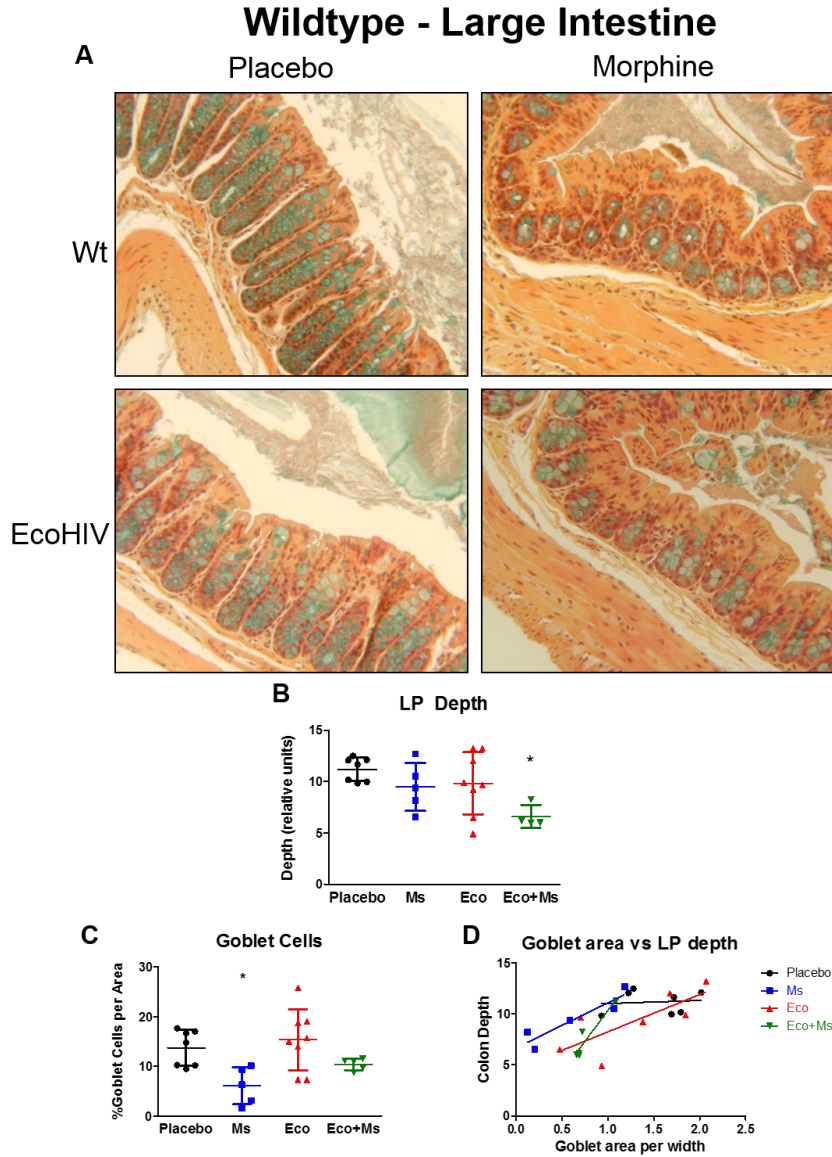
Fig 2. 7 Large intestine shows morphological changes only in EcoHIV+morphine at 5 days post-infection

(A)Large intestine was stained with Hematoxylin (cell counter stain, brown), Alcian Blue (goblet cells, blue), and Saffron (connective tissue, yellow). (B) Large intestine sections were measured for LP depth, where only EcoHIV+morphine showed a decrese. Goblet cells showed a decreased count per LP in morphine (C) and a positive correlation with count versus LP depth implying EcoHIV+Ms have fewer goblet cells due to a shorter depth (D). *p<.05. Magnification: 100X

A

Beclin-1

B
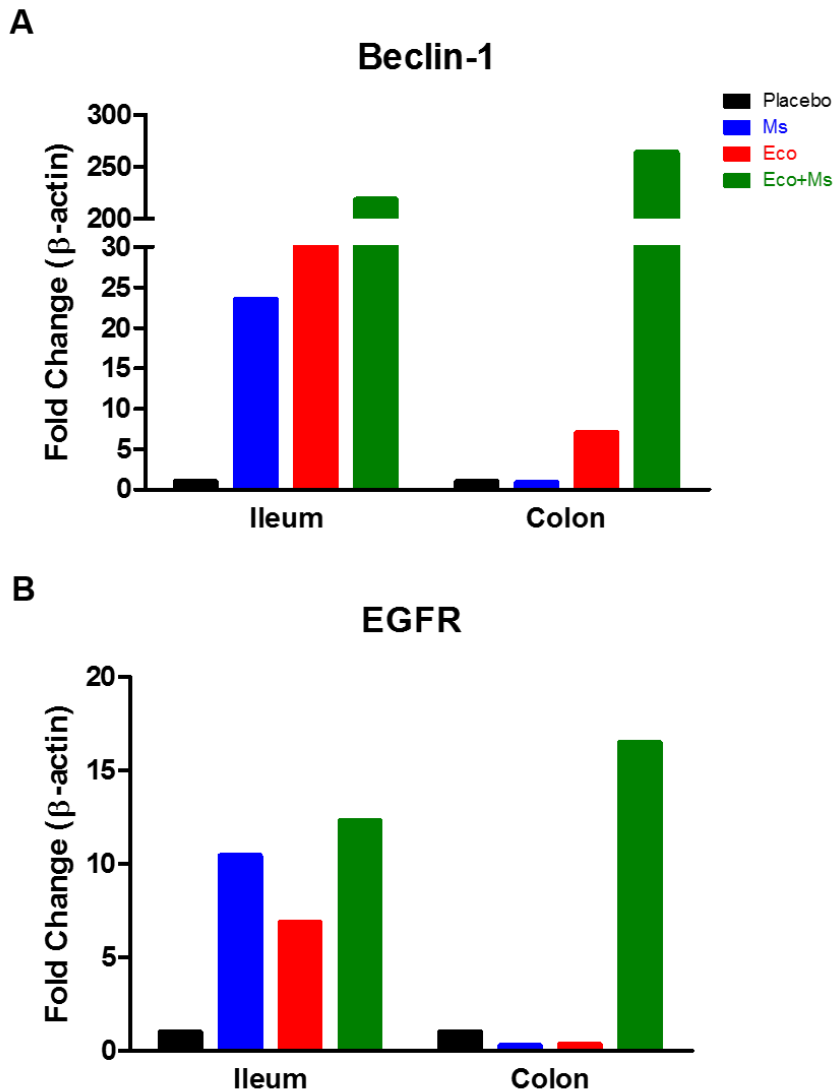
EGFR

Fig 2. 8 Stress markers are increased in epithelial cells of both small and large intestine at 5 days post-infection

Changes were examined in Beclin-1, a marker of autophagy, and EGFR, a growth promoter, which are both known to be upregulated in response to damage. (A) Beclin-1 expression increases with morphine and EcoHIV treatments in small intestine, and drastically higher in EcoHIV+morphine in both small and large intestine. (B) Similarly, EGFR expression increases with morphine, EcoHIV, and EcoHIV+morphine treatments in small intestine, and increases large intestine expression in EcoHIV+morphine only.

74

2 days infection

A

MORKO

MORKO - Small Intestine

B Placebo   Morphine

Wt
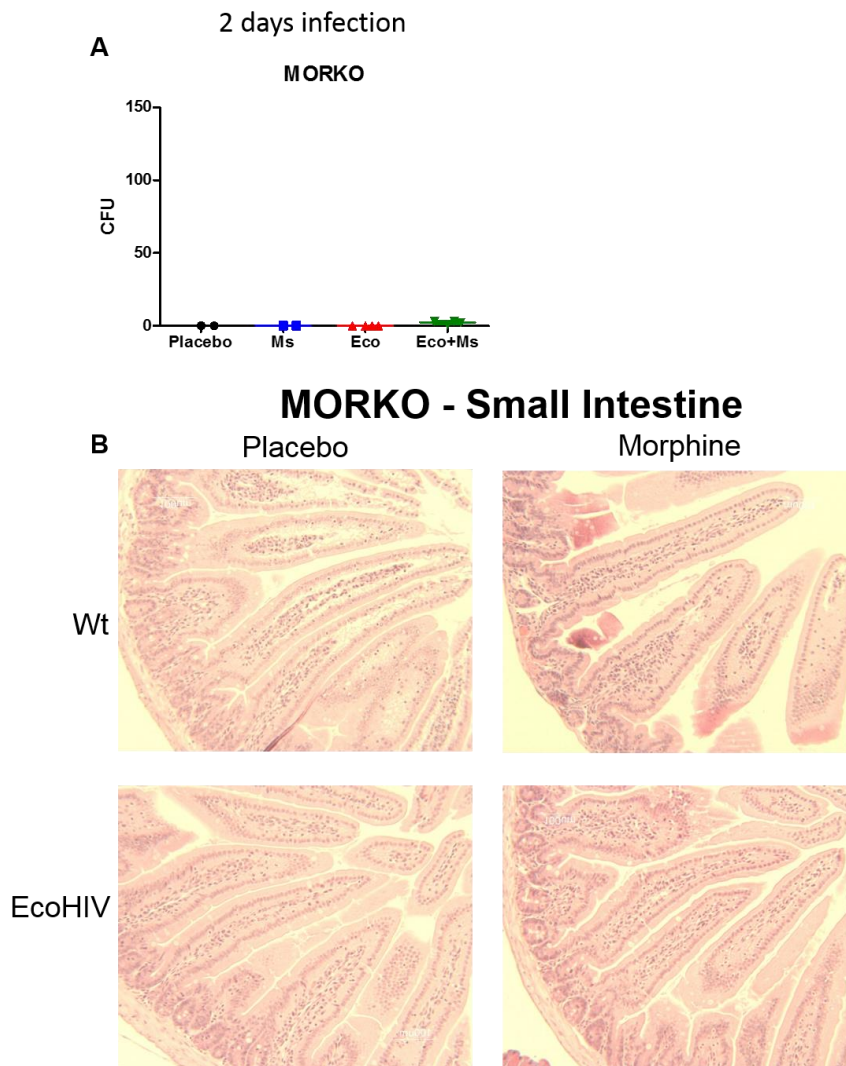
EcoHIV

Fig 2. 9 MORKO mice show a protection from bacterial translocation and morphological changes from EcoHIV and morphine in small intestine at 5 days post-infection

(A)Bacterial translocation was performed on the livers of mice at 2 days post-infection when translocation was observed in wildtype animals; none was observed in MORKO. (B) H&E staining shows that MORKO protects from morphological changes in the small intestine observed in wildtype animals. Magnification: 100X

MORKO - Large Intestine

Placebo   Morphine
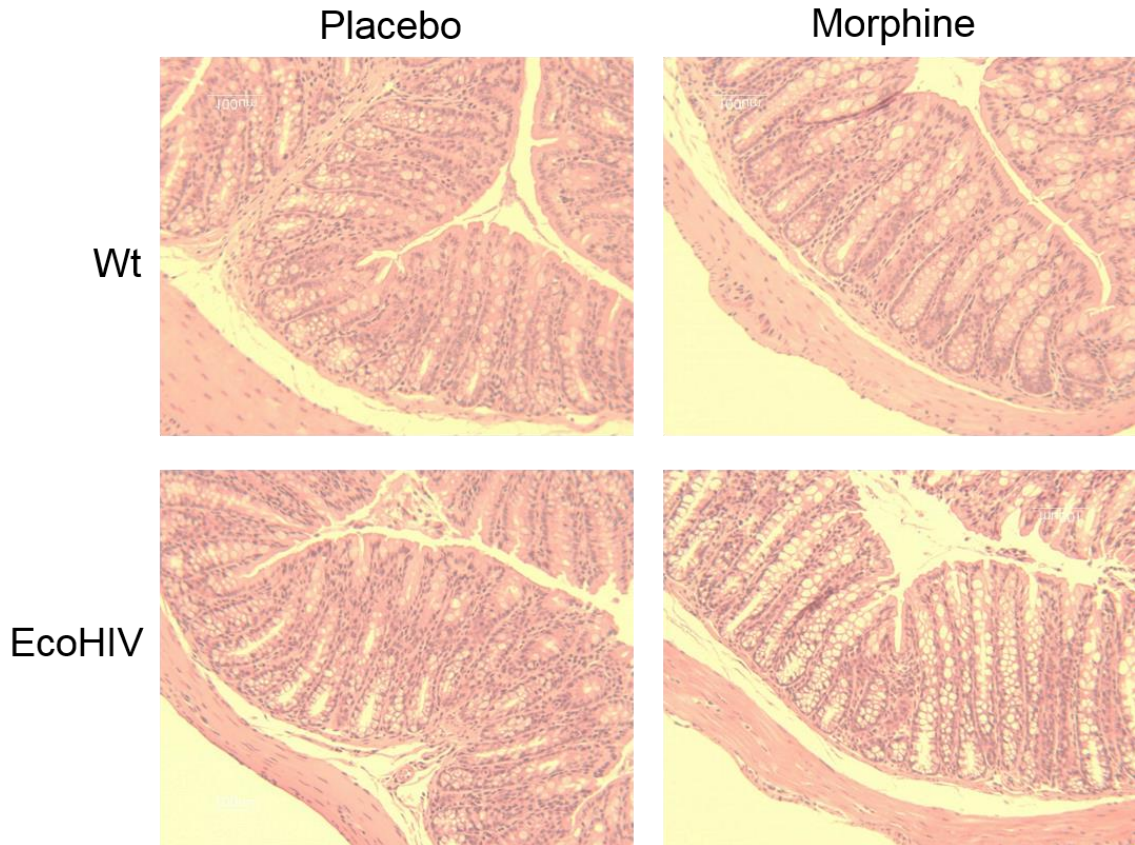
Fig 2. 10 MORKO protects from morphological changes by EcoHIV and morphine in large intestine at 5 days post-infection

H&E staining shows that MORKO protects from morphological changes in the large intestine observed in wildtype animals. Magnification: 100X

A
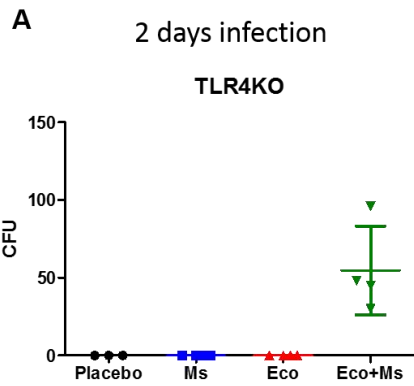
2 days infection

TLR4KO - Small Intestine
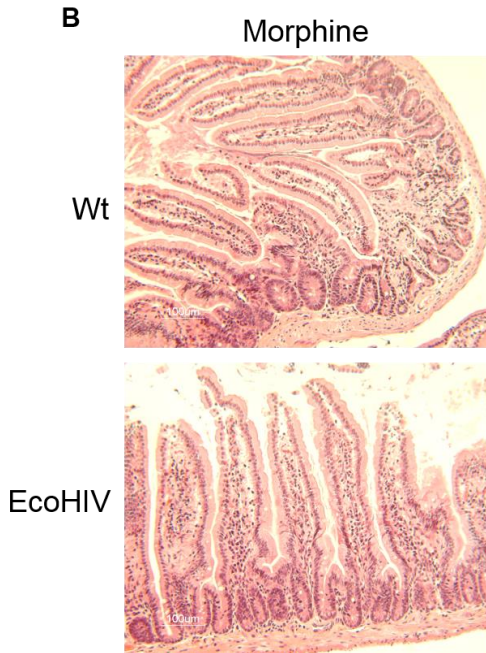
Fig 2. 11 TLR4KO mice show protection from bacterial translocation and morphology changes by EcoHIV and morphine in small intestine at 5 days post-infection

(A)Bacterial translocation was performed on the livers of mice at 2 days post-infection when translocation was observed in wildtype animals; none was observed in TLR4KO. (B) H&E staining shows that TKR4KO protects from morphological changes in the small intestine observed in wildtype animals. Magnification: 100X

TLR4KO - Large Intestine

Morphine

Wt
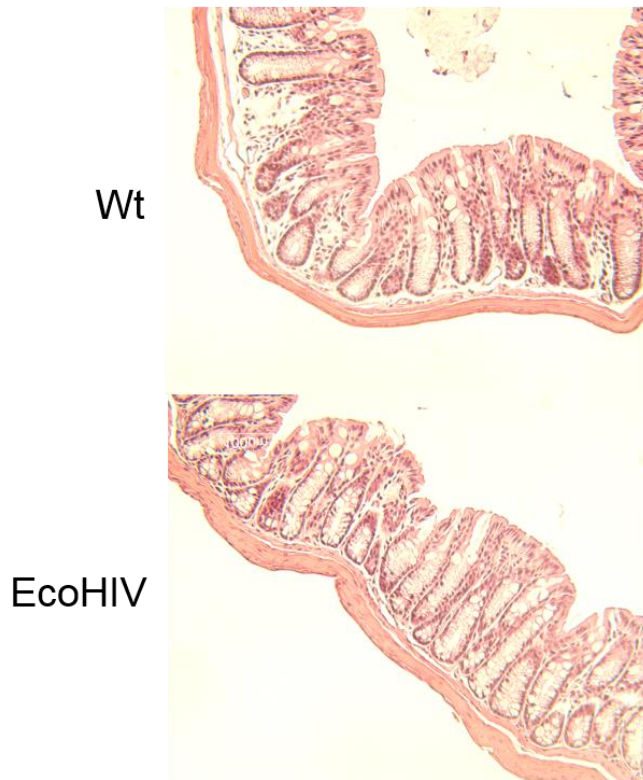
EcoHIV

Fig 2. 12 MORKO protects from morphological changes by EcoHIV and morphine in large intestine at 5 days post-infection

H&E staining shows that MORKO protects from morphological changes in the large intestine observed in wildtype animals in EcoHIV+morphine animals. Magnification: 100X
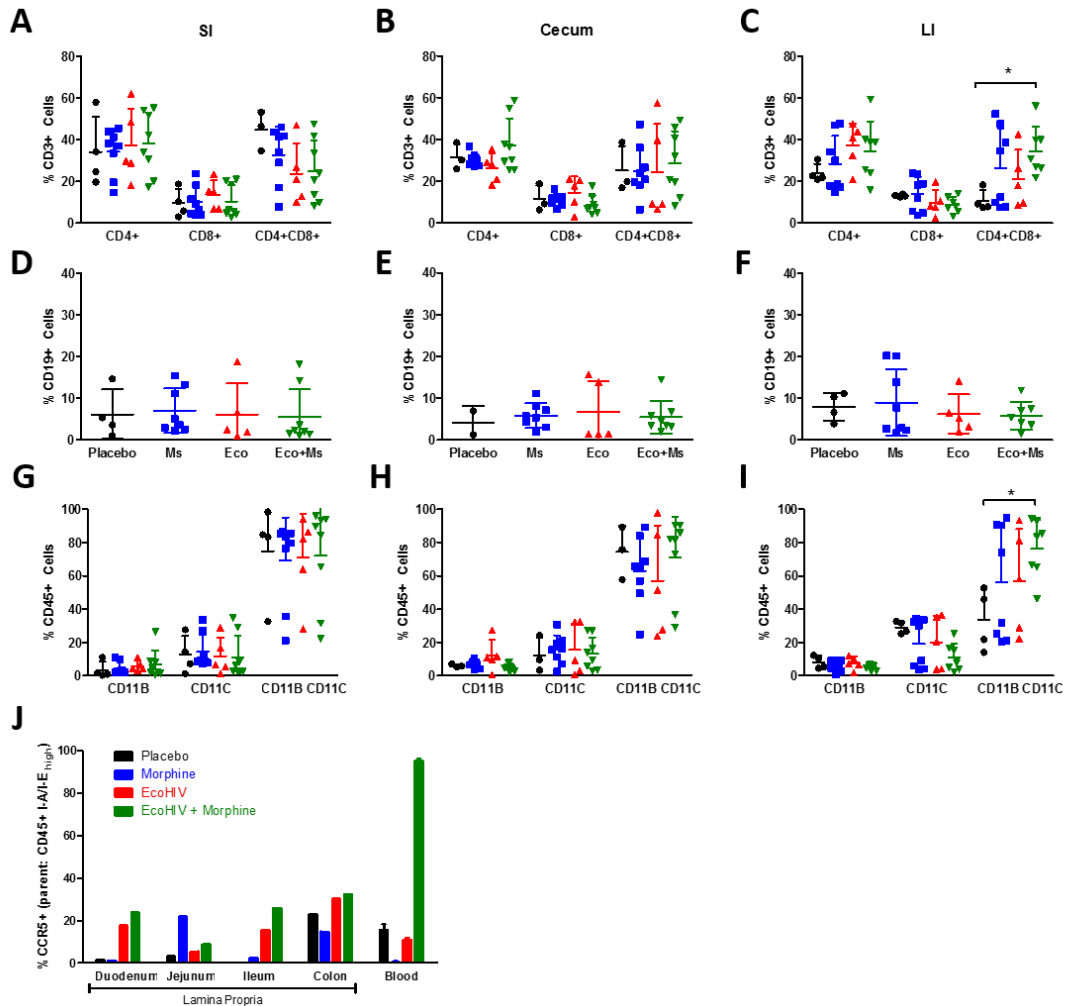
Fig 2. 13 EcoHIV with morphine does not greatly alter proportions of immune cells within the gut at 5 days post-infection.

Gut cells were collected from homogenized distal SI (A,D,G), Cecum (B,E,H), or colon (C,F,I) and stained for FACS analysis. CD3+ T-cells were gated and values of CD4, CD8, or CD4/CD8 double positive were examined (A,B,C), with the only significant change in DP cells being higher in morphine, EcoHIV, and EcoHIV+morphine. CD19+ B-cells were examined as a percentage of live cells (D,E,F) and no significant change was observed. CD45+ monocyte cells were gated and values of CD11B, CD11C, or CD11B/CD11C double positive were examined (G,H,I), with the only significant change in large intestine DP cells in morphine, EcoHIV, and EcoHIV+morphine. Cells were gated for CD45+ and MHCII high to see CCR5 expression in macrophages, which saw trending increases at all locations, most notably in EcoHIV+morphine. *p<.05

79

RAW macrophage cell line
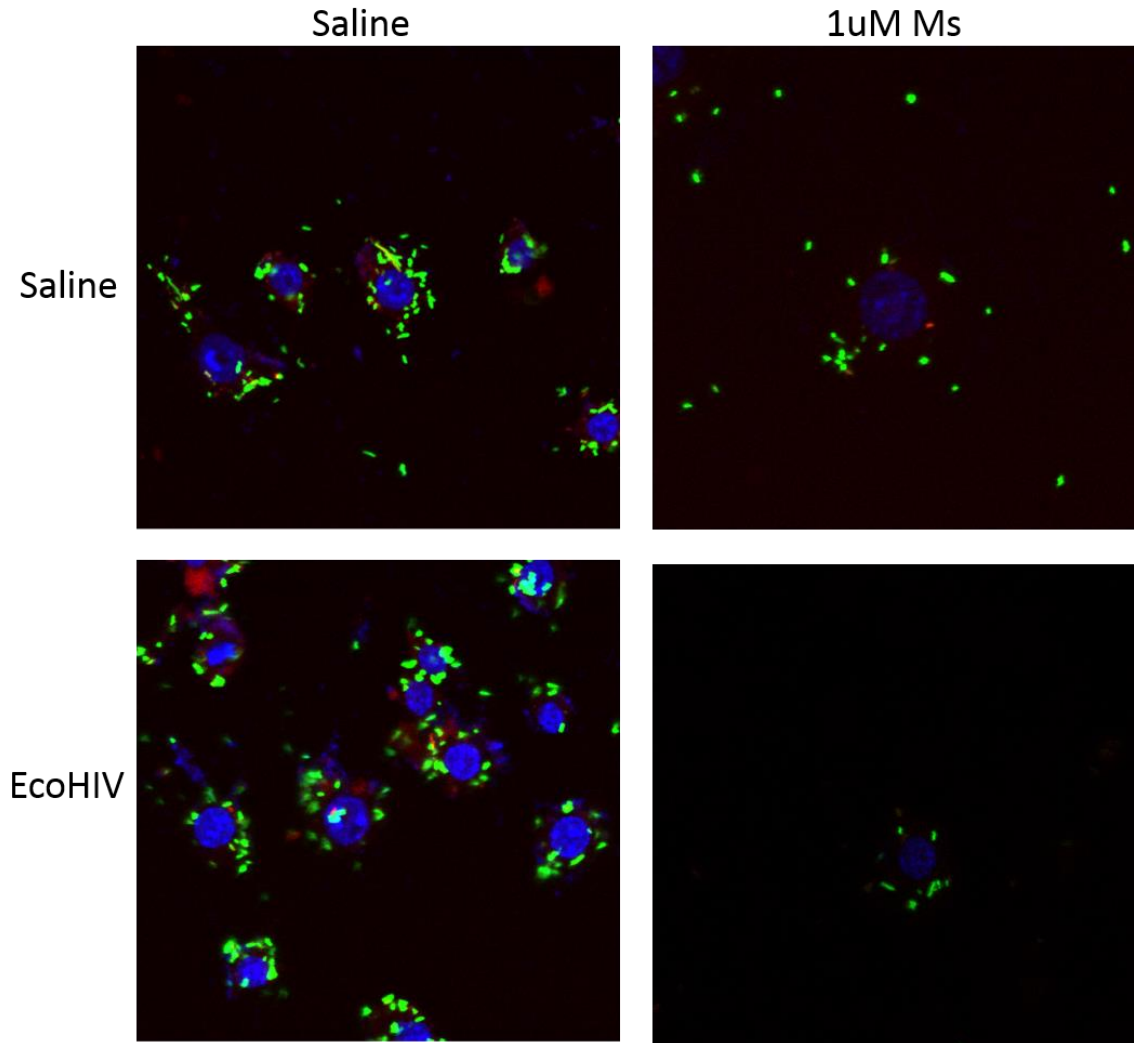
Fig 2. 14 RAW macrophages show a reduced capacity for phagocytosis with EcoHIV and morphine

Cells were incubated with GFP-*E.coli* (green), following which wells were quenched so that any green observed is intracellular. Morphine (upper right) and EcoHIV+morphine (lower right) both show a reduced amount of bacteria per cell. Magnification: 400X
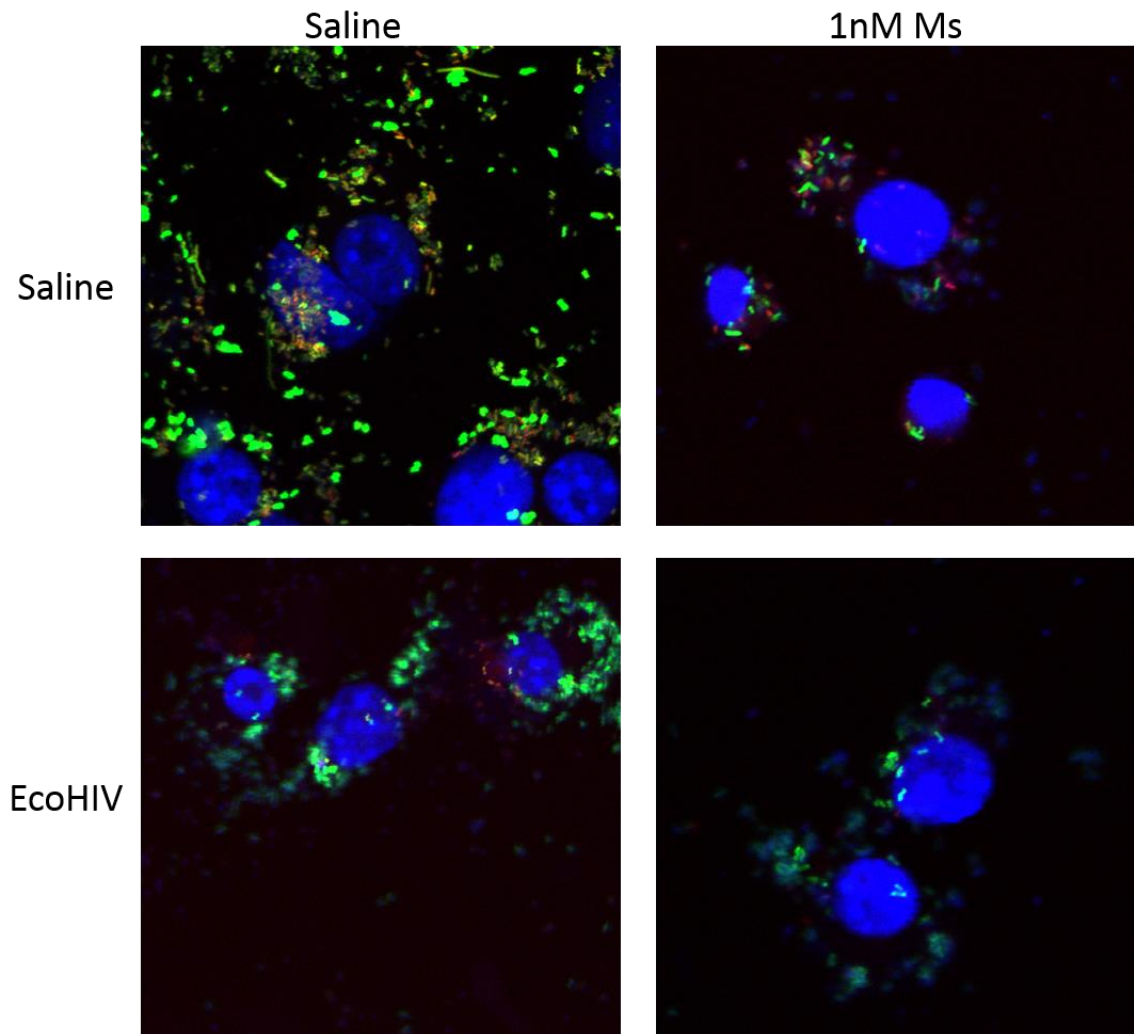
Fig 2. 15 J774 macrophages show a reduced capacity for phagocytosis with EcoHIV and morphine

Cells were incubated with GFP-*E.coli* (green), following which wells were quenched so that any green observed is intracellular. Morphine (upper right), EcoHIV (lower left), and EcoHIV+morphine (lower right) all show a reduced amount of bacteria per cell. Magnification: 400X
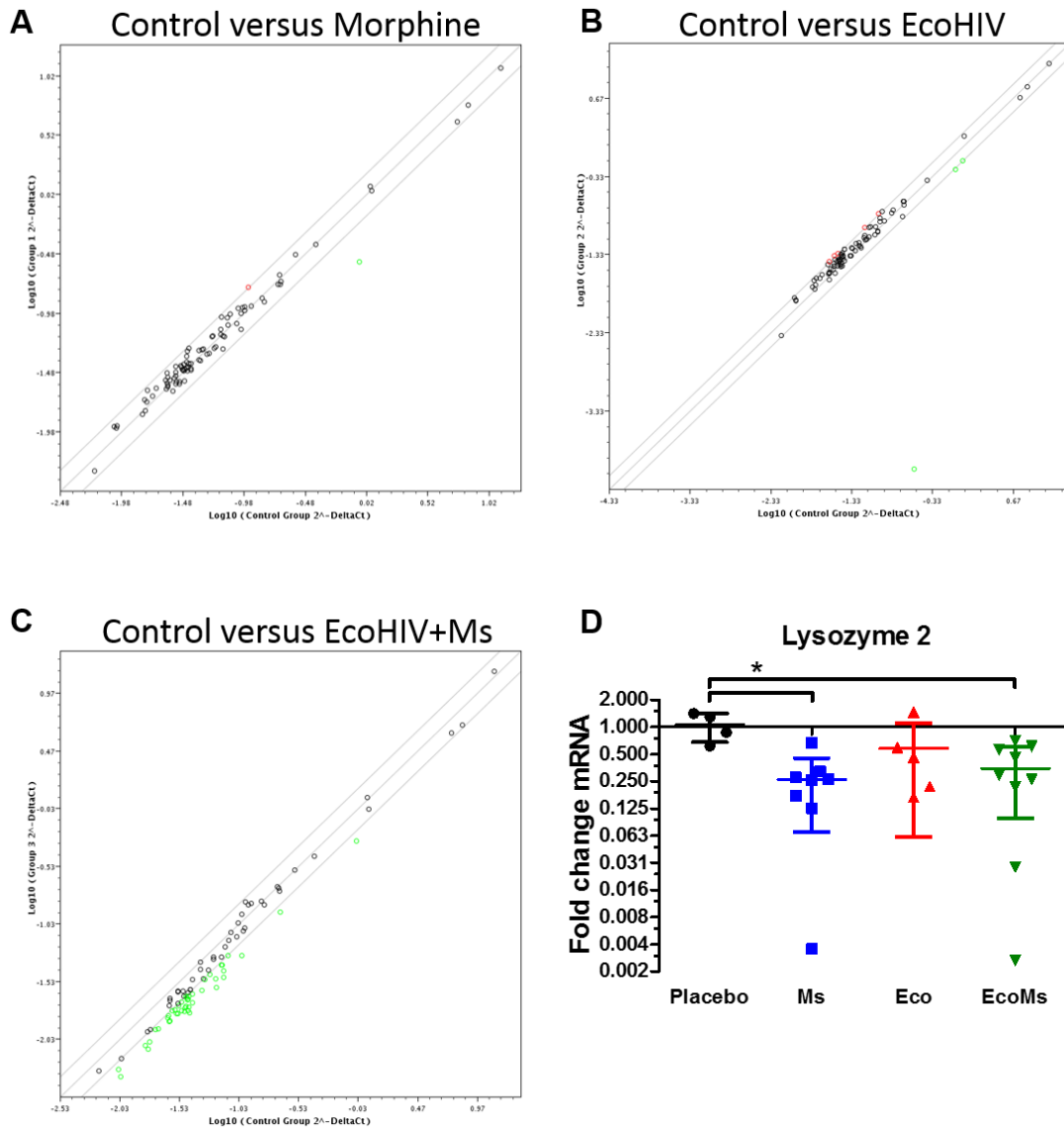
Fig 2. 16 EcoHIV (5 days post-infection) and morphine induce few global changes observed in RNA expression from small intestine aside from Lysozyme

RNA array was run with adaptive and innate immune markers on global small intestine RNA pooled from treatment group animals (5 days post EcoHIV infection). Morphine (A) and EcoHIV (B) showed few changes from control. EcoHIV+Ms showed a greater shift in markers that were downregulated (C). Total changes are summarized in Table 2.2; lysozyme2 was a common thread. (D) Lysozyme2 expression was verified in individual animals and found to be significantly downregulated in both morphine and EcoHIV+morphine. $P<.05$

82

Table 2. 2 RNA array identified genes altered >1.5 fold change vs placebo

Gene	Morphine	EcoHIV	EcoHIV+morphine
Fasl			-2.2925
Il6			-2.2925
MGDC			-2.139
Cd40lg			-2.1242
Tlr7			-2.1242
Il17a			-2.095
Rag1			-1.9957
Tnf			-1.9957
Tlr3			-1.9819
Ifnb1			-1.9547
Ifng			-1.875
Il1a			-1.875
Il4			-1.875
Il2			-1.8621
Il5			-1.8621
Tbx21			-1.8621
Ifna2			-1.8492
Tlr6			-1.8492
Lyz2	**-3.2038**	**-1.5758**	**-1.8365**
Cd80			-1.8238
Crp			-1.8238
Nlrp3			-1.8112
Ccr8			-1.7862
Foxp3			-1.7495
Mx1			-1.7374
Il10			-1.7135
Il23a			-1.6782
Ccr4			-1.6666
Gata3			-1.6551
Ccl5			-1.6437
Csf2			-1.6437
Cd40			-1.6323
Ccr5			-1.621
Nod1			-1.6098
Tlr4			-1.6098
Cd86			-1.5987
Ccl12			-1.5877
Tlr8			-1.5767
Ccr6			-1.5658
Tlr2			-1.5658
Mbl2			-1.555
Il1b			-1.5443
Slc11a1			-1.5336
Il1r1			-1.5125
Hsp90ab1		-1.5116	
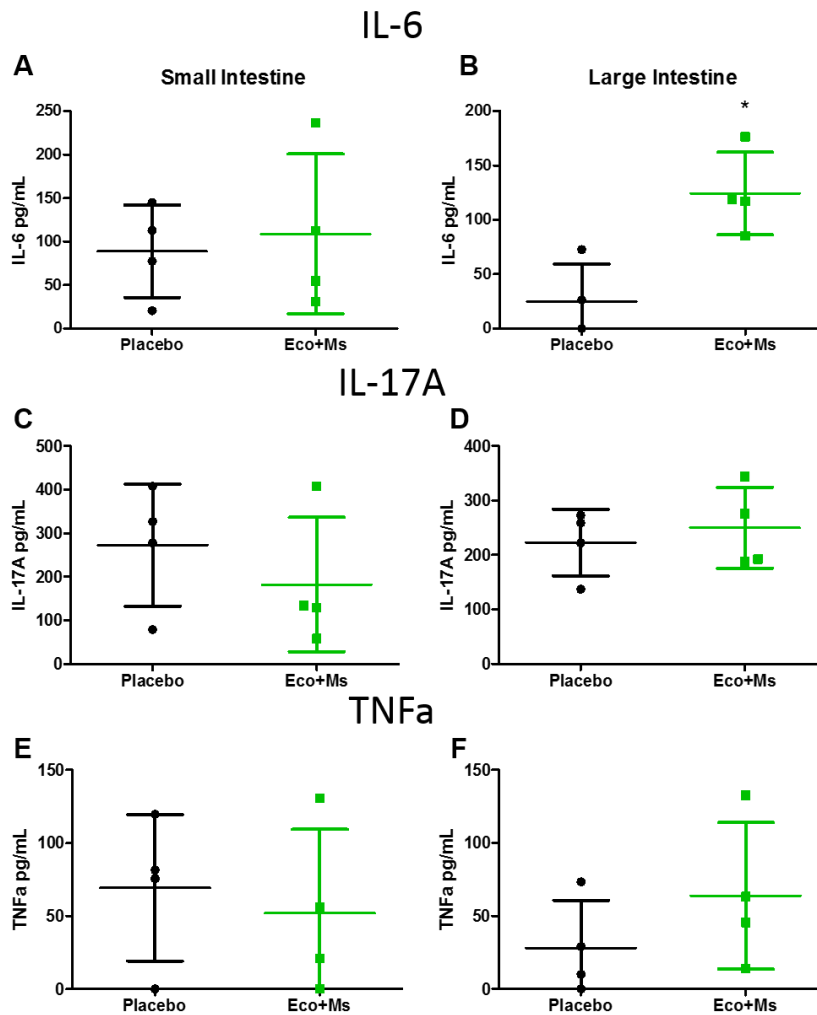
Fig 2. 17 Intestinal supernatant shows little difference in inflammatory cytokines with EcoHIV+morphine at 5 days post infection.

Intestinal homogenate was prepared from 2cm sections of distal small intestine and large intestine and ELISAs were performed. IL-6 in SI (A) showed no change while LI (B) showed a significant increase with EcoHIV+morphine. IL-17A in both SI (C) and LI (D) showed no change. TNFα in SI (E) and LI (F) showed no change. *p<.05
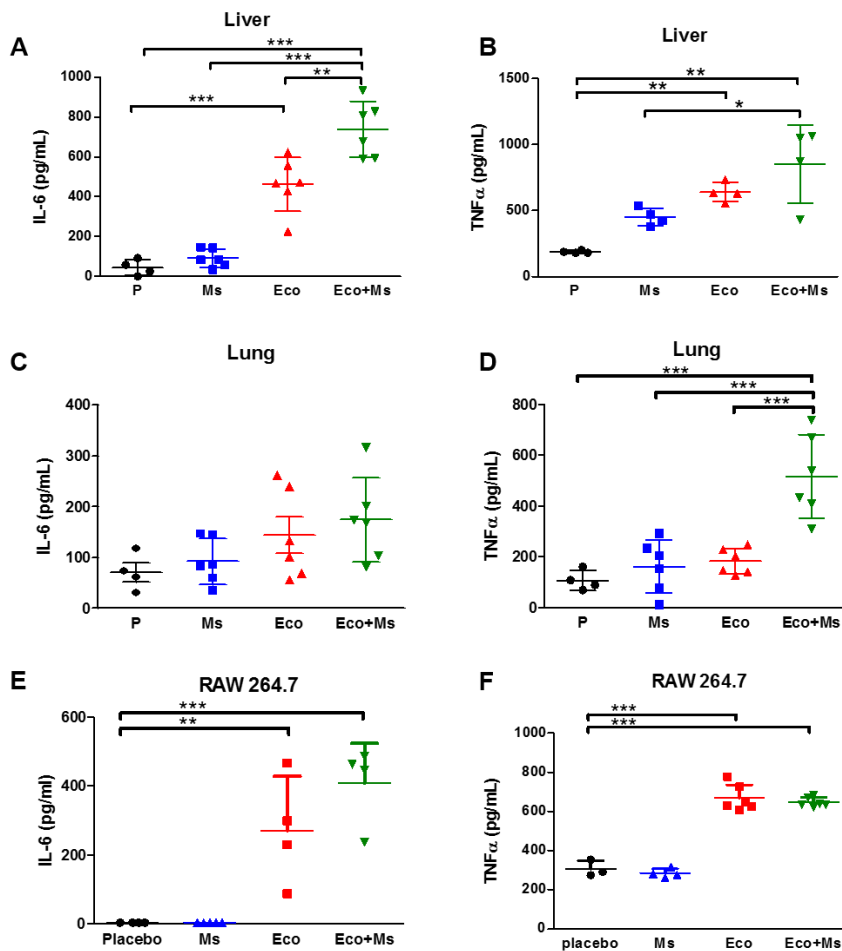
Fig 2. 18 EcoHIV increases IL-6 and TNFα systemically, which is exacerbated by morphine at 5 days post-infection

(A) IL-6 ELISA was performed on liver supernatant which had significantly higher levels in EcoHIV and EcoHIV+morphine treatments compared with placebo, and significantly higher levels in EcoHIV+morphine compared with EcoHIV or morphine alone. (B) TNFα in the liver showed similar results, with EcoHIV and EcoHIV+morphine having significantly higher levels than placebo, and EcoHIV+morphine having significantly higher levels than morphine alone. Lung IL-6 (C) and TNFα (D) levels were examined, which showed EcoHIV+morphine had significantly higher levels of TNFα compared to all other groups and IL-6 trended that way but did not achieve significance. To elucidate the potential source of cytokines, supernatant from RAW264.7 cells were examined and shown to have both higher IL-6 (E) and TNFα (F) levels in EcoHIV and EcoHIV+morphine treatments. *p<.05, **p<.01, ***p<.001
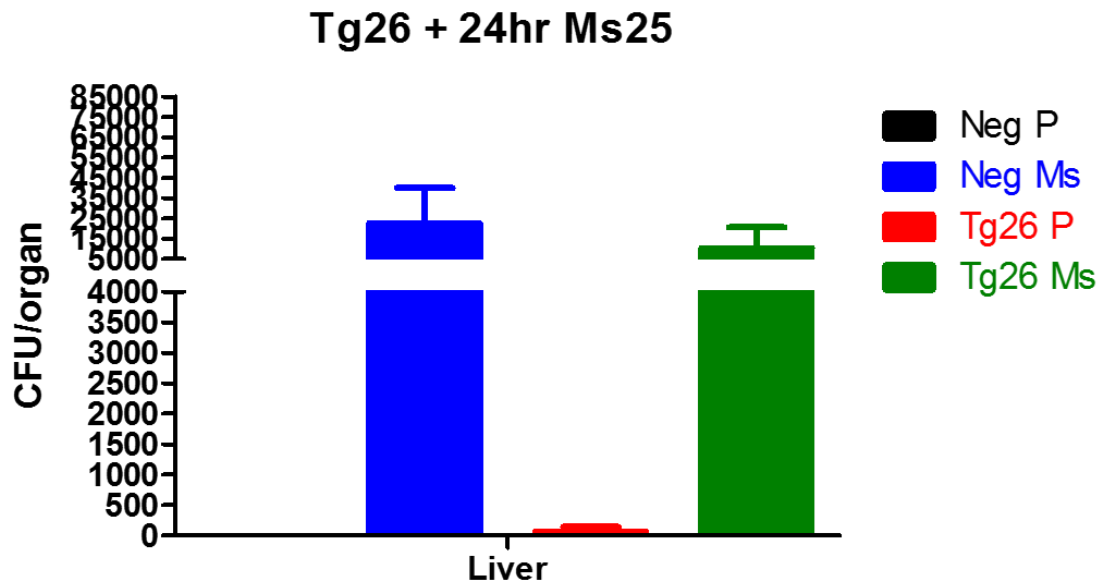
Fig 2. 19 Tg26 mice with morphine show no difference in bacterial translocation compared to Tg26 negative controls with morphine

Liver was homogenized and cultured on blood agar plates in aerobic conditions to count live CFUs. Tg26 negative (-/-) or Tg26 positive (+/-) mice treated with morphine for 24hr. Neg+morphine and Tg26+morphine both showed translocation, but there was not a significant difference between them.
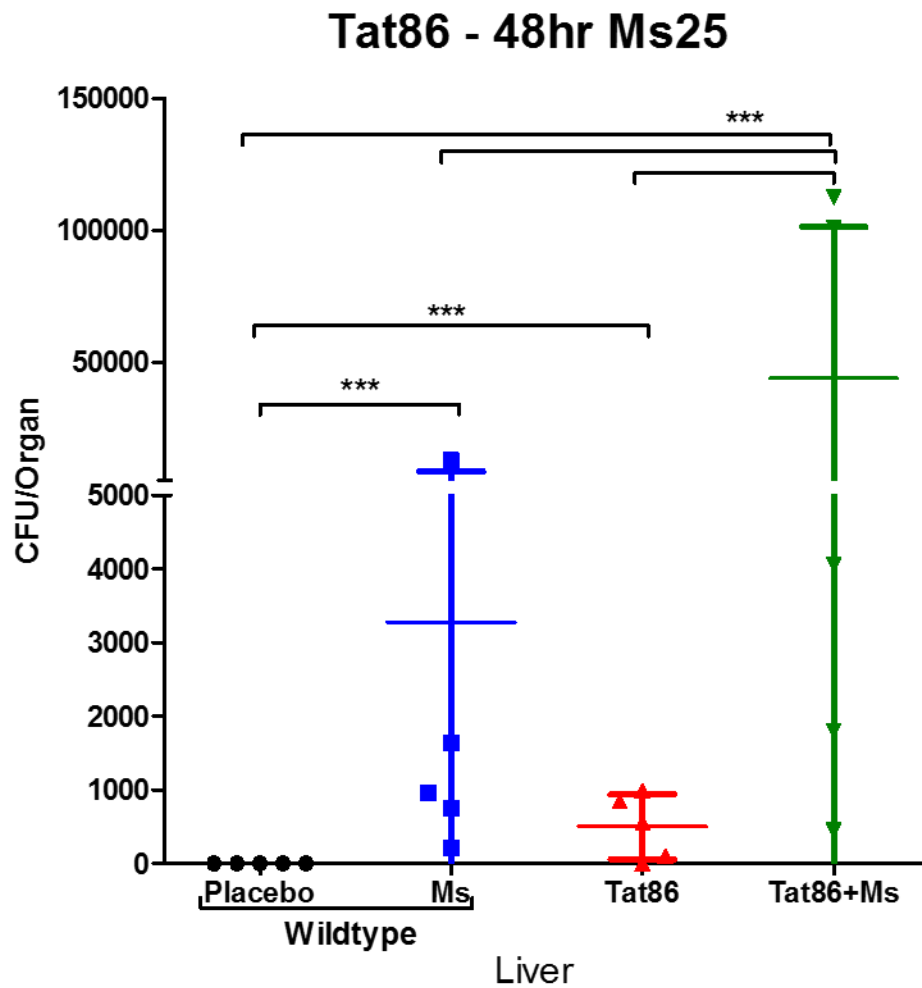
Fig 2. 20 Tat86 mice with morphine show a high induction of bacterial translocation
Liver was homogenized and cultured on blood agar plates in aerobic conditions to count live
CFUs. Tat86 mice treated with morphine for 24hr. Neg+morphine and Tg26+morphine both
showed translocation, but there was not a significant difference between them.

Small Intestine - Occludin

Placebo Morphine

Wildtype

Tat86
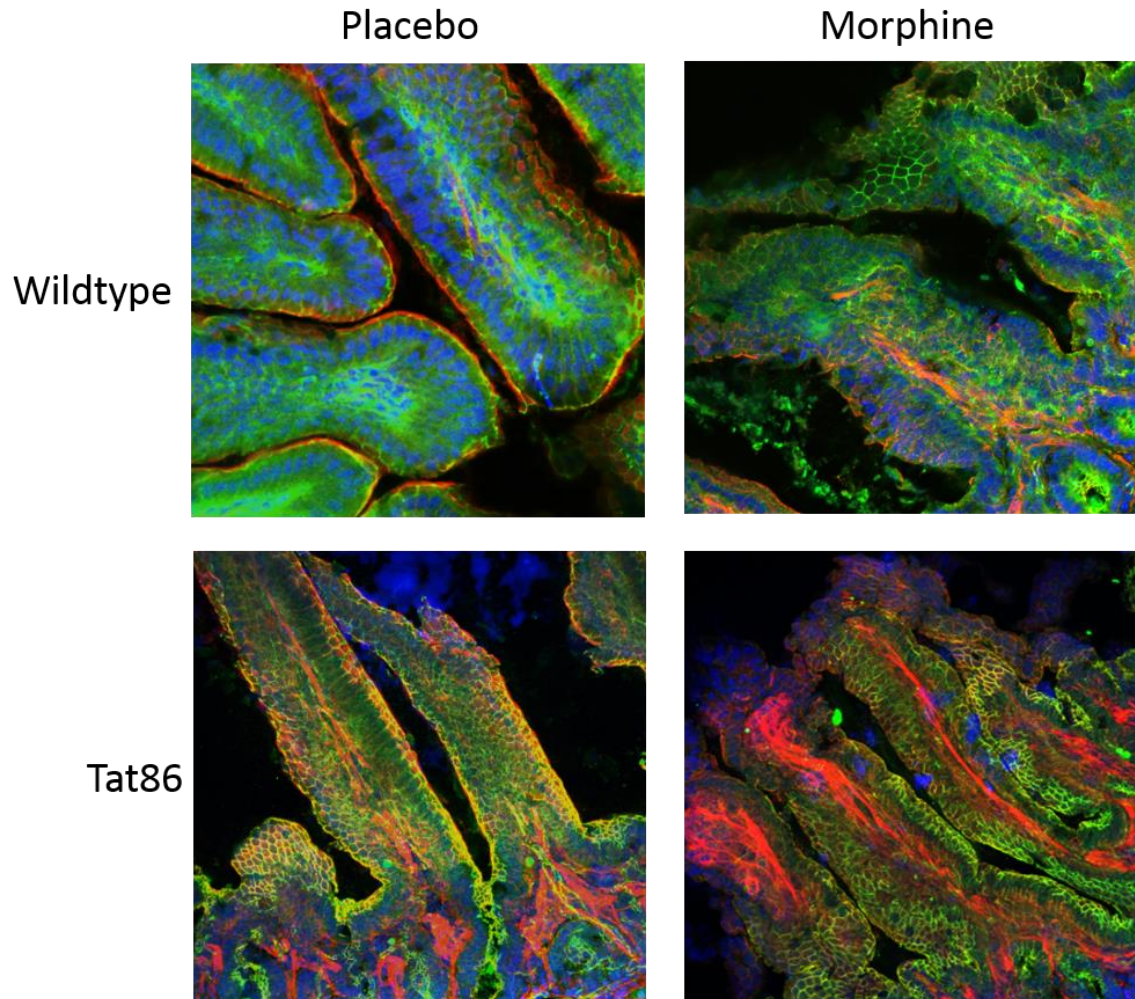
Fig 2. 21 Tight junction protein occludin is disrupted by Tat and morphine in small intestine

Frozen distal small intestine (ileum) was stained with Occludin (green), Phalloidin (F-actin, red) and dapi (nuclei, blue). Co-localization of occludin and phalloidin at the tight junction show up as yellow. Morphine alone (upper right panel) shows reduction in the yellow co-localization between the lumen (black) and the epithelial boundary. EcoHIV+morphine (lower right panel) shows representative picture of drastic reduction in yellow co-localization staining, similar to the results observed in EcoHIV. Magnification: 400X

Large Intestine - Occludin

Placebo	Morphine
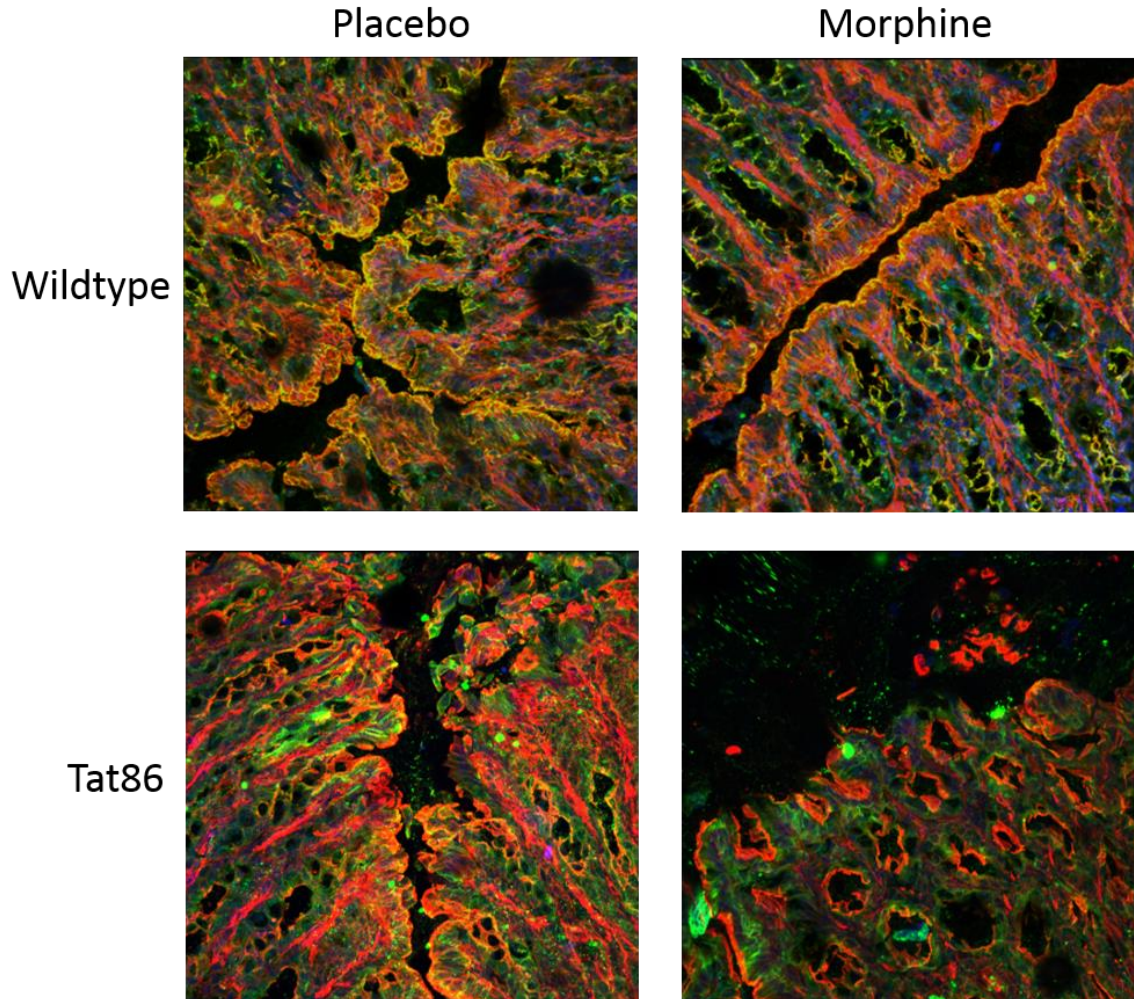
Fig 2. 22 Tight junction protein occludin is disrupted by Tat and morphine in large intestine

Frozen large intestine was stained with Occludin (green), Phalloidin (F-actin, red) and dapi (nuclei, blue). Co-localization of occludin and phalloidin at the tight junction show up as yellow. As expected, Tat86 and morphine alone (upper right panel) shows no reduction in the yellow co-localization between the lumen (black) and the epithelial boundary. EcoHIV+morphine (lower right panel) shows representative picture of drastic reduction in yellow co-localization staining, similar to the results observed in EcoHIV. Magnification: 400X

Small Intestine
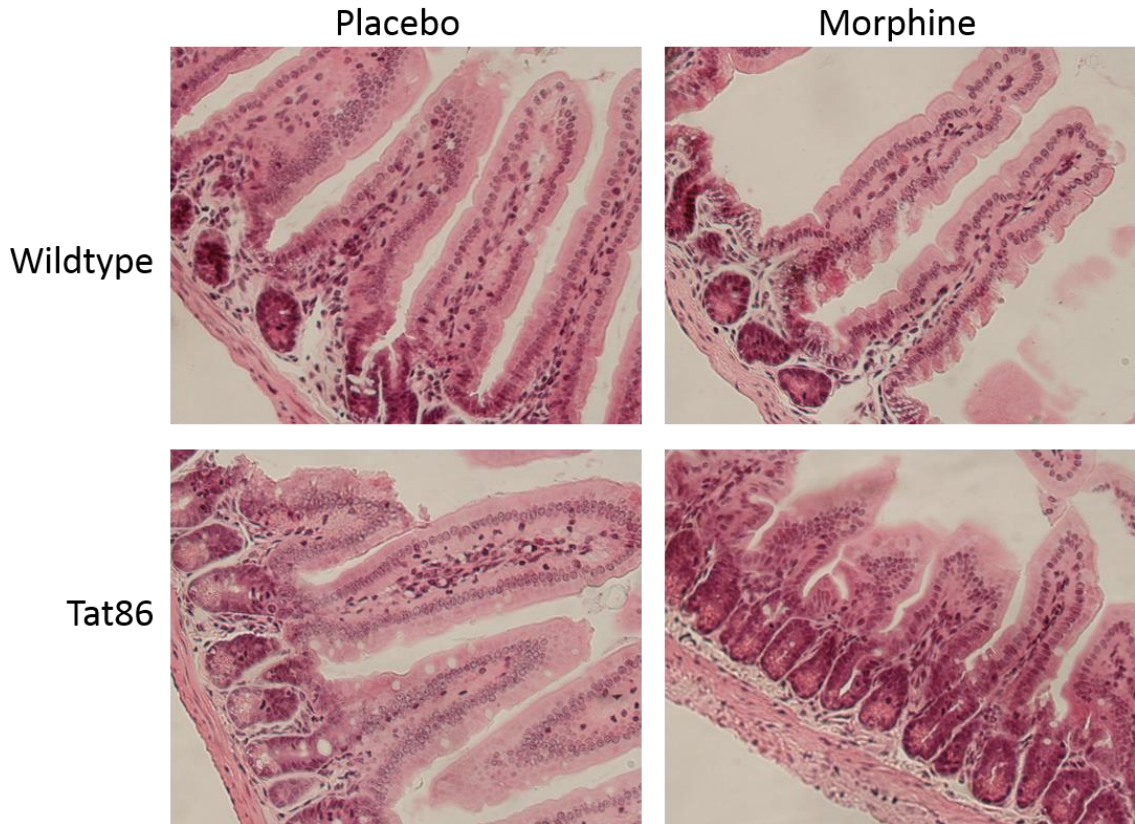
Fig 2. 23 Tat86 background induces morphological changes with morphine in small intestine

H&E staining shows that Tat86+morphine (lower right panel) induces morphological changes at 24hr after morphine treatment in the small intestine compared to what is observed in wildtype animals (upper panels) or Tat86 alone (lower right panel). Magnification: 100X

Large Intestine

Placebo | Morphine
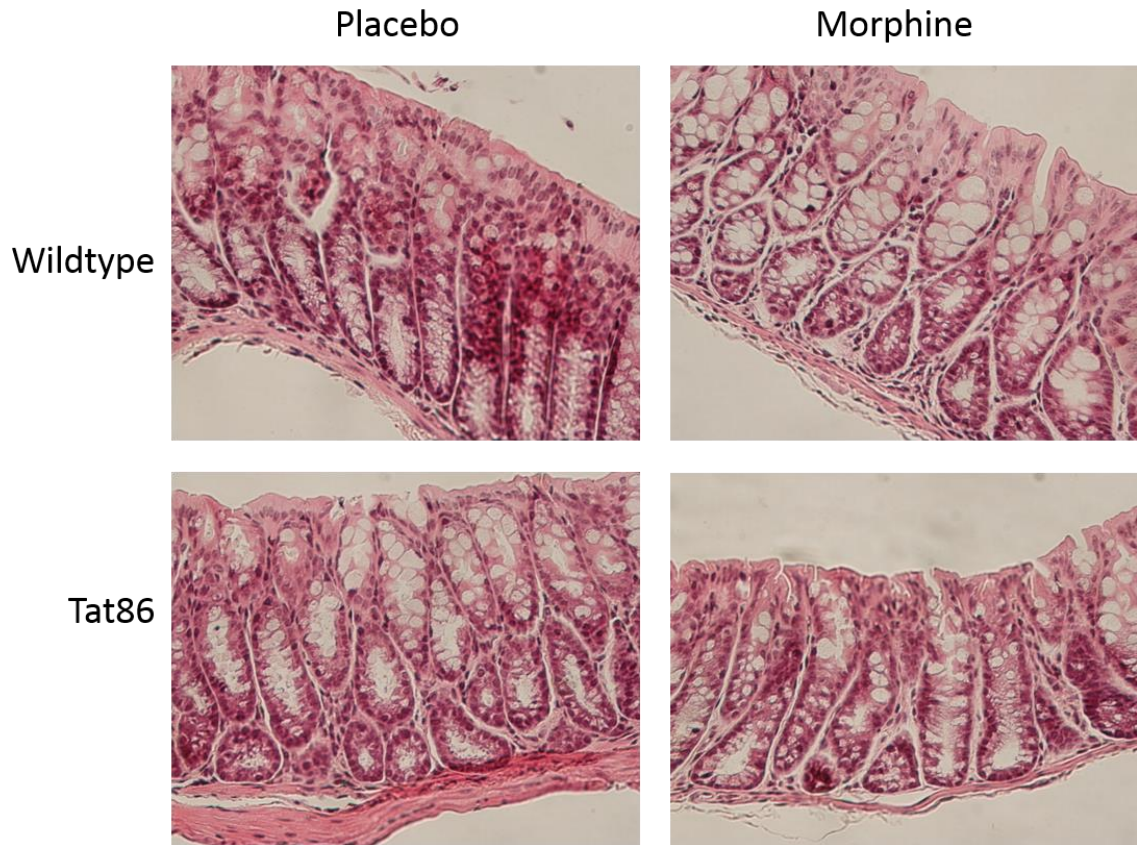
Wildtype

Tat86

Fig 2. 24 Tat86 background does not induce morphological changes with morphine in large intestine

H&E staining shows that Tat86+morphine (lower right panel appears consistent with wildtype with or without morphine (upper panels) or Tat86 alone (lower left panel) at 24hr after morphine treatment in the large intestine. Magnification: 100X
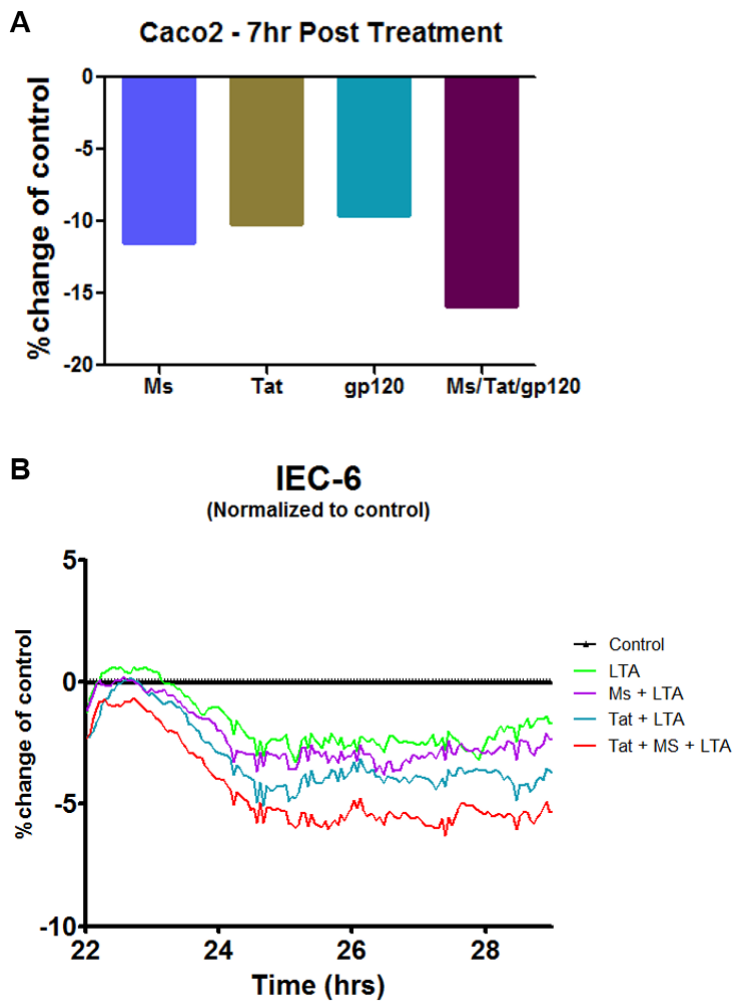
Fig 2. 25 Tat is capable of disrupting tight junctions of epithelial cells in culture which is worsened with morphine and TLR activation

Cells were cultured in ECIS chamber slides to monitor for changes in electrical permeability between the cells, interpreted as changes in tight junctions. (A) Caco2 cells were pretreated with morphine and monitored after Tat and/or gp120 were added to wells, which showed a reduction in permeability by Tat and gp120 alone, and exacerbated with both in combination with morphine. (B) IEC-6 cells were pre-treated with morphine and Tat, when TLR2 agonist LTA was added to the culture, which showed that in combination with Tat and morphine had to lowest permeability reduction.
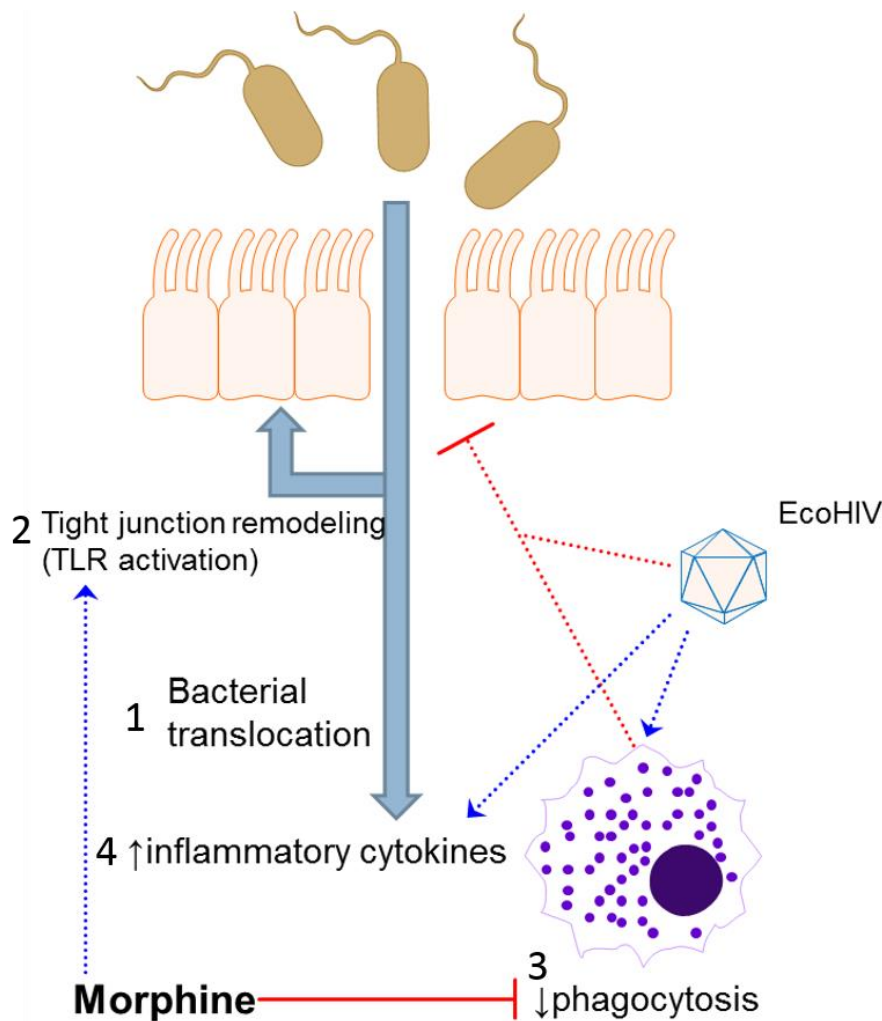
Fig 2. 26 Model of EcoHIV and morphine induced bacterial translocation.

Bacterial translocation is induced likely by a combination of morphine altering tight junction expression [97] and EcoHIV activating an inflammatory response. (1) Bacteria is able to translocate across the epithelial barrier which alters gut morphology (2), likely by activating basolateral TLRs, (3) Phagocytosis of bacteria by macrophages is diminished, which allows the spread of bacteria systemically to tissues such as liver. (4) Continued inflammation was observed in both the liver and brain tissues, despite the clearance of translocated bacteria. This may result from prolonged TLR4 activation, as TLR4KO mice had decreased translocation in this study. TLR4 typically undergoes tolerance following activation however this has been shown to be disrupted with morphine leading to long term activation [98]..

Chapter 3. <u>Dysbiosis in gut microbiome induced by opioids and interactions with HIV infection</u>

3.1.   Chapter Summary

HIV infection and opioid use are common comorbidities, with HIV patients including up to 40% drug abusers in some populations.[1] Studies have suggested that opioids in combination with HIV increase viral replication and disease progression.[2] HIV pathogenesis is known to alter gut homeostasis, leading to bacterial translocation and systemic inflammation that drives HIV replication and disease progression.[63,111] While the loss of gut homeostasis is strongly believed to occur at least in part through changes in the host defenses in the gut, namely on immune populations and epithelial barrier integrity, recent evidence suggests that the microbiome of late stage HIV infected individuals is altered and may contribute to the observed disruption.[7,6,5] This goal of this study was to investigate the microbiome in early HIV infection to see if dysbiosis occurs, and whether opioids are associated with earlier changes. This study found, using two animals models of infectious HIV, that microbial dysbiosis was not observed at early time points of infection in either model. However, this study shows for the first time that morphine induced strong changes in the microbiome, which likely occurs via a combination of constipation and immune mediated effects. Altogether, these findings suggests another mechanism for morphine influencing HIV pathogenesis at early stages of disease.

3.2.   Introduction

The microbiome plays a key role in homeostasis within the gut, acting in concert with the host immune and epithelial cells, to protect against pathogens and provide essential nutrients to the host. Microbial dysbiosis, or a change in the normal microbiome, is a hallmark of interrupted gut homeostasis and has been observed in numerous diseases.[58] Dysbiosis can occur as a direct effect of a pathogen outcompeting commensal bacteria, such as in *C. dificil*[198] or indirectly as a result of altered host immunity that acts with either too little or too great of a response, as in inflammatory bowel disease (IBD).[199]

Opioids have been shown to disrupt gut homeostasis leading to bacterial translocation.[78] There is a wealth of studies characterizing the effects of morphine on systemic immunity,[79] and recent evidence also shows its effects in the gut as well, including on gut epithelial cells.[97] However, whether dysbiosis occurs with opioids has not been examined to our knowledge. A recent study of opioid-independent constipation showed dysbiosis, suggesting that constipation induced by opioids could also cause dysbiosis in addition to altered bacteria by immune dysfunction.[94]

HIV is commonly found in opioid using populations with a prevalence of up to 40%.[105] HIV on its own is capable of disrupting gut homeostasis leading to bacterial translocation, and the resulting inflammation is believed to be integral for driving HIV replication.[63,71] Thus, it is not surprising that HIV, and SIV in

nonhuman primates, has been shown to induce dysbiosis in the gut.[7,6,131,200,201]

The limitation in these studies is that they all examine late stages of disease,

making it difficult to know when the dysbiosis occurs.

Opioids have been observed to hasten the pathogenesis of HIV and

worsen symptoms such as inflammation and toxicity in the brain.[138,147,165] Notably,

opioids have also been shown to increase bacterial translocation in SIV infection

compared with non-using individuals,[4] suggesting its role in the disruption of gut

homeostasis, but to our knowledge has not been examined further.

The goal of this study is to examine the role of opioids on microbial

dysbiosis in the absence or presence of early stage HIV infection. Using early

stages of infection will allow us to assess when HIV mediated dysbiosis occurs.

Opioids were hypothesized to induce microbial dysbiosis and that, in the context

of HIV, dysbiosis may be more severe at early time points of infection compared

with either HIV or opioids alone. To accomplish this, both mice (EcoHIV[154]) and

nonhuman primate (SIV) models of HIV were utilized to examine very early

points of infection (6 days in mice and 3/8/15/22 days in nonhuman primates).

3.3.   Methods

Mice

All studies using mice in Dr. Roy's laboratory were approved by the University of

Minnesota Animal Care and Use Committee and were conducted in full

compliance with NIH guidelines. Male C57Bl/6 and NSG mice were purchased

from the Jackson Laboratory, while Mu Opioid Receptor Knock Out (MORKO)

and Toll-Like Receptor 2 Knock Out (TLR4KO) mice were bred in house. All

animals were between 10-16 weeks of age at the beginning of each experiment.

Morphine treatment

Mice were implanted with either a placebo or 25mg slow-release morphine pellet.

In EcoHIV infection, morphine pellet implantation occurred 24 hr prior to infection.

Pellets were generously provided by NIH/NIDA.

EcoHIV infection

The EcoHIV constructs used in the present work were EcoHIV/NL4-3 which was

constructed on the backbone of HIV-1/NL4-3 (Potash). For brevity, the virus is

called EcoHIV. The viruses were propagated in HEK293TN cells as previously

described.[154] Mice were injected in the intraperitoneal cavity with 1mL of either

saline or 1×10^6 pg of p24 of EcoHIV as measured by p24 ELISA following

manufacturer's instructions (ZeptoMetrix Corporation). *In vitro* work performed in

macrophage cell lines (J774 or RAW) were treated with 1×10^3 pg of p24 of

EcoHIV per 1×10^6 cells.

Bacterial Translocation

Tissue was harvested and homogenized in sterile PBS with 100µM cell strainers (BD) following aseptic techniques. Homogenized tissue was then plated on blood agar plates and incubated at 37°C overnight. Colonies were counted and normalized for varying protein concentrations in the tissue homogenate.

Nonhuman primates

NHP samples were donated in kind by Dr. Shilpa Buch, University of Nebraska. Animals used in this study were male Rhesus macaques between 2-3 years of age. Feces were collected at the dates indicated (see Fig 3.22).

Sequencing and 16S DNA analysis

Fecal content was collected from gut region encompassing distal cecum and approximately one inch of the colon and frozen on dry ice. The fecal matter was lysed using glass beads in MagnaLyser tissue disruptor (Roche) and total DNA isolated using Power-soil/fecal DNA isolation kit (Mo-Bio) as per manufacturer's specifications. All samples was quantified via the Qubit® Quant-iT dsDNA Broad-Range Kit (Invitrogen, Life Technologies, Grand Island, NY) to ensure that they met minimum concentration and mass of DNA and submitted to either Second genome Inc. or University of Minnesota Genomic Center for microbiome analysis as follows: To enrich the sample for the bacterial 16S V4 rDNA region, DNA was

amplified utilizing fusion primers designed against the surrounding conserved regions which are tailed with sequences to incorporate Illumina (San Diego, CA) flow cell adapters and indexing barcodes. Each sample was PCR amplified with two differently bar coded V4 fusion primers and were advanced for pooling and sequencing. For each sample, amplified products were concentrated using a solid-phase reversible immobilization method for the purification of PCR products and quantified by electrophoresis using an Agilent 2100 Bioanalyzer®.The pooled 16S V4 enriched, amplified, barcoded samples were loaded into the MiSeq® reagent cartridge, and then onto the instrument along with the flow cell. After cluster formation on the MiSeq instrument, the amplicons were sequenced for 250 cycles with custom primers designed for paired-end sequencing. Using QIIME, sequences were quality filtered and demultiplexed using exact matches to the supplied DNA barcodes. Resulting sequences were then searched against the Greengenes reference database of 16S sequences, clustered at 97% by uclust (closed-reference OTU picking).

Mass Spectrometry

Fecal samples were collected as for 16S DNA analysis. Samples were shipped on dry ice to Metabolon, Inc., who prepared and analyzed the samples.

Predictive metabolic profile (PICRUSt)

OTU tables from closed-reference picking were uploaded to Huttenhower lab
public Galaxy domain containing the PICRUSt module
(huttenhower.sph.harvard.edu/galaxy/).[202] OTU tables were normalized by copy
number, predicted metagenome, and categorized by function using KEGG
pathways with three levels of depth.

Analysis and Statistics

OTU tables were rarefied to the sample containing the lowest number of
sequences in each analysis. Qiime 1.8 was used to calculate alpha diversity
(alpha_rarefaction.py) and to summarize taxa
(summarize_taxa_through_plots.py). OTU table and PICRUSt output was
visualized and analyzed using Statistical Analysis of Metagenomic Profiles, or
STAMP, software.[203] Principal Coordinate Analysis was done within this program
using observation ID level. Heatmaps were generated using family level (L5)
taxonomic data. Indicator species analysis was performed in R using the
IndicSpecies package with combined taxonomic output from the summarize taxa
command above.[204]

3.4.   Results

Morphine-mediated dysbiosis

Morphine has previously been shown to induce gut barrier disruption and significant bacterial translocation.[97] Immune activation was also observed to be induced by morphine,[78,97] and described in chapter 2 of this dissertation. However, the role of microbial dysbiosis in this process has not been examined. Bacterial translocation was observed in animals examined for microbial dysbiosis following 72 hr of exposure to a 25mg slow release morphine pellet (Ms-WT) which was not observed in placebo-treated animals (Pl-WT) (Fig 3.1A). Bacterial translocation was prevented when the mu-opioid antagonist naltrexone was implanted with morphine (MN-WT) (Fig 3.1A). Species richness, or alpha diversity, was assessed within the large intestinal fecal content in these animals. No meaningful difference was observed in the number of operational taxonomic units, putative species of sequences clustered at 97% or greater homology, between the three treatment groups (Fig 3.1B). To verify this, the three groups were compared at 48230 sequences, which was minimum sequences per sample and no significance was found (Fig 3.1C). While the number of species did not change between samples, the composition of species was compared between treatments, which includes the number within each species. Ms-WT (blue) caused a noticable shift in 5 out of 6 animals along the x-axis, which encompasses 55.3% of total variability between the samples of a Principal

Coordinate Analysis (PCoA) compared with PI-WT (black, points enclosed with black dashed line). As observed with bacterial translocation, the community shift observed in Ms-WT animals was abolished in the MN-WT animals (red) (Fig 3.1D). Together, this implies that microbial dysbiosis occurs in morphine treated animals in conjunction with bacterial translocation, and that dysbiosis is mediated by the mu-opioid receptor.

Based on the PCoA analysis, specific taxa were examined that changed in the Ms-WT animals. An indicator species analysis was performed to measure taxa whose presence can predict groups or combinations of groups (Fig 3.2). Indicators were found for PI-WT (black) and MN-WT (red) treated groups when considered together, but not in either treatment alone, which supports the overlap in beta diversity between these two groups observed in Fig 3.1. Indicator taxa which overlap PI-WT and MN-WT are taxa reduced in the morphine treatment group. Taxa in this category include the family *Peptococcaceae* from the *Firmicutes* phylum and the order *Streptophyta* from the *Cyanobacteria* phylum. Conversely, many taxa were identified with Ms-WT animals alone(blue circle); these taxa are increased with morphine treatment compared to the other two groups. Of those identified, all were gram positive bacteria belonging to the Firmicutes phylum, including *Bacillaceae*, *Enterococcaceae*, *Erysipelotrichaceae*, *Staphylococcaceae*, and *Streptococcaceae*. Interestingly, the serotype of the translocated bacteria were from the same families: *Enterococcaceae*,

Bacillaceae, and *Staphylococcaceae* (Table 3.1; Meng et al, submitted).

Altogether, the data suggests that morphine induced-bacterial dysbiosis results in

the outgrowth of certain families within the Firmicutes phylum which are also the

translocated bacteria in the morphine treated group.

Since the bacterial outgrowth observed was predominantly from the gram

positive community, which is recognized by the innate pathogen sensing receptor

TLR2, the next experiment examined if morphine causes dysbiosis within

TLR2KO mice. Validating previous data, TLR2KO animals treated with either

placebo or morphine pellets have significantly less bacterial translocation

compared to wild type mice treated with morphine (Fig 3.3A). Interestingly,

species composition analysis still showed a distinct clustering in the morphine-

treated TLR2KO (Ms-TLR2KO, light blue) versus placebo-treated TLR2KO (Pl-

TLR2KO, grey, enclosed by grey dotted line) (Fig 3.3B). When plotted together,

TLR2KO animals (grey and light blue, respectively) cluster distinctly from WT

animals along the y-axis (23.7% variability) (Fig 3.3C). Interestingly, Ms-WT

animals (blue) still cluster distinctly from the Pl-WT (black, enclosed by black

dashed line) and MN-WT (red) on the x-axis (33.1% variability). However,

distinct differences between the Pl-TLR2KO (grey, enclosed by grey dotted line)

and Ms-TLR2KO (light blue) animals are no longer visible (Fig 3.3C). Together,

this highlights that TLR2 may play an important role in morphine-induced

microbial dysbiosis, and when TLR2 is absent global changes are not as

obvious. The reduced dysbiosis observed in Ms-TLR2KO animals also

correlates with decreased bacterial translocation.

Since distinct clustering could be observed when Pl-TLR2KO was

compared with Ms-TLR2KO, an indicator species analysis was performed on

TLR2KO animals and compared with wild type animals (Fig 3.4). Given the shift

in microbial composition observed in beta diversity between WT and TLR2KO

animals (Fig 3.3C), it makes sense that indicator taxa were found for wild type

animals compared with TLR2KO animals (Fig 3.4). Changed taxa likely play a

role in the shift observed in beta diversity between the two groups along the y-

axis (Fig 3.3C). The gram-positive order *Bifidobacteriales* was indicated in WT

animals (overlap of black, blue, and red circles), meaning that this order is

decreased in TLR2KO animals. Conversely, TLR2KO animals were indicated by

higher levels of gram-positive Streptococcaceae, as well as the gram-negative

Desulfovbrionaceae family of the *Proteobacteria* phylum. Comparing Ms-

TLR2KO and Ms-WT animals, an enrichment in the following taxa were

observed: *Erysipelotrichaceae*, *Enterococcaceae*, and *Streptococcaceae*

families. However, Ms-WT animals had a number of significant indicators that

were not observed in TLR2KO morphine animals, which included

Staphylococcaceae, *Planococcaceae*, and *Bacillaceae*. Thus, these taxa may be

contributing to the shift observed in the species composition of Ms-WT that was

not observed in Ms-TLR2KO (Fig 3.3C). Based on these studies, species

105

increased by morphine may play a contributing role in bacterial translocation in Ms-WT animals since bacterial translocation was not observed in Ms-TLR2KO.

In addition to disrupted TLR2 signaling in the gut epithelium,[97] morphine has been shown to alter immune responses[79] which likely plays a role in both the microbial translocation and dysbiosis observed. TLR2KO animals have deficient TLR2 on both epithelial as well as immune cells. To examine the role immune cells play in this process, Nod scid gamma (NSG) mice, which lack a functional immune system, were examined. Interestingly, NSG animals treated with morphine (Ms-NSG) showed no bacterial translocation compared with animals treated with placebo pellets (Fig 3.5A). Similarly to TLR2KO animals, a shift in beta diversity was observed between PI-NSG (black, enclosed by black dashed line) and morphine (blue) treated NSG animals (Fig 3.5B), however the average distance between groups in NSG (~.2) was reduced compared to WT mice (~.4, Fig 3.1D). Dysbiosis in NSG-Ms occurred despite having an incompetent immune system, suggesting that morphine acts to induce dysbiosis partially through mechanisms independent of immune function such as constipation. However, dysbiosis was blunted compared to Ms-WT animals, implying that the immune system contributes to the dysbiosis induced by morphine. Also, as no bacterial translocation was observed in either the NSG or TLR2KO animals, an intact and functional immune system is critical for the bacterial translocation observed in Ms-WT animals.

To identify the taxa that was driving the shift in beta diversity within NSG animals, an indicator species analysis was performed (Fig 3.6). Pl-NSG animals (black) had one significant indicator: the *Lachnospiraceae* family of the *Firmicutes* family which was decreased in the morphine-treated animals. As in WT, Ms-NSG animals had a greater number of hits which included *Peptostreptococcaceae*, *Enterococcaceae*, *Staphylococcaceae*, *Ruminococcaceae*, *Clostridiaceae*, and *Erysipelotrichaceae* families. Overall, these taxa level changes may be contributing to the shift observed in beta diversity, however as in TLR2KO animals there were fewer changes induced by Ms-NSG than Ms-WT which again implicates that immune activation correlates with bacterial translocation.

Comparing the results in WT, TLR2KO, and NSG mice, it is clear that both immunocompromised backgrounds share similarities, but not all changes that are observed in Ms-WT animals (Table 3.2). *Enterococcaceae* and *Erysipelotrichaceae* families were increased by morphine independent of background, implying that these changes in these taxa by morphine may not be dependent on an intact immune system. *Streptococcaceae* family was an indicator taxa with morphine in both TLR2KO and WT, but not NSG animals. Similarly, Staphylococcaceae was an indicator species in both NSG and WT, but not TLR2KO mice. Differences between the strains may be attributed to genetic differences in the background, particularly between wildtype C57Bl/6 and NSG.

However, it is likely also due in part to changes in immune function which morphine has been shown to modulate.

While it is apparent that bacterial populations are changing with morphine, the next analysis examined whether bacterial dysbiosis has any functional impacts on the host by measuring metabolites within the fecal matter via mass spectrometry. Compounds were compared between groups to look for significant changes (Table 3.3). Similar to changes observed in taxa, Ms-WT animals induced 73 and 84 significant metabolite changes compared with both Pl-WT and MN-WT, respectively. The majority of the metabolite changes in Ms-WT compared with Pl-WT were decreased (57 versus 16). Interestingly, MN-WT had 34 significant metabolite changes compared with placebo despite taxa being mostly similar, with the majority again being decreased. As changes were observed in taxa between TLR2KO and WT animals, it was no surprise that metabolite changes occured between placebo or morphine treated animals of each background, 63 and 36 respectively. Once again, the majority of the metabolite were decreased (59 versus 4; 28 versus 8). Ms-TLR2KO animals showed 50 significant metabolite changes compared with Pl-TLR2KO animals. The distribution of change was relatively equivalent with 29 increased by morphine and 21 decreased. Metabolite changes observed by both Ms-WT and Ms-TLR2KO followed the same pattern that is observed with taxa level changes,

supporting that taxonomic changes are contributing to alterations in the metabolic function of the host.

As each group had a distinct profile when compared to other groups, group profiles were tested to blindly predict sample grouping. By using a random forest confusion matrix, all samples were assessed to see which groups they classified with (Table 3.4). Overall, samples were predicted with 97% accuracy. The only animal which was classified incorrectly was a Ms-WT animal that was predicted to be Ms-TLR2KO, highlighting that morphine causes some consistent changes in both genotypes. The accuracy of this test further validates that each group had a distinct signature of metabolites.

When the signature of metabolites from each sample was compared via principal coordinate analysis (Fig 3.7a), clustering is obvious with PI-WT (black, enclosed by black dashed line) and MN-WT (red). Similarly, Ms-WT (blue) and Ms-TLR2KO morphine (light blue) clustered together, which illustrates how one of the Ms-WT animals could be classified as Ms-TLR2KO in the Random Forest analysis. Again, differences in the signature of metabolites between Ms-WT and Ms-TLR2KO are likely prioritized on lower priority axis and not visualized when all groups are compared. TLR2KO placebo (grey, enclosed by grey dotted line) were intermediately changed compared to the other two clusters. The profile of metabolites was then prioritized to show which compounds had the largest changes and the best accuracy of predicting treatment groups (Fig 3.7b).

Interestingly, many top metabolites altered were associated with lipid metabolism. Among these, changes among bile acids were strikingly common, including deoxycholate, alpha-muricholate, beta-muricholate, taurodeoxycholate, lithocholate, chenodeoxycholate, and cholate.

Initially, primary bile acids are produced in the host liver from cholesterol. Primary bile acids are then trafficked and secreted to the lumen of the gut and play a role in digestion and nutrient absorption as well as preventing bacterial outgrowth.[205–207] Cholate, a primary bile acid, was significantly decreased in Ms-WT compared to both PI-WT and MN-WT (Fig 3.8A). Unexpectedly, cholate in PI-TLR2KO animals had a lower baseline than PI-WT animals, which made it difficult to tell if Ms-TLR2KO induced a similar reduction in cholate compared with Ms-WT animals. In the GI tract, primary bile acids are converted into secondary bile acids by bacteria. Similar to primary bile acids, a reduction was observed in secondary bile acids such as deoxycholate in both Ms-WT and Ms-TLR2KO animals (Fig 3.8B). Together this implies that morphine is altering the host ability to secrete primary bile acids into the lumen and secondary bile acids are lowered as a consequence. Interestingly, coprostanol, a direct metabolite of cholesterol via bacterial conversion, is increased in both Ms-WT and Ms-TLR2KO animals. This suggests that cholesterol availability in the gut may increase and accumulate as a counterpoint to having lower bile acid metabolism.

Morphine was measured as a biochemical in the fecal matter and was present in high levels in the treatment groups that were given morphine pellets: Ms-WT, MN-WT, and Ms-TLR2KO (Fig 3.9). This is direct evidence that morphine was excreted through the gastrointestinal tract in these animals, which has been shown to be a source of excretion of morphine along with the urinary tract.[208]

As a comparison to mass spectrometry, a predictive metabolic analysis was utilized to determine whether taxa changes could predict the metabolite shifts observed in mass spectrometry. If similar findings were shown, predictive metabolites could be used in subsequent studies. Metabolites changes were predicted using Phylogenetic Investigation of Communities by Reconstruction of Unobserved States, or PICRUSt.[202] Comparing the predicted metabolic profile of each sample, clustering was observed similar to the species composition shown above (Fig 3.10A). Pl-WT (black, enclosed by dashed black circle) and MN-WT (red) overlapped, while Ms-WT (blue) was separated along the x-axis which included 88.6% of variability among the samples. 2 out of the 6 morphine samples showed less of a shift from the other two groups; one of these animals was consistent with the animal that did not shift in the analysis of species composition (Fig 3.3C). A heatmap was generated to compare the significantly changed metabolites that were predicted by PICRUSt between Pl-WT, Ms-WT, and MN-WT animals (Fig 3.10B). While not all hits are relevant as they are

predicted to gene homologs, it is interesting to note that lipid metabolism was a category that showed up in many of the hits validating the mass spectrometry analysis. The samples were clustered as expected, with 4 of the 6 Ms-WT (blue) animals clustering distinctly from the other samples (Fig 3.10B, top dendogram). The remaining Ms-WT samples clustered separately but were closer to the PI-WT (black) and MN-WT (red) animals (Fig 3.10B, top dendogram). Secondary bile acids were not predicted to have changed, however this is not surprising given that primary bile acids are host derived and may drive the deficiency in secondary bile acids that was observed. Overall, the PICRUSt analysis grossly encompasses changes observed in lipid metabolites. However, the resolution of PICRUST is unable to look for changes in particular compounds, such as bile acids, that were measured as significantly changed via mass spectrometry.

Dysbiosis with EcoHIV+Morphine

As HIV has been shown to induce microbiome changes in human studies,[7,6,132] EcoHIV infected micel[154] was examined for changes in the murine microbiome either with or without morphine. Mice in subsequent experiments were treated with morphine for 6 days as opposed to 3 days in the previous studies in order to accommodate a longer infection (5 days) with EcoHIV.

Species richness, or alpha diversity, was first assessed for each group (Fig 3.11A). No significant change was observed between placebo (PI-WT), morphine (Ms-WT), and EcoHIV (Eco-WT) animals. However, a significant

112

decrease in species was observed in EcoHIV+morphine (EcoMS-WT) animals compared with PI-WT animals at 980 sequences. Individual animals were stratified at 980 sequences to again illustrate the significant difference between EcoMs-WT and PI-WT animals (Fig 3.11B). No other group comparisons had significance. This implies that EcoHIV and morphine treatments combine additively to decrease the species found in large intestinal fecal content.

Next, the composition of species was examined, comparing PI-WT with the three treatment groups. As in earlier studies at three days treatment, six days Ms-WT (blue) caused a shift in the species composition compared with PI-WT (black, enclosed by dashed black line) (Fig 3.12A). Eco-WT (red) did not show a distinct clustering from PI-WT (black, enclosed by dashed black line), however the Eco-WT animals were spread beyond the tightly clustered PI-WT (black, enclosed by dashed line) which suggests that small changes occur (Fig 3.12B). EcoMs-WT (green) induced changes similar to Ms-WT, however 2 out of 5 animals were not very different from PI-WT (black, enclosed by dashed line) animals (Fig 3.12C). When all treatments were compared in the same plot, Ms-WT (blue) and 3 out of 5 EcoMs-WT (green) animals clustered together, supporting that morphine is causing consistent microbial shifts in these animals. Compared to previous experiments at 3 days exposure to morphine, 6 days morphine exposure still induced microbial shifts, but these shifts were smaller which may reflect a lower dose of morphine pellet which has been previously

113

shown at this time point.[175] EcoHIV caused relatively small microbial shifts at this time point of infection and did not alter the shift induced by morphine when infected in combination.

To see if a particular species were causing the shifts in microbial composition, an indicator species analysis was performed on the four treatment groups (Fig 3.13). Despite similar clustering in the PCoA, few changes were significantly different with morphine treatment. *Coriobacteriaceae* family in the *Actinobacteria* phylum were significantly associated with PI-WT and Eco-WT, which implies that this family was reduced in both groups treated with morphine. Unexpectedly, nothing was significantly enriched consistently by morphine. EcoMs-WT had *Erysipelotrichaceae* family as an indicator taxa, which was also enriched in the 3 day morphine studies, however Ms-WT did not. *Mogibacteriaceae* and *Enterococcaceae* were associated with PI-WT, Eco-WT, and EcoMs-WT groups, indicating a reduction in Ms-WT animals. Though not many indicator species were identified, four families had significantly different means between groups: *Erysipelotrichaceae*, *Mogibacteriaceae*, *Peptocococcaceae*, and *Clostridiaceae*. *Erysipelotrichaceae* was identified for an indicator species for EcoMs-WT and increased to significantly higher levels than the other three groups (Fig 3.14A). *Mogibacteriaceae* was identified as an indicator for PI-WT, Eco-WT, and EcoMs-WT, which is validated by a reduction in 3 out of 5 animals Ms-WT (Fig 3.14B). While not significant, *Mobibacteriaceae*

also had a trend toward an increase in Eco-WT and EcoMs-WT compared with PI-WT (Fig 3.14B). *Peptococcaceae* was not identified as an indicator, however was significantly increased by EcoMs-WT from PI-WT (Fig 3.14C). The final hit, C*lostridiaceae*, was decreased in both Ms-WT and EcoMS-WT supporting that morphine treatment may be contributing to these changes (Fig 3.14D). A heatmap of these four families shows a clustering that is similar to the species diversity plot shown earlier, with PI-WT and Eco-WT clustering together, and Ms-WT and EcoMs-WT clustering in a different branch (Fig 3.14E). These findings were quite different from the experiments with three day morphine treatment group, which showed an enrichment of many taxa by morphine. The differences between these time points suggest that morphine effects may be transient in the mice probably due to decrease in morphine release over time.[175] Eco-WT did not induce changes from PI-WT as demonstrated by the indicator species analysis nor did it cluster distinctly based on the significantly altered families.

Mu opioid receptor knockout (MORKO) animals were utilized to block the ability of morphine to act on the host. Unexpectedly, the composition of species among each placebo animal (PI-MORKO, black, enclosed by dashed line) were not clustered tightly as in other experiments which made comparisons to treatment groups more ambiguous (Fig 3.15). Despite this, morphine (Ms-MORKO, blue) and EcoHIV+morphine (EcoMs-MORKO, green) clustered closely with the PI-MORKO animals. EcoHIV (Eco-MORKO, red) also clustered closely

115

with Pl-MORKO as occurred in WT animals. Families that were significantly changed in WT animals were examined in MORKO animals to see if any changes were consistent (Fig 3.18). *Erysipelotrichaceae* (Fig 3.18A), *Mogibacteriaceae* (Fig 3.18B), and *Peptococcaceae* (Fig 3.18C), and *Clostridiaceae* (Fig 3.18D) were all protected from changes induced in Ms-WT animals. This is reflected in a heatmap using these four families; where Ms-WT and EcoMs-WT animals clustered distinctly (Fig 3.14E), MORKO animals show no clustering of treatment groups (Fig 3.16E). This supports that MORKO protects from microbiome shifts induced by morphine, and adds evidence that the host response is what shifts the microbiome rather than morphine acting directly on bacteria.

TLR2KO animals were similarly examined for shifts in microbial composition due to the consistent increase of gram positive bacteria. Species composition of morphine (Ms-TLR2KO; blue) and EcoHIV+morphine (EcoMs-TLR2KO; green) is shifted from placebo (Pl-TLR2KO; black, enclosed by dashed black line) similar to WT animals (Fig 3.17). Two out of three EcoHIV (Eco-TLR2KO; red) animals were also shifted along the x-axis to the same extent as EcoMs-TLR2KO. Interestingly, EcoMs-TLR2KO was positioned as a cluster between Ms-TLR2KO and Eco-TLR2KO implying that the combination leads to intermediate shifts. The four families that were significantly altered in wildtype animals were examined in TLR2KO animals, which showed that absence of

116

TLR2 lead to protection from morphine induced modulation of

Erysipelotrichaceae (Fig 3.18A), *Mogibacteriaceae* (Fig 3.18B), and

Peptococcaceae (Fig 3.18C). Unexpectedly, *Clostridiaceae* significantly

increased in Ms-TLR2KO and EcoMs-TLR2KO animals, which decreased in Ms-

WT and EcoMs-WT animals. The heatmap of these 4 families clustered 3 out of

4 Ms-TLR2KO and 1 out of 4 EcoMs-TLR2KO distinct from other samples; these

samples had the highest levels of *Clostridiaceae* which drove the clustering as

the other families did not change (Fig 3.18E). Overall, it appears that TLR2KO

protects from morphine-induced microbiome shifts similarly to what was

observed in the three day experiments discussed earlier.

   As in the three day experiment with morphine, the next question asked

was if shifts observed in the microbiome had functional implications. Mass

spectrometry was not performed in these experiments, so PICRUSt

metagenomic predictions of metabolic changes was utilized. Pl-WT animals

(black, enclosed by black dashed line) clustered tightly on the primary x-axis

aside from one outlier (Fig 3.19A). Ms-WT (blue) and EcoMs-WT (green) all had

shifts to the right on the x-axis compared to the cluster of Pl-WT animals. Eco-

WT (red) predominantly clustered with the Pl-WT animals, although two out of six

animals clustered to the right as well which may imply a variation in response to

the infection. When significantly changed metabolite groups were plotted as a

heatmap, Ms-WT (blue) and EcoMs-WT (green) animals clustered distinctly from

PI-WT (Fig 3.19B). Together, this indicates that morphine is inducing a functional shift at this extended timepoint. EcoHIV infection does not seem to have much impact on the predicted metabolites.

When MORKO animals were similarly analyzed, no shift was observed between Ms-MORKO (blue) or EcoMs-MORKO and PI-MORKO animals (black, enclosed by black dashed line) along the primary x-axis as was observed in WT animals (Fig 3.20A). Eco-MORKO (red), similarly to WT animals, also clustered closely with PI-MORKO. A heatmap was plotted of significant metabolite changes between MORKO treatment groups, which had fewer changes compared to WT (MORKO, Fig 3.20B; WT, Fig 3.19B). Unlike in WT animals, no treatment groups in MORKO animals clustered distinctly based on metabolite changes (Fig 3.20B). This matches what was observed in the species composition of MORKO animals discussed earlier, and again highlights that deletion of the mu opioid receptor protects from functional shifts in the microbiome induced by morphine.

PICRUSt analysis was also performed on samples from TLR2KO animals to look for predicted metabolite changes based on altered taxa. Clustering using the metabolite profile shows that Ms-TLR2KO (blue) and EcoMs-TLR2KO (green) clusters very closely with PI-TLR2KO (black, enclosed by dashed line) (Fig 3.21A). As was expected from the species composition, two out of three Eco-TLR2KO animals (red) clustered distinctly from PI-TLR2KO. Using the

118

significantly changed metabolites, a heatmap was generated that again shows the same two Eco-TLR2KO (red) samples clustering distinctly from all other samples (Fig 3.21B). Unlike WT animals, Ms-TLR2KO (blue) and EcoMs-TLR2KO (green) clustered with Pl-TLR2KO (black) animals. This protection in the absence of functional TLR2 further highlights the role that TLR2 plays in changes to microbial composition and metabolites observed in Ms-WT.

Dysbiosis with SIV+morphine

SIV is currently the best infectious model for human HIV infection, and is the gold standard to compare with the EcoHIV model. Microbiome dysbiosis has been shown in SIV,[200,201] as in human HIV infections,[7,6,132] however, these studies have looked at later time points of infection. Also, no studies have been published examining microbial changes in SIV in combination with opioid drugs. To fill this void, pre-treatment sample were obtained from 14 male rhesus macaques (Pre-NHP) (Fig 3.22). Animals with morphine treatment were given injections of 2 mg/kg morphine three times daily for 14 days, and then transitioned to 4mg/kg three times daily. Four animals were only given morphine (Ms-NHP; blue), with collections at D21, D64, and D84 in addition to a pre sample (Fig 3.22, top panel). Four animals were treated solely with SIV (SIV-NHP; red), and samples were collected 3, 8, 15, and 22 days post infection in addition to a pre sample (Fig 3.22 middle panel). Finally, SIV+morphine animals were treated with morphine (Ms-NHP; blue) for 70 days prior to receiving SIV

infection (SIVMs-NHP;green) (Fig 3.22 bottom panel). Samples were collected

at 21 and 64 days, which were analyzed as morphine alone. Following SIV

infection, samples were collected at 73 days morphine/3 days SIV, 78 days

morphine/8 days SIV, 84days morphine/14 days SIV, and 92 days morphine/22

days SIV. The collections with SIV in these animals mirror the time points of

fecal collections in SIV alone animals following infection.

Species number, or alpha diversity, was analyzed and no difference was

found when all time points within each treatment were grouped together (Fig

3.23A). Each group was then stratified over the time points collected to see if

any changes occurred over time. There were no changes observed in Ms-NHP

animals (Fig 3.23B), SIV-NHP (Fig 3.23C), or SIVMs-NHP (Fig 3.23D) animals

compared to Pre-NHP samples in each group. This suggests that the treatments

do not change the number of species in the microbiome at early time points.

The composition of species was analyzed to examine for changes among

the treatments. Similar to mouse experiments presented above, clustering by

Ms-NHP samples (various shades of blue) is distinct from Pre-NHP (black,

enclosed by black dashed line) (Fig 3.24A) with the exception of one sample. A

heatmap was generated using families that were significantly changed between

groups, which shows that Pre-NHP (black) samples clustered distinctly from Ms-

NHP (Fig 3.24B). Again, similar time points did not cluster together implying that

this shift occurs early and is relatively stable over the course of treatment.

120

Interestingly, *Methanobacteriaceae* of the kingdom *Archaea* was enriched in

many of the Ms-NHP samples. In contrast to what was observed in mice treated

with morphine, *Streptococcaceae* of the phylum *Firmicutes* was decreased in Ms-

NHP collections. SIV-NHP animals (various shades of red) also had a slight shift

in microbial composition compared to matched Pre-NHP samples (Fig 3.25A).

While not as distinct as clustering in Ms-NHP, a heatmap of the significantly

altered families shows clustering among SIV-NHP samples (Fig 3.25B). Not all

Pre-NHP samples clustered together, however the SIV-NHP samples that cluster

closely with Pre-NHP samples (black) are animal matched, suggesting that SIV

did not induce changes in these animals. Of these, 3 day SIV-NHP (dark red)

clusters most commonly with the Pre-NHP samples, which suggests that SIV

may progressively alter the microbiome and that any shifts in the microbiome are

among the earliest changes to occur. SIVMs-NHP (green) samples show

microbial composition shifts similarly to matched Ms-NHP (blue) time points (Fig

3.26A). A heatmap was constructed of the families significantly changed

between groups, which showed placebo (black) clustering distinctly from the

majority of morphine (blue) and SIV+morphine (green) samples (Fig 3.26B). Of

note, similar to morphine alone, methanobacteriaceae from the Archaea kingdom

were enriched while Streptococcaceae was diminished in morphine and

SIV+morphine samples.

Finally, the species composition of all samples was compared as a dendogram (Fig 3.27). This grossly highlights the shifts observed in Ms-NHP (blue) and SIVMs-NHP (green), which cluster distinctly from matched Pre-NHP samples (black). SIV-NHP (red) clusters more closely with matched Pre-NHP samples, again highlighting smaller changes compared with morphine. Morphine treatment causes a distinct shift in microbial composition, which clustered distinctly from all other Pre-NHP samples. SIV infection alone also induced a shift in microbial composition, especially at later time points of infection. However, ignoring the time points of infection, the microbial shifts in SIV-NHP are smaller than in Ms-NHP and SIVMs-NHP, which cluster distinctly (bottom of dendogram) from SIV-NHP and Pre-NHP (top of dendogram). Thus, at this stage of infection, SIV does not shift the microbiome beyond the dysbiosis that morphine has already induced.

To understand if particular taxa were driving the clustering in the species composition, an indicator species analysis was performed on the Pre-NHP and terminal collection timepoints (D84 morphine, D22 SIV, D92 morphine/D22 SIV) for each group (Fig 3.28). *YRC22* genus of the *Paraprevotella* family and *TM7* phylum are indicators of morphine alone, while morphine decreased the *Gammaproteobacteria* class. SIV alone increased the *Fibriobacteriaceae* family and *Gammaproteobacteria*, including *Enterobacteriaceae* family. SIVMs-NHP was found to decrease the *Streptococcaceae* family, which was also found to be

significantly changed compared with Pre-NHP (Fig 3.26B). Overall, while these

changes further validate that microbial dysbiosis does occur, the low amount of

predictable hits also imply that the clustering observed in the species

composition may result from many small changes rather than large distinct

changes in a few taxa.

Finally, to see if the shifts observed have functional consequences,

PICRUSt was again utilized to predict shifts in the bacterial metabolite profile.

The composition of predicted metabolites is shown among all treatment groups

without regard to time point of collection, which highlights variation from the tight

clustering of Pre-NHP (black, enclosed by black dashed line) samples (Fig 3.29).

Distinct clustering was not observed, however the variation among all treatments

again implies that small shifts are occurring in the microbiome which can

cumulatively alter the global metabolic profile. For each of the treatment groups,

a heatmap of the significantly changed metabolite groups were plotted.

Interestingly, Ms-NHP (various shades of blue) samples clustered distinctly from

their Pre-NHP (black, enclosed by black dashed line) samples (Fig 3.30).

Notable significant metabolites include methane metabolism, which was

expected from the increase in *Methanobacteriaceae*, as well as decreased

secondary bile acids (not shown in heatmap, p<.047). As expected due to fewer

shifts in the microbial composition, SIV-NHP (red) samples had fewer hits

compared with morphine (Fig 3.31). However, the majority of samples (12 out of

123

16) still clustered distinctly from pretreatment. SIVMs-NHP showed a more complex heatmap (Fig 3.32). Many metabolite groups were predicted to be significantly different between time points, however this did not provide obvious clustering: four of the pretreatment samples clustered closely, but two others clustered in the right third of the heatmap. The samples that clustered closely with the two Pre-NHP on the right were treatment time points from the same animals, indicating that changes may not occur as robustly in all animals. Still, the majority of treated samples clustered separately from the matched Pre-NHP samples. Aside from the two Pre-NHP samples that clustered with some of the treated samples from the same animals, there was no clustering when animals were grouped rather than treatment (not shown). Together, the PICRUSt analysis shows that functional metabolic shifts are likely to occur, which would impact the host gastrointestinal environment. However, especially at this very early stage of SIV infection, this alteration may not occur in a predictable matter between different animals but may stabilize at later time points.

3.5. Discussion

This study showed that morphine and EcoHIV/SIV induce microbial dysbiosis at very early stages of HIV infection. At both 3 days and 6 days morphine exposure in mice, dysbiosis occurred, as well as at time points from 21 up to 92 days in nonhuman primates. Both models of HIV infection were examined at time points earlier than previous studies of HIV-induced microbial

124

dysbiosis, including 5 days in EcoHIV infected mice and 3 to 22 days in SIV infected NHP. Interestingly, shifts in the microbial composition were apparent however the cumulative shift was not as robust as studies examining later time points have suggested.[7,6,132,200,201] Consequently, there was no greater shift in the microbiome of HIV models with morphine greater than what was observed in morphine alone. EcoHIV and SIV showed relatively small changes at the time points examined, suggesting that morphine effects are dominant when both treatments are present. Later time points of HIV infection may likely have stronger shifts, and need to be examined in the context of opioid drugs.

A major consequence of opioid use is constipation, which is reversible by blocking the mu opioid receptor.[209] Constipation has been shown to alter the gut microbiome independent of opioids,[94] and likely plays a role in the dysbiosis observed in both the mice and primate models treated with morphine. However, our group has shown that a low fiber diet model of constipation showed no significant bacterial translocation (Meng et al, in submission). An opioid-independent constipation control was not utilized in this study to assess whether bacterial shifts still occur, however future studies are needed to address this issue.

Opioids have also been reviewed to cause drastic systemic immune modulation of the host.[79] Likewise, immune modulation by opioids have also been shown in the gut, which leads to bacterial translocation and altered

tolerance to bacteria-mediated inflammation.[78,97,98,187,210] Morphine-induced bacterial translocation was hypothesized to drive immune activation in the GI tract that would induce bacterial dysbiosis. Indeed, morphine induced microbial dysbiosis in both mice and NHP animals. As predicted, the immune response plays an important role in morphine-induced dysbiosis as experiments showed that modulating the immune system (NSG and TLR2KO mice) showed protection from morphine-induced dysbiosis (Table 3.2). As NSG and TLR2KO animals both have active mu opioid receptors, they should experience constipation similarly to wildtype. Constipation of animals exposed to morphine was not quantified by this study, but will need to be addressed in future work. *Enterococcaceae*, and *Erysipelotrichaceae* families were consistent between the three groups, which suggest that these families may be altered by constipation. Differences observed between the genetic backgrounds can be attributed to the immune changes. The majority of populations enriched by morphine were gram-positive bacteria, which are primarily recognized by the innate TLR2 on epithelial and immune cells. TLR2KO animals did not experience morphine-induced changes in many of the taxa that were significantly altered in WT, highlighting the important role that TLR2 plays in morphine-induced dysbiosis. This model cannot differentiate which TLR2 expressing cell plays the most important role for morphine-induced dysbiosis, however epithelial cells are a good candidate that are regularly exposed to the bacteria in the gut lumen and have been showed to

126

have increased TLR2, as well as TLR4, expression in the presence of morphine.[97] NSG animals, which lack immune cells but maintain epithelial tight junctions, as no bacterial translocation was observed in these animals, and epithelial TLR expression, also had reduced morphine-induced dysbiosis compared with WT. The bacterial communities that were changed in NSG mice by morphine had additional members compared with TLR2KO animals. This difference between NSG and TLR2KO mice further supports the importance of TLR2 in morphine-induced modulation of the microbiome. Future experiments using adoptive transfer will be needed to delineate the importance on the role of epithelial cells versus immune cells in these functions.

Another potential mechanism by which morphine alters the microbiome can be as suggested in a recent article that certain bacteria may be able to sense and react to the presence of morphine, including chemotaxis.[100] Fecal content was found to have high levels of morphine in animals treated with morphine pellets. This gives the possibility that morphine is available to bacteria within the gut, and could possibly induce virulence factors and translocation through chemotactic mechanisms as is suggested in the literature. If this were happening changes would be expected in the microbiome signature of MORKO mice. MORKO animals do not have receptors available to bind morphine to act on whereas the bacteria within the gut are theoretically unchanged and, if capable, should still be able to sense morphine. In MORKO animals, at 6 days exposure

to morphine pellets, morphine induced changes were prevented. The observed protection should also be true in mice co-treated with morphine and naltrexone, however in this case naltrexone may be available in the lumen of the gut and could interfere with potential bacterial sensing. Regardless, complete protection was observed in mice co-treated with morphine and naltrexone three days after exposure. Together this implies that morphine is not acting directly on the bacteria but rather through host mediated effects including constipation and immune modulation.

Temporally, morphine caused fewer changes after six days of exposure to morphine pellets compared with three days of exposure. This may be a limitation of the morphine pellet at the time point examined, which has been shown to achieve peak serum levels at 24-48 hr and diminish significantly by 96 hr, or 4 days.[175] This time point was chosen initially to have morphine on board prior to EcoHIV infection, and to allow the infection time to establish itself. Nonhuman primate samples showed a shift in the microbiome induced by morphine independent of days of exposure. While dysbiosis in NHP with long term exposure to morphine suggests that the shift of microbiome is not limited by tolerance of morphine, this cannot be ruled out with these studies as NHP were subjected to escalating doses of morphine and different delivery compared to mice. Regardless, future studies utilizing the murine EcoHIV infection model will

be needed to utilize injections or a slow-release pump to overcome dosing limitations that are observed with the slow release pellet.

Dysbiosis has been observed in the gut microbiome at later stages of HIV infection, but it is currently unknown if it happens in early stages of pathogenesis.[6,132,200] In this study two infectious models of HIV, mouse EcoHIV and nonhuman primate SIV, were examined at very early time points of infection in order to overcome this gap. Mice infected with EcoHIV were examined at 5 day post-infection, which was chosen due to previous data that showed bacterial translocation occurring at 2 days post-infection. As previous studies have shown a link between dysbiosis and bacterial translocation,[76,77] dysbiosis was expected to occur shortly after translocation was observed. Unfortunately, dysbiosis was not apparent in Eco-WT animals, which may suggest that this time point was too early to observe shifts in the microbiome induced by HIV. EcoMS-WT induced dysbiosis that was similar to morphine alone, supporting that EcoHIV was causing relatively few microbial shifts beyond what is observed with morphine at this time point. Future studies will incorporate additional time points of later collections to resolve whether the infection in the presence of morphine is capable of inducing greater dysbiosis than infection alone. Similarly to EcoHIV experiments, NHP infected with SIV were examined at very early time points: 3 days, 8 days, 15 days, and 22 days post-infection. Microbial dysbiosis was induced by SIV-NHP compared to matched Pre-NHP samples, especially at time

points beyond 3 days post-infection. However, the microbial shifts observed were differential and not large enough to observe any distinct clustering. Samples from SIV-infected animals clustered distinctly from pretreatment samples in all animals. This suggests that SIV infection alone at these early time points did not significantly induce microbial shifts compared to pretreatment at the early time points examined. Previous studies showing microbial shifts have examined predominantly late stages of HIV infection when symptoms occur[7,6,200,201], however future studies will need to examine intermediate time points between those studies and this one to isolate the timing of microbial shifts. This would allow for interventional therapies to be developed, as the microbial shift that occurs is likely to play a role in disrupting gut homeostasis that helps drive HIV replication.

Additionally, SIVMs-NHP did not cluster distinctly from Ms-NHP collections in matched animals, supporting that SIV was having a minor impact on the microbiome compared with morphine at these time points. As with EcoHIV, later time points of SIV infection may be useful to see if dysbiosis occurs more overtly. Very few, if any, immune changes were observed systemically at time points examined in SIV infection (not shown), although gut specific immunity remains to be examined. Morphine has been shown to greatly increase HIV and SIV pathogenesis,[158,168] so SIV+morphine were expected to induce dysbiosis earlier

than SIV alone but this could not be mapped well at this early stage of SIV infection.

Interestingly, the significant indicator taxa were relatively few in nonhuman primate samples despite the observed clustering in PCoA. Morphine samples clustered consistently with samples from 21 days to 92 days, suggesting that morphine can stably alter the microbiome compared to the pretreatment samples. Animals were not taken off morphine to see if the microbiome reverted to pretreatment. Morphine may act differentially depending on the genetics of the host as well as the baseline microbiome, however the data from NHP suggests that morphine will still cause dysbiosis if long term opioids are prescribed which could have detrimental consequences.

Consequences from microbial dysbiosis induced functional shifts in the samples measured, as changes were observed in both predicted and measured metabolites. Metabolite shifts can contribute to host pathologies and disruption of gut homeostasis, including further changes in the gut microbiome.[211,212] Predicted metabolites using PICRUSt has been validated to correlate with actual metabolic changes, and performed on all microbiome samples.[202] In the first set of experiments using three days of morphine exposure, metabolic chemicals from fecal content were measured with mass spectrometry which allowed us to validate the relevance of PICRUSt in these experiments. Interestingly, the biggest change observed in mass spectrometry was among bile acids, however

131

bile acids were not detected as changed by PICRUSt. The discrepancy between

mass spectrometry and PICRUST suggests that, while PICRUSt is useful for

looking at gross changes, it may miss changes that are due to low abundance

bacteria since it doesn't take into account the volume capability of the bacteria,

solely the amount of DNA observed through sequencing. Through the majority of

these experiments, PICRUSt showed differential clustering between treatment

groups which suggests that the predicted metabolic profile of morphine at

multiple time points, EcoHIV/SIV, and in combination are altered. These findings

correlate very closely with the bacterial signature, which should come as no

surprise. While bacteria could change but the metabolic function stays the same,

this is unlikely as bacteria are competing for resources and a changing

microbiome likely reflects a selection for bacteria better able to compete in the

given environment.[57]

Bile acids were a notable change detected by mass spectrometry in the

morphine treated samples due to their established role in preventing bacterial

overgrowth and translocation.[205–207] Both primary and secondary bile acids were

decreased by morphine, which implies that secondary bile acid is reduced due to

lower availability of primary bile acid from the host. This suggests that morphine

alters the ability of the host to produce bile acids in the liver, or the capacity of

primary bile acid to traffic to the gut. The experiments discussed here could not

resolve this question, however future studies will analyze host metabolites

including the liver to elucidate the source of change. As PICRUSt could not predict the bile acid changes observed with mass spectrometry, it will be very useful to assess the effects of EcoHIV/SIV with or without morphine on bile acids. Finally, looking at bile acids temporally with morphine treatment will be important as well. If it is an early step in the disruption of gut homeostasis, it may be a therapeutic target for preventing microbial dysbiosis and bacterial translocation.

Overall, these studies show that morphine induces drastic microbial dysbiosis regardless of time point and model. Morphine was evaluated in the context of HIV models, however an early stage of infection was examined where discreet changes were not obvious. Minor changes were observed in the HIV models relative to morphine, however dysbiosis likely continues to develop further along in pathogenesis of HIV. In both morphine and HIV conditions, bacterial dysbiosis predicted changes in metabolites, and found measured metabolite changes resulting from morphine. Altered metabolites can have detrimental impacts on the host and the host immune responses, including to HIV and opportunistic infections. This study was conducted using time points much earlier than has been previously studied in HIV, but there remains a need to look at intermediate time points of HIV infection to ultimately uncover the mechanisms and timing of dysbiosis.
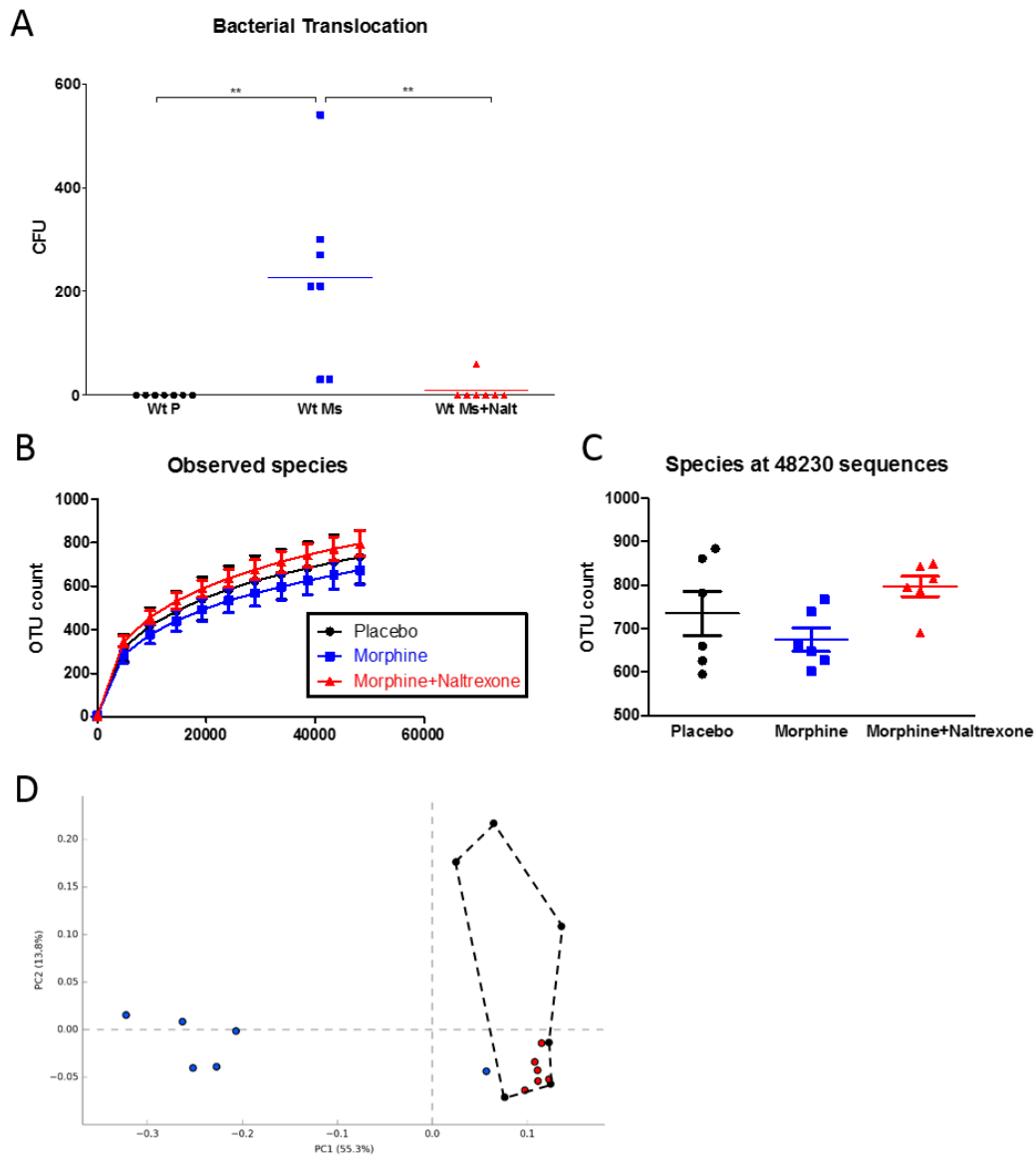
Fig 3. 1 Morphine Induces bacterial translocation and shifts in microbial composition
(A)Ms-WT induces translocation to liver following 72hr exposure to 25mg morphine pellet, which is reversible by naltrexone. (B)Alpha diversity, or number of observed species, is unchanged between treatments. (C)Number of observed species in individual animals at 48230, the minimum number of sequences in each sample, is unchanged. (D)Ms-WT animals (blue) show a distinct shift in composition of species away from both PI-WT (black, enclosed by dashed black line) and MN-WT(red).**P<.01

134

↓Morphine (PI-WT / MN-WT)

Phylum	Class	Order	Family	Genus	stat	p value
					0.975	0.006
Firmicutes	Clostridia	Clostridales	Peptococcaceae	rc4-4	0.975	0.006
					0.88	0.018
					0.88	0.018
					0.88	0.018
					0.88	0.018
Cyanobacteria	Chloroplast	Streptophyta	unid.	unid.	0.88	0.018

↑Morphine (Ms-WT)

Phylum	Class	Order	Family	Genus	stat	p value
					0.99	0.017
					0.81	0.011
			unid.	unid.	0.81	0.011
					0.9	0.002
				unid.	0.91	0.001
			Bacillaceae	Anaerobacillus	0.9	0.001
					1	0.001
				unid.	0.99	0.001
				Lysinbacillus	0.91	0.001
			Planococcaceae	Ureibacillus	0.91	0.001
					0.99	0.009
				Salinicoccus	0.82	0.011
		Bacillales	Staphylococcaceae	Staphylococcus	0.99	0.009
					0.9	0.007
					0.9	0.007
		Gemellales	unid.	unid.	0.9	0.007
					0.9	0.001
			Carnobacteriaceae	Granulicatella	0.9	0.001
					0.99	0.004
				unid.	0.91	0.003
			Enterococcaceae	Enterococcus	1	0.001
					0.89	0.001
	Bacilli	Lactobacillales	Streptococcaceae	unid.	0.9	0.001
					0.86	0.027
			Christensenellaceae	unid.	0.86	0.027
	Clostridia	Clostridales	Ruminococcaceae	Anaerotruncus	0.95	0.001
Firmicutes	Erysipelotrichi	Erysipelotrichales	Erysipelotrichaceae	Allobaculum	1	0.001

Fig 3. 2 Indicator species of morphine and non-morphine treatments
Indicator species analysis of treatment groups revealed a distinct profile of taxa that were upregulated by Ms-WT (blue), which are predominantly gram positive from the phylum Firmicutes. Taxa that were higher in PI-WT and MN-WT animals (black+red overlay) are decreased by morphine, which included one gram positive of Firmicutes and one gram negative of phylum Cyanobacteria.

135

	Families increased in WT-Ms
Bacteria translocated to liver (serotyped*)	Enterococcaceae Staphylococcaceae Bacillaceae
Not found in bacteria translocated to liver	Carnobacteriaceae Christensenellaceae Erysipelotrichaceae Planococcaceae Ruminococcaceae Streptococcaceae

*serotyping data courtesy of Jingjing Meng

Table 3. 1 Comparison of enriched families in fecal matter and translocated bacteria to liver induced by morphine
Serotyping was performed on bacteria which translocated to the liver of Ms-WT animals. The three families that were identified overlapped with families found to be increased in the fecal content of Ms-WT animals. Other families increased in Ms-WT fecal content were not translocated.

136
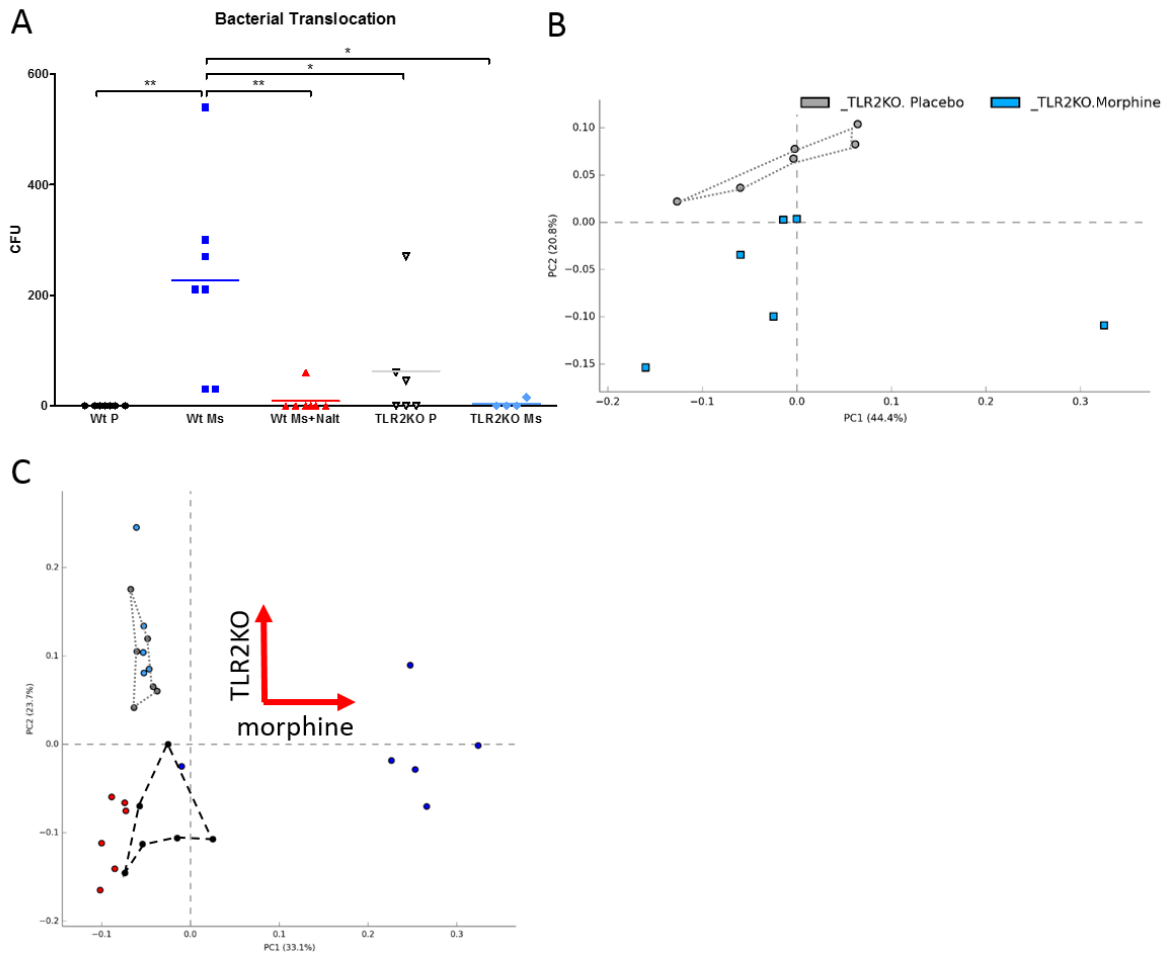
Fig 3. 3 TLR2KO mice show protection from bacterial translocation and dysbiosis
(A) Bacterial translocation to liver that is induced in Ms-WT animals is abolished in Ms-TLR2KO animals. (B) Ms-TLR2KO animals (light blue) show a shift from Pl-TLR2KO animals (grey, enclosed by grey dotted line). (C) When compared with changes in WT animals, the difference between Pl-TLR2KO (grey, enclosed by grey dotted line) and Ms-TLR2KO (light blue) disappears. Ms-WT (dark blue) induces a shift along the x-axis compared with Pl-WT (black, enclosed by black dashed line) and MN-WT (red), whereas Pl-TLR2KO and Ms-TLR2KO are shifted up on the y-axis compared with placebo animals.

137

PI-TLR2KO

↑All TLR2KO

Phylum	Class	Order	Family	Genus	stat	p value
Firmicutes	Bacilli	Lactobacillales	Streptococcaceae	Streptococcus	0.84	0.001
Proteobacteria	Deltaproteobacteria	Desulfovibrionales	Desulfovibrionaceae	Bilophilia	0.82	0.002

Ms-TLR2KO

↑Morphine (WT&TLR2KO)

Phylum	Class	Order	Family	Genus	stat	p value
	Erysipelotrichi	Erysipelotrichales	Erysipelotrichaceae	Allobaculum	0.996	0.001
					0.955	0.001
				Enterococcus	0.955	0.001
			Enterococcaceae	unid.	0.863	0.001
			Streptococcaceae	unid.	0.906	0.001
					0.707	0.019
Firmicutes	Bacilli	Lactobacillales	unid.	unid.	0.707	0.019

↑Ms-WT

Phylum	Class	Order	Family	Genus	stat	p value
					0.952	0.022
					0.805	0.006
			unid.	unid.	0.805	0.006
					0.878	0.007
				unid.	0.9	0.002
				Anaerobacillus	0.843	0.004
			Bacillaceae	Bacillus	0.694	0.032
					0.983	0.003
				unid.	0.949	0.001
				Lysinibacillus	0.912	0.003
			Planococcaceae	Ureibacillus	0.833	0.003
					0.929	0.017
				Salinicoccous	0.816	0.005
		Bacillales	Staphylococcaceae	Staphylococcus	0.927	0.018
					0.871	0.002
					0.871	0.002
		Gemellales	unid.	unid.	0.871	0.002
					0.767	0.014
	Bacilli	Lactobacillales	Carnobacteriaceae	Granulicatella	0.757	0.02
Firmicutes	Clostridia	Clostridiales	Ruminococcaceae	Anaerotruncus	0.946	0.001

↑All WT

Phylum	Class	Order	Family	Genus	stat	p value
					0.97	0.001
					0.97	0.001
Actinobacteria	Actinobacteria	Bifidobacteriales	Bifidobacteriaceae	Bifidobacterium	0.97	0.001

PI-WT

MN-WT

Ms-WT

Fig 3. 4 Indicator species differ between Ms-TLR2KO and Ms-WT animals

138

Indicator species analysis of treatment groups revealed a distinct profile of taxa that were unique to TLR2KO (overlay of grey and light blue) and WT animals (overlay of black, red, and dark blue). Ms-TLR2KO animals share indicators with Ms-WT (overlay of light blue and dark blue). However, Ms-WT have distinct indicator species from TLR2KO morphine, implying that Ms-TLR2KO animals are protected from morphine-induced dysbiosis.

Fig 3. 5 NSG mice show protection from bacterial translocation and dysbiosis
(A) Bacterial translocation to liver that is induced in Ms-WT animals is abolished in Ms-NSG animals. (B) Ms-NSG animals (blue) show a shift from PI-NSG animals (black, enclosed by black dashed line).

PI-NSG

↓Morphine

Phylum	Class	Order	Family	Genus	stat	p value
Firmicutes	Clostridia	Clostridiales	Lachnospiraceae	Anaerostipes	0.99	0.01

↑Morphine

Phylum	Class	Order	Family	Genus	stat	p value
					0.993	0.01
					0.993	0.01
		Bacillales	Staphylococcaceae	Staphylococcus	0.993	0.01
					0.999	0.01
	Bacilli	Lactobacillales	Enterococcaceae	Enterococcus	0.999	0.01
					0.955	0.01
			Clostridiaceae	unid.	0.936	0.01
					1	0.01
			Peptostreptococcaceae	unid.	1	0.01
	Clostridia	Clostridiales	Ruminococcaceae	Anaerotruncus	0.99	0.016
Firmicutes	Erysipelotrichi	Erysipelotrichales	Erysipelotrichaceae	Coprobacillus	0.894	0.045

Ms-NSG

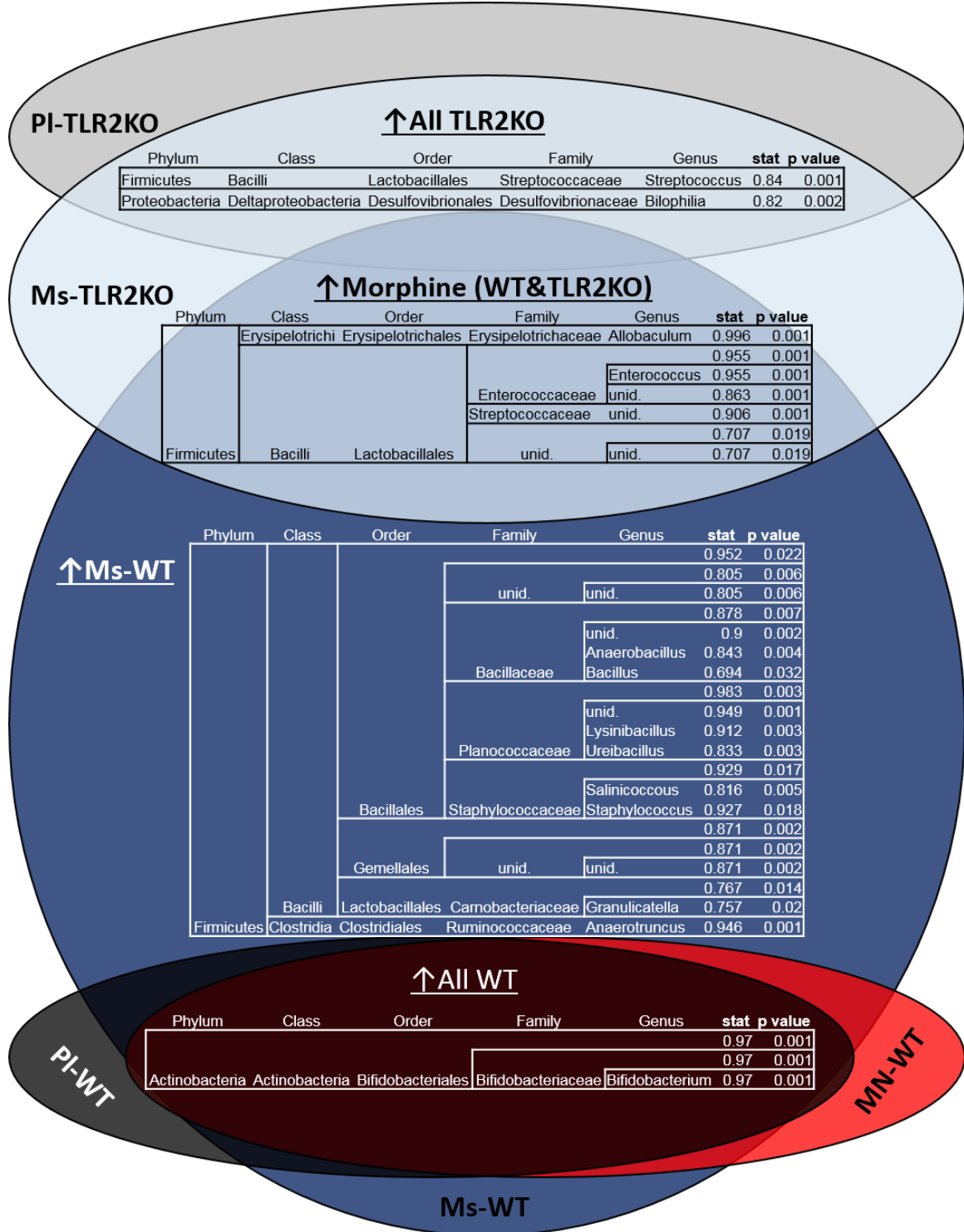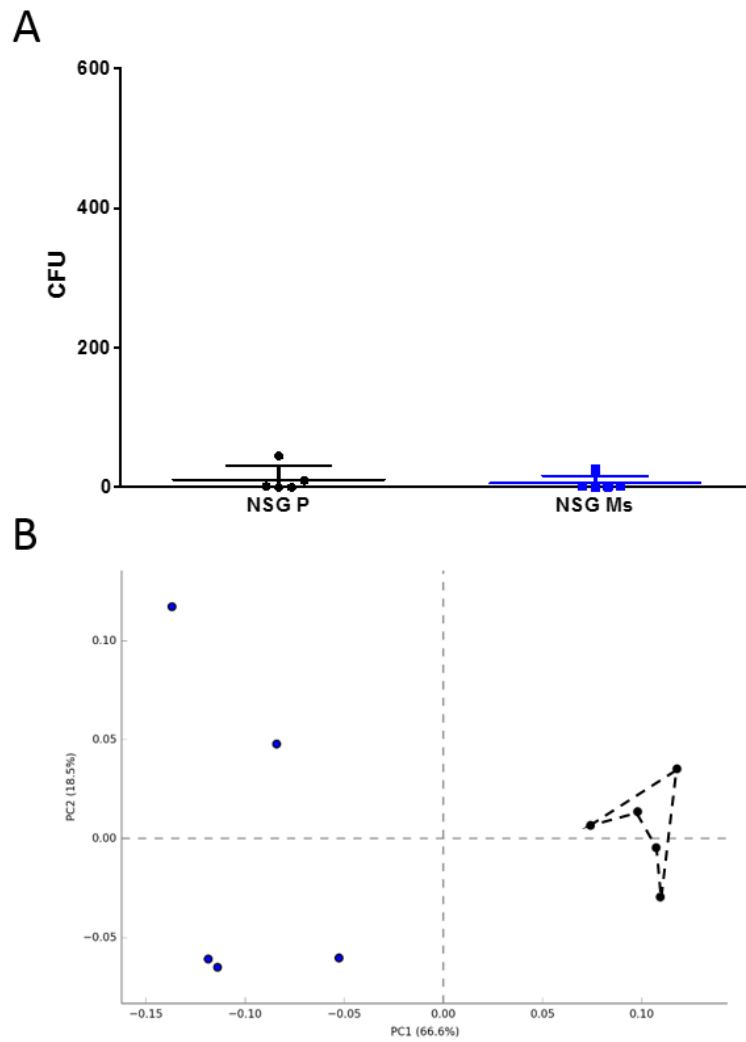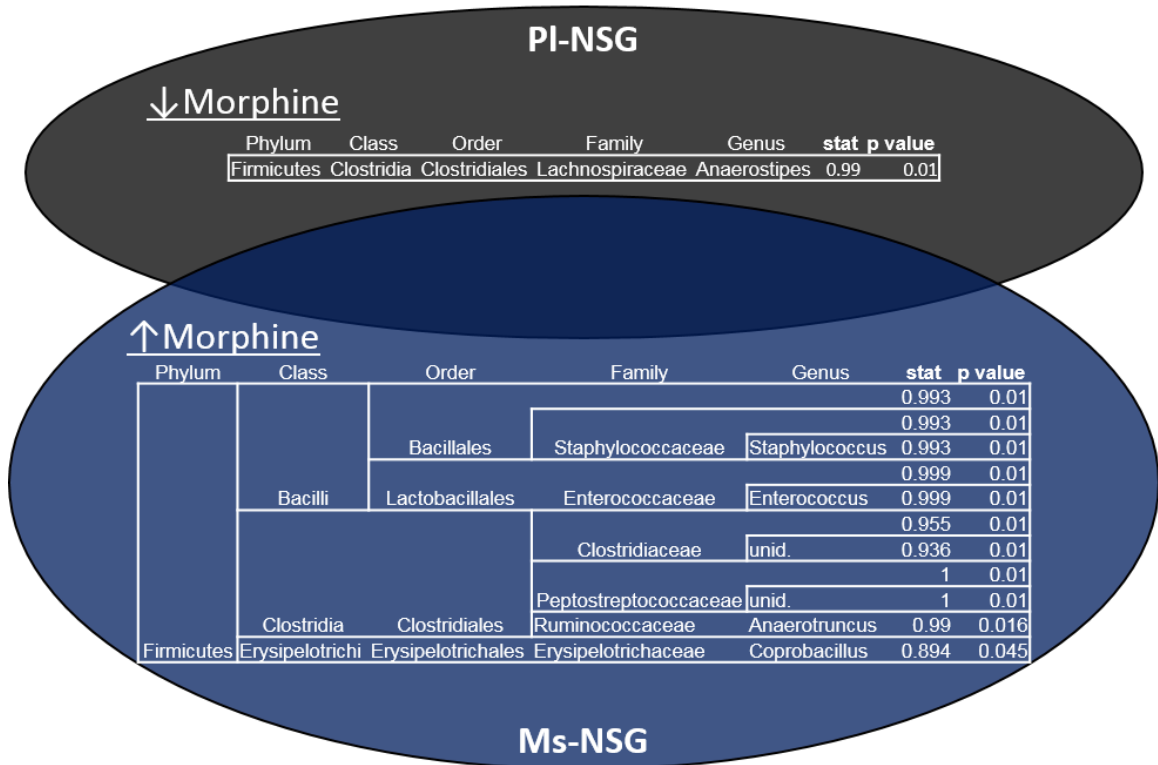**Fig 3. 6 Indicator species of Ms-NSG animals**

Indicator species analysis of treatment groups revealed a distinct profile of taxa that were unique to Ms-NSG animals (blue) compared with PI-NSG (black). This profile shared commonalities but was shorter than Ms-WT, implying that having a functional immune response plays a role in dysbiosis.

141

Strain	Families increased by Morphine	Families decreased by Morphine
Ms-WT	Bacillaceae Carnobacteriaceae Christensenellaceae Enterococcaceae Erysipelotrichaceae Planococcaceae Ruminococcaceae Staphylococcaceae Streptococcaceae	Peptococcaceae
Ms-TLR2KO	Enterococcaceae Erysipelotrichaceae Streptococcaceae	
Ms-NSG	Clostridiaceae Enterococcaceae Erysipelotrichaceae Peptostreptococcaceae Ruminococcaceae Staphylococcaceae	Lachnospiraceae

Table 3. 2 Comparison of Indicator species by morphine treatment between WT, TLR2KO, and NSG mice
Indicator species associated with morphine treatment were compiled to obtain families increased and decreased within each genotype. Ms-TLR2KO and Ms-NSG mice share commonalities with Ms-WT (taxa in red), however each share only part of the list from Ms-WT.

Statistical Comparisons			
Welch's Two-Sample *t*-Test	WT+Morphine WT+Placebo	WT+Morphine+NTX WT+Placebo	TLR2 KO+Placebo WT+Placebo
Total biochemicals $p \leq 0.05$	73	34	63
Biochemicals (↑↓)	16 | 57	10 | 24	4 | 59
Total biochemicals $0.05 < p < 0.10$	28	23	26
Biochemicals (↑↓)	10 | 18	6 | 17	7 | 19
Welch's Two-Sample *t*-Test	WT+Morphine+NTX WT+Morphine	TLR2 KO+Morphine WT+Morphine	TLR2 KO+Morphine TLR2 KO+Placebo
Total biochemicals $p \leq 0.05$	84	36	50
Biochemicals (↑↓)	48 | 36	8 | 28	29 | 21
Total biochemicals $0.05 < p < 0.10$	30	24	32
Biochemicals (↑↓)	15 | 15	11 | 13	10 | 22

Table 3. 3 Statistical comparison of metabolite biochemical changes in Ms-WT and Ms-TLR2KO animals
Collected fecal matter was isolated for mass spectrometry and assessed for known biochemical metabolites. All comparisons saw a change in metabolites, either upregulated (red) or downregulated (green). The number of significant changes in Ms-WT compared with Pl-WT and MN-WT was relatively equivalent, and higher than between MN-WT and Pl-WT. TLR2KO animals saw changes from WT, which was expected due to microbial shifts observed. Ms-TLR2KO animals did see a shift compared with Pl-WT, however the number of metabolites significantly altered implies that TLR2KO is protecting from changes associated with morphine.

Random Forest Confusion Matrix
Predicted Group

Actual Group	TLR2 KO Morphine	TLR2 KO Placebo	WT Morphine	WT Morphine +NTX	WT Placebo	Class Error
TLR2 KO Morphine	6	0	0	0	0	0.000
TLR2 KO Placebo	0	6	0	0	0	0.000
WT Morphine	1	0	5	0	0	0.167
WT Morphine +NTX	0	0	0	6	0	0.000
WT Placebo	0	0	0	0	6	0.000
Predictive accuracy = 97%						

Table 3. 4 Metabolic profiles could accurately predict treatment groups
Following mass spectrometry, the profile of metabolites analyzed were utilized in a random forest matrix to see if metabolites could predict which group they belonged to. All samples were accurately predicted, aside from one Ms-WT sample which was misclassified as Ms-TLR2KO.
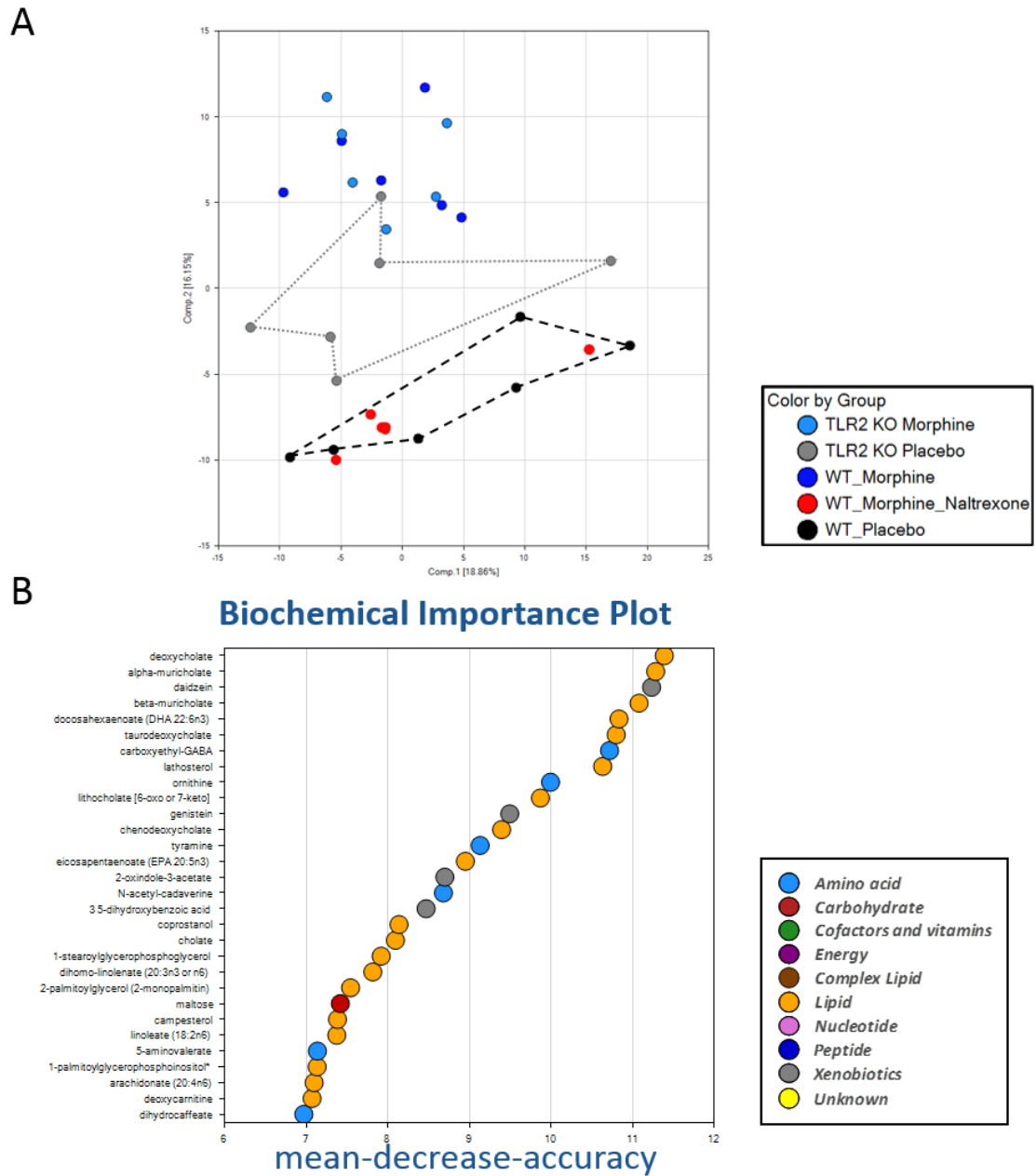
Fig 3. 7 Metabolic signature of morphine animals cluster distinctly from placebo independent of TLR2KO

(A) PCoA of metabolites shows distinct clustering of Pl-WT (black) with MN-WT (red); also Ms-WT (blue) with Ms-TLR2KO (light blue). Pl-TLR2KO placebo (grey) is an intermediate between the other two clusters. (B) Metabolites with the highest change between groups were graphed, which showed lipids were the most commonly change and bile acids had numerous hits.

145
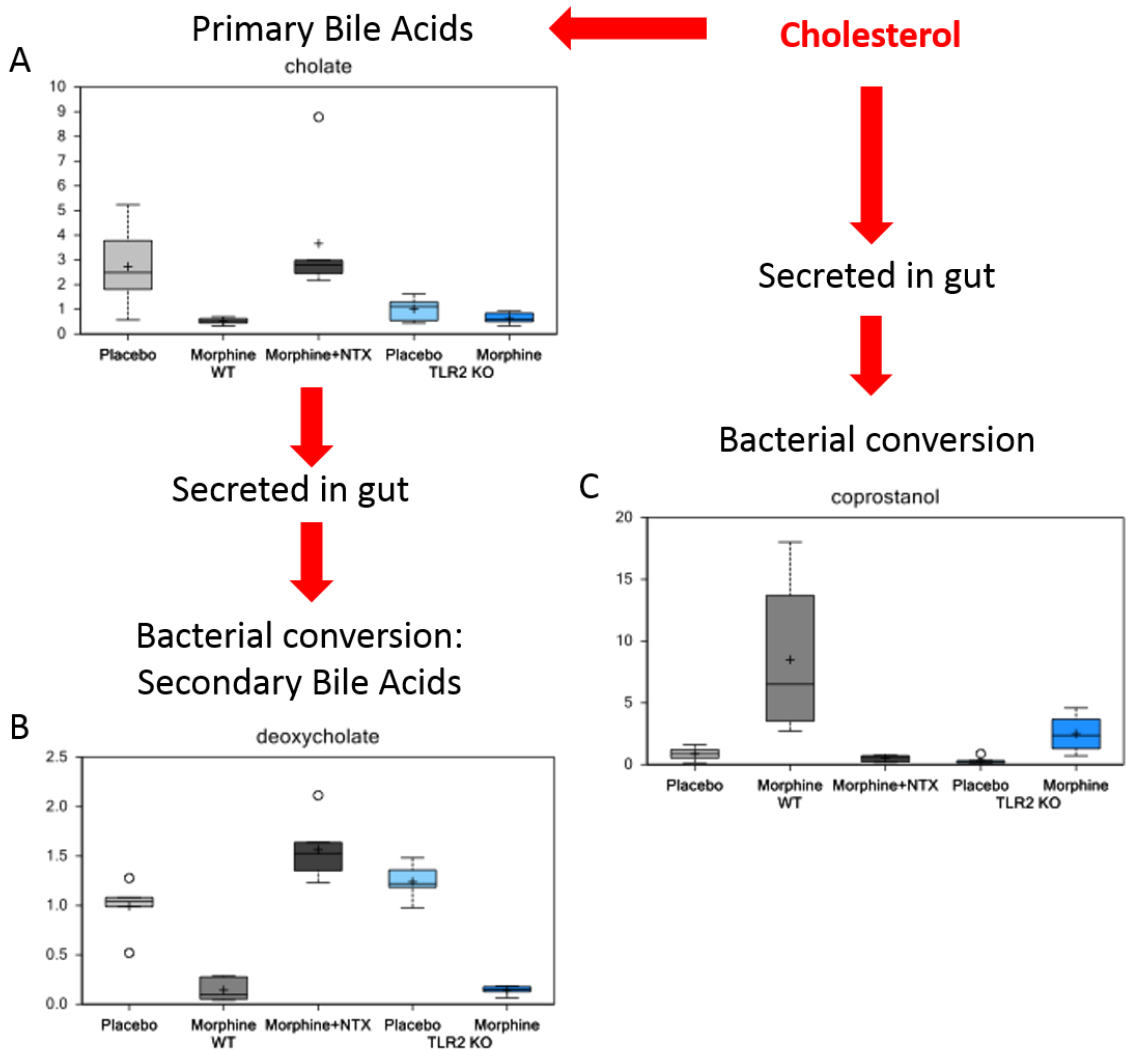
Fig 3. 8 Bile acids were changed by morphine, which was replaced by coprastanol
(A) Primary bile acid cholate was decreased in Ms-WT compared with Pl-WT and MN-WT animals. Pl-TLR2KO animals had a lower baseline than Pl-WT, which made Ms-TLR2KO not appear changed. (B) Secondary bile acids were similarly lowered in Ms-WT animals as well as Ms-TLR2KO animals, suggesting that primary bile acids are reduced by morphine in both backgrounds. (C) Cholesterol can be directly secreted into the gut and converted to coprostanol, which is increased in Ms-WT and, albeit less, Ms-TLR2KO animals.

146
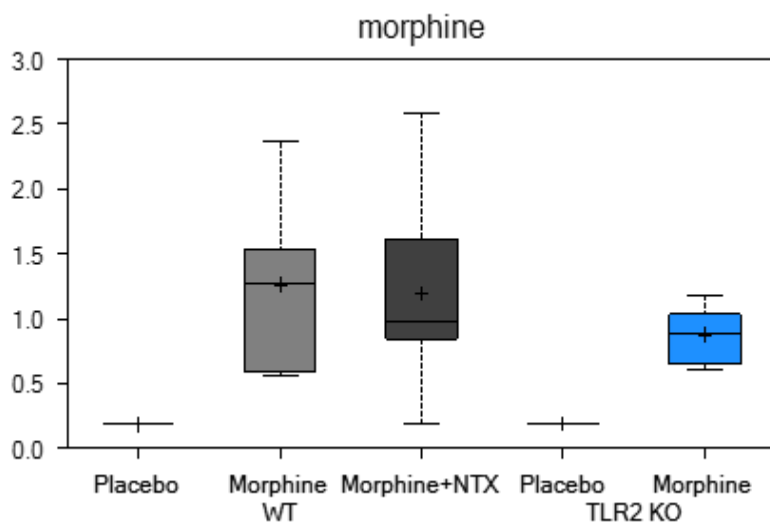
Fig 3. 9 Morphine is detectible by mass spectrometry in the fecal matter
Morphine was analyzed in samples, and was found at high levels in Ms-WT, MN-WT, and Ms-TLR2KO. This highlights the gastrointestinal tract as a major excretion pathway of morphine, and introduces the possibility that bacteria are directly exposed to morphine.
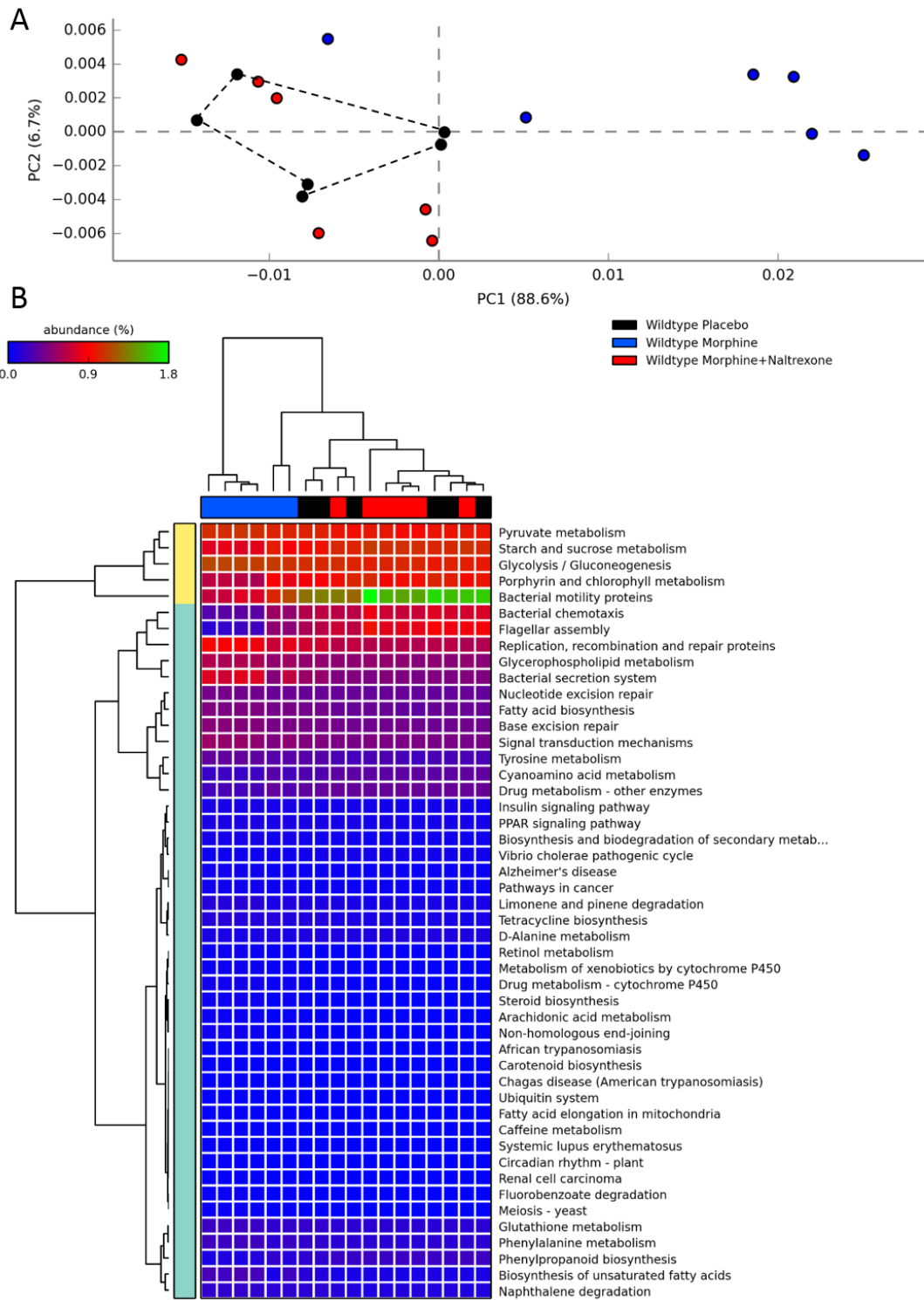
Fig 3. 10 Morphinie induces changes in predictive metabolomics

(A) Predictive metabolites were predicted via PICRUSt algorithm, which showed that Ms-WT (blue) was predicted to cluster distinctly from both Pl-WT (black, enclosed by dashed black line) and MN-WT (red) samples. (B) Heatmap of significantly changed metabolites (p<.05) shows clustering of Ms-WT (blue) compared to Pl-WT (black) and MN-WT (red).
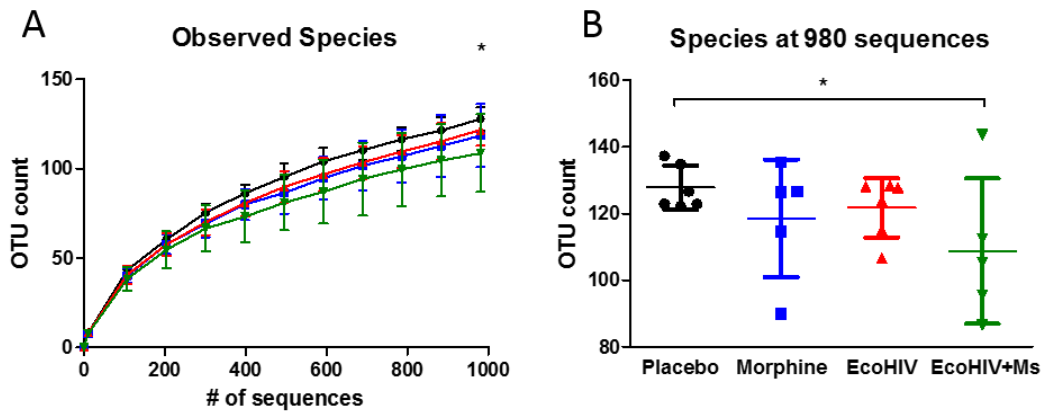
Fig 3. 11 Number of species in EcoMs-WT animals is reduced compared to other groups
(A) Pl-WT (black), Ms-WT (blue), Eco-WT (red) and EcoMs-WT (green) was compared for
number of observed species. A significant increase was found between EcoMs-WT and Pl-WT at
980 sequences, which was the minimum number of sequences among the samples. (B)
Observed species at 980 sequences showing individual animals, where the comparison of
EcoMs-WT and Pl-WT was significantly different. *p<.05

150
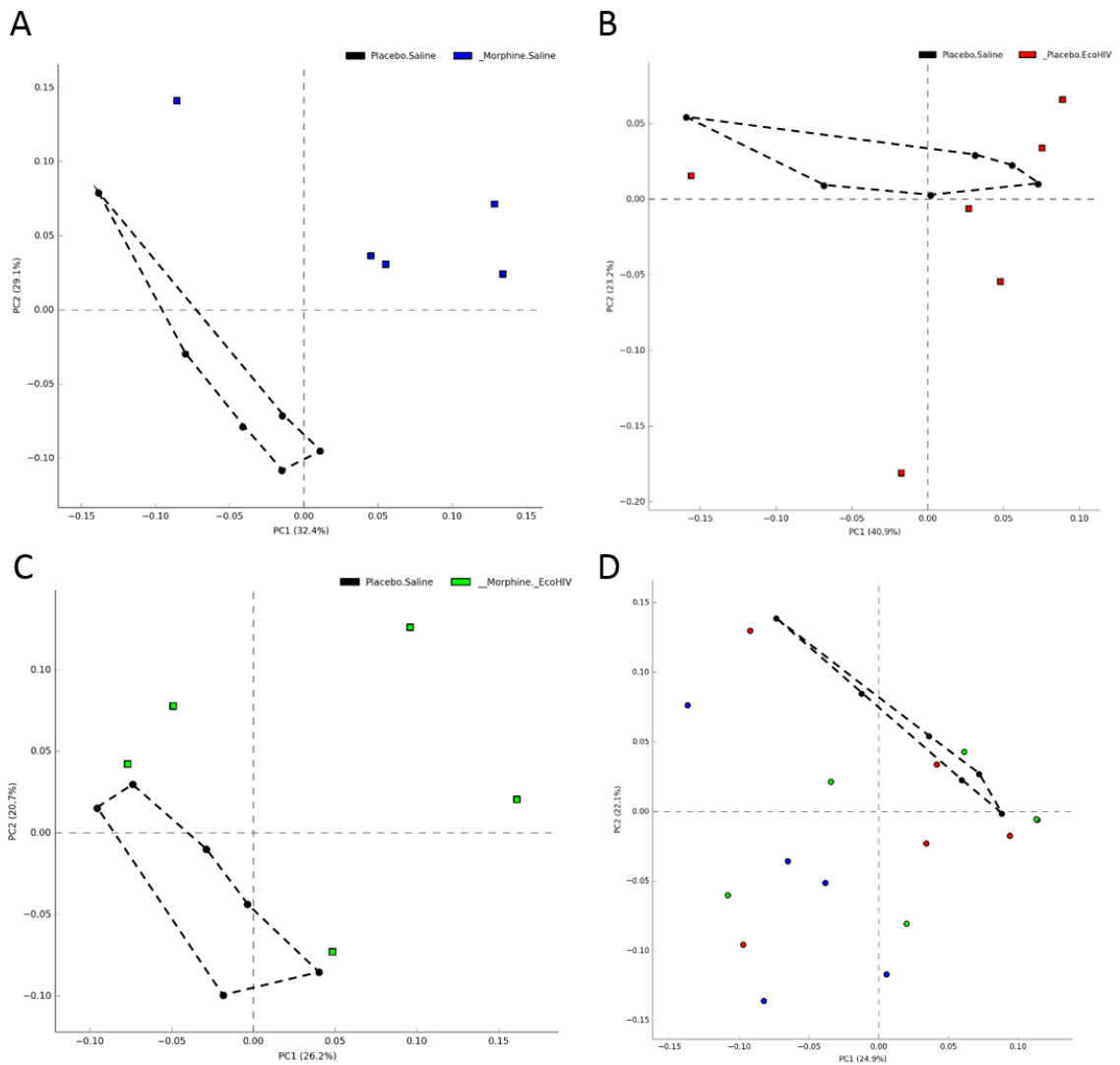
Fig 3. 12 Morphine in the absence or presence of EcoHIV induces dysbiosis
(A) Ms-WT (blue) shows distinct clustering from Pl-WT (black, enclosed by black dashed line).
(B) Eco-WT (red) does not show distinct clustering from Pl-WT (black, enclosed by black dashed line). (C) EcoMs-WT (green) shows clustering separate from Pl-WT (black, enclosed by black dashed line), in 3 out of 5 animals. (D) Combined, morphine induces distinct clustering from Pl-WT (black, enclosed by dashed black line) in both EcoMs-WT (green) and Ms-WT (blue). Eco-WT (red) alone does not induce change at this time point.
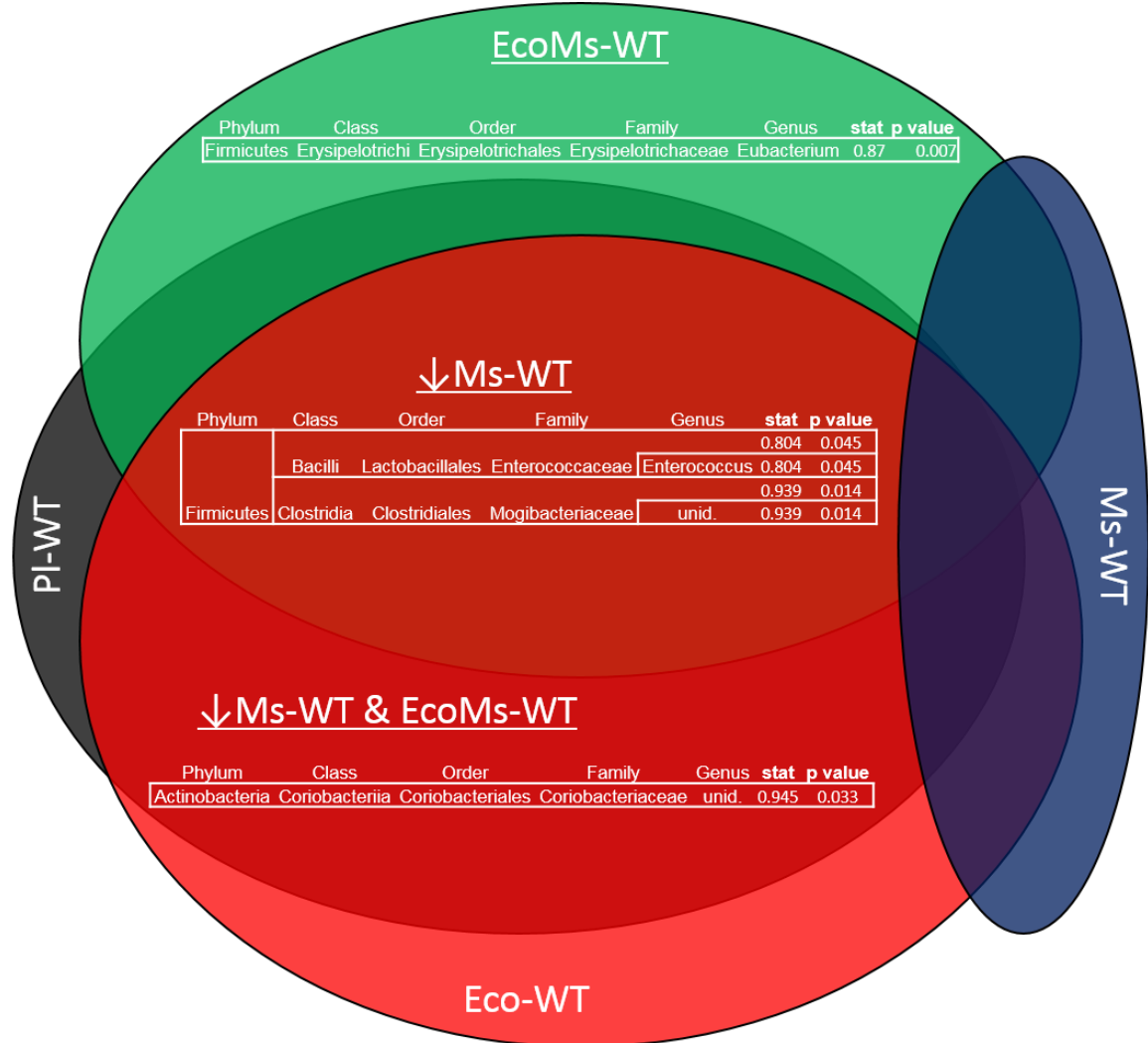
Fig 3. 13 Indicator species of 6 days morphine with and without EcoHIV infection
Closed-reference-picked species from wildtype animals treated with morphine for six days and/or EcoHIV infection for five days. Indicator species analysis of treatment groups revealed a distinct profile of taxa that were associated with EcoMs-WT (green). Taxa indicated by PI-WT and Eco-WT animals (black+red overlay) are taxa that are decreased in Ms-WT and EcoMs-WT animals. Interestingly, the largest category indicated PI-WT, Eco-WT, and EcoMs-WT (Black, red, green overlay) which indicated a decrease in Ms-WT animals. The outgrowth of populations in Ms-WT animals was not observed here at 6 days exposure as it was in Ms-WT at 3 days exposure.
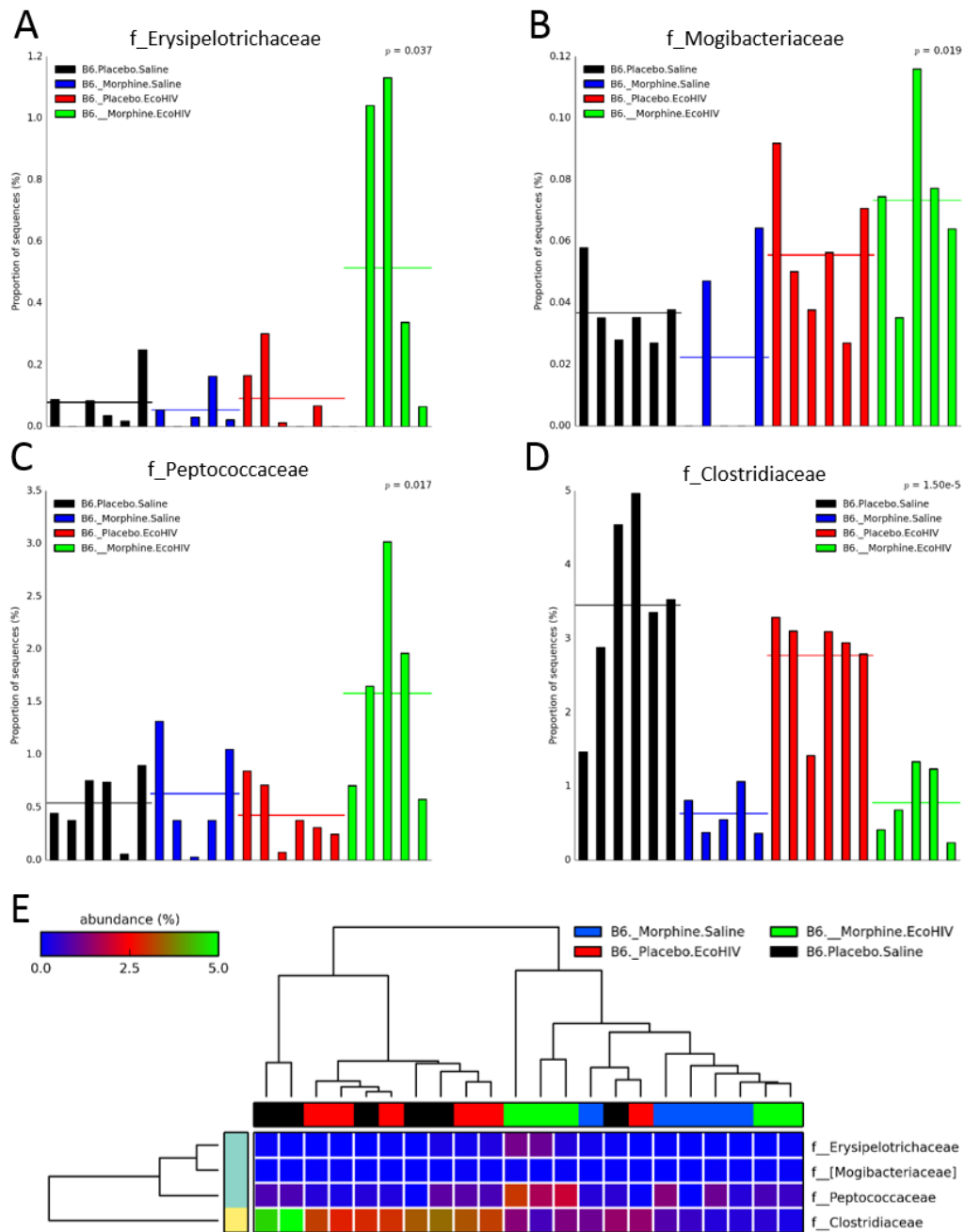
Fig 3. 14 Families significantly changed with Ms-WT and Eco-WT
6 days exposure to morphine and 5 days EcoHIV infection leads to significant family changes in wildtype animals. (A) Erysipelotrichaceae is significantly upregulated by EcoMs-WT. (B) Mogibacteriaceae is significantly upregulated by EcoMs-WT and trends upwards in Eco-WT alone. (C) Peptococcaceae is increased by EcoMs-WT. (D) Clostridiaceae is downregulated in Ms-WT and EcoMs-WT. (E) Performing a heatmap of these four families results in a clustering of Ms-WT (blue) and EcoMs-WT (green), but not Eco-WT (red), samples distinctly from Pl-WT (black).

153
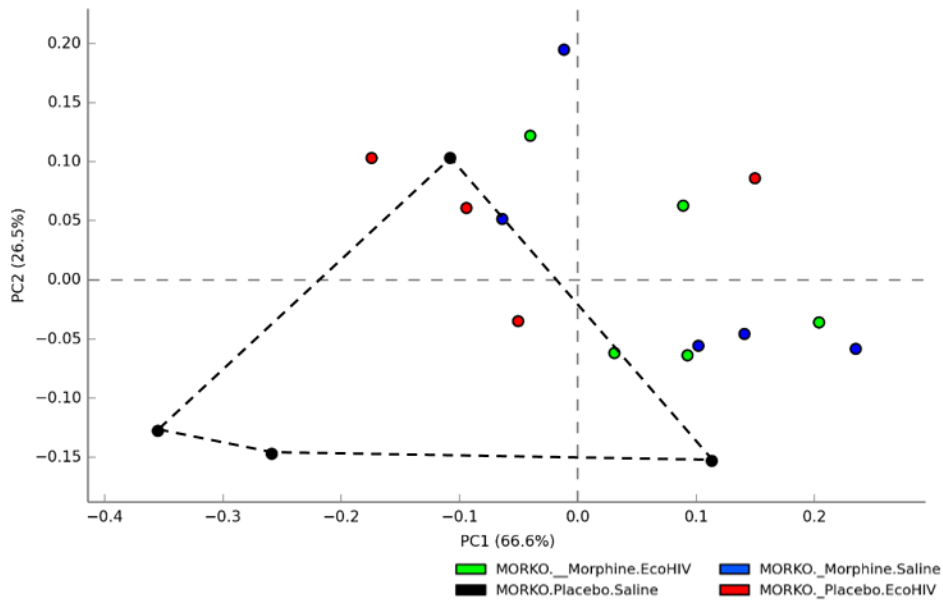
Fig 3. 15 MORKO mice are protected from dysbiosis induced by morphine and EcoHIV
Closed-reference-picked species from MORKO animals treated with morphine for six days and/or
EcoHIV infection for five days were analyzed by PCoA. Ms-MORKO (blue), Eco-MORKO (red),
and EcoMs-MORKO (green) did not cluster distinctly from PI-MORKO (black, enclosed by black
dashed line).
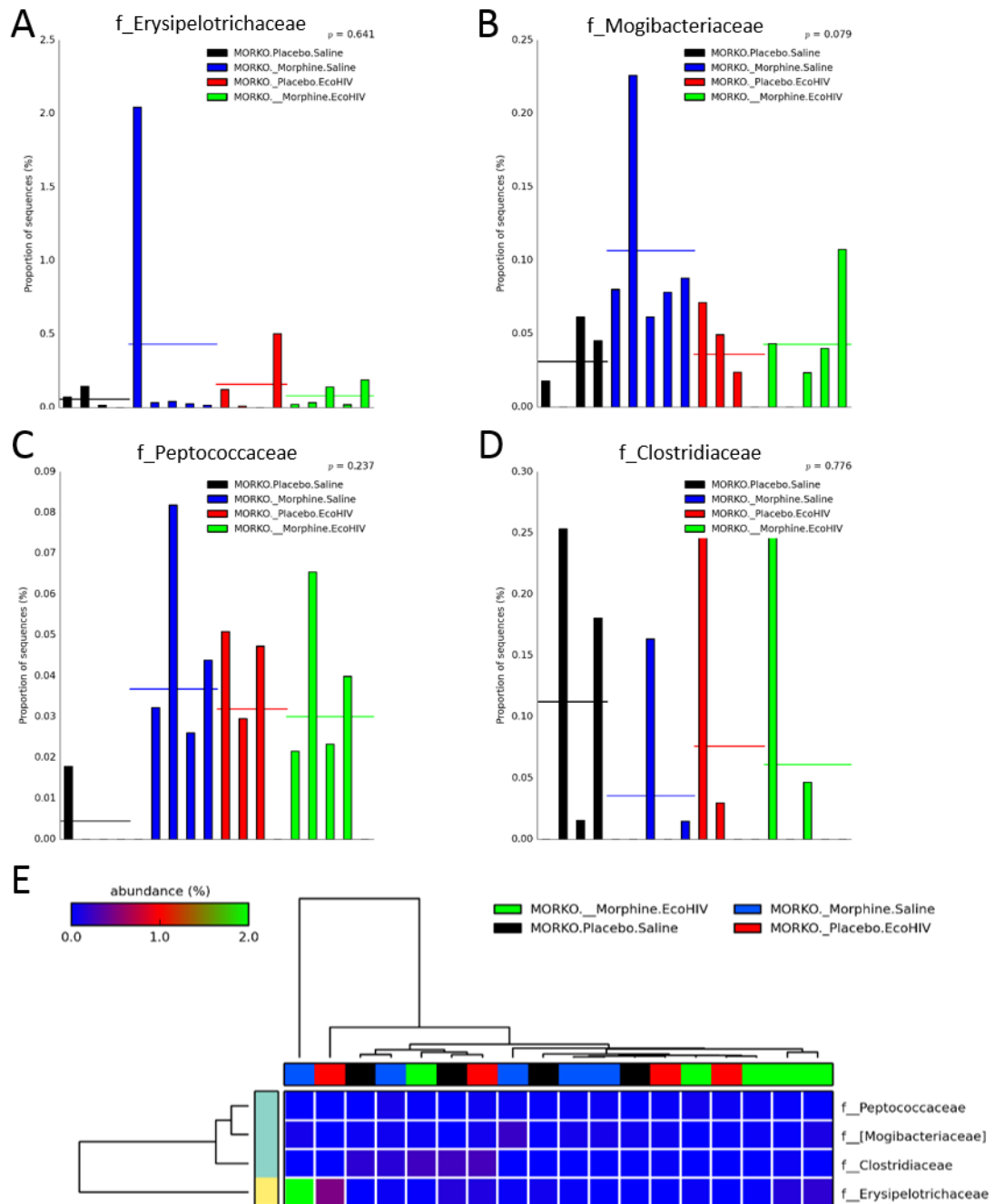
Fig 3. 16 Ms-MORKO is protected from changes in families that were altered in Ms-WT animals

Significant families in closed-reference-picked species from MORKO animals treated with morphine for six days and/or EcoHIV infection for five days. Erysipelotrichaceae (A), Mogibacteriaceae (B), Peptococcaceae (C), and Clostridaceae (D) had no significant changes in Ms-MORKO, Eco-MORKO, or EcoMs-MORKO animals. (E) A heatmap of these families produced no clustering between treatment groups.

155
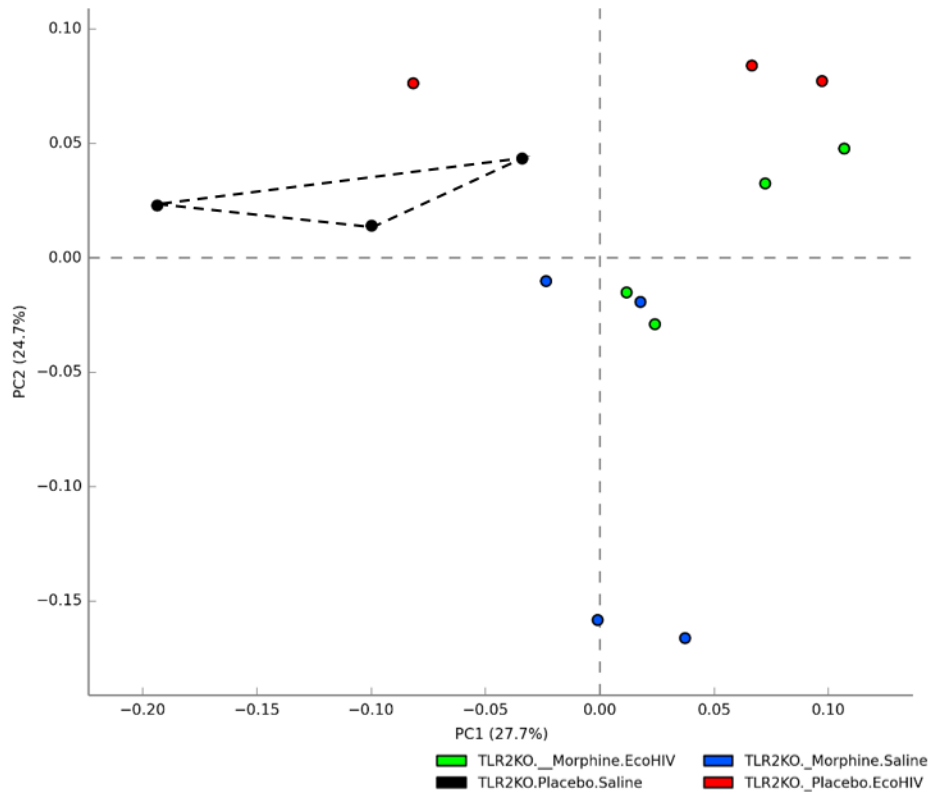
Fig 3. 17 TLR2KO shows dysbiosis in morphine and EcoHIV treated animals
Closed-reference-picked species from TLR2KO animals treated with morphine for six days and/or
EcoHIV infection for five days were analyzed by PCoA. Ms-TLR2KO (blue) clusters distinctly
from PI-TLR2KO (black, enclosed by black dashed line). Eco-TLR2KO (red) also clusters
distinctly from PI-TLR2KO. EcoMs-TLR2KO (green) clusters distinctly from PI-TLR2KO, and lies
as an intermediate between Ms-TLR2KO and Eco-TLR2KO alone.

156
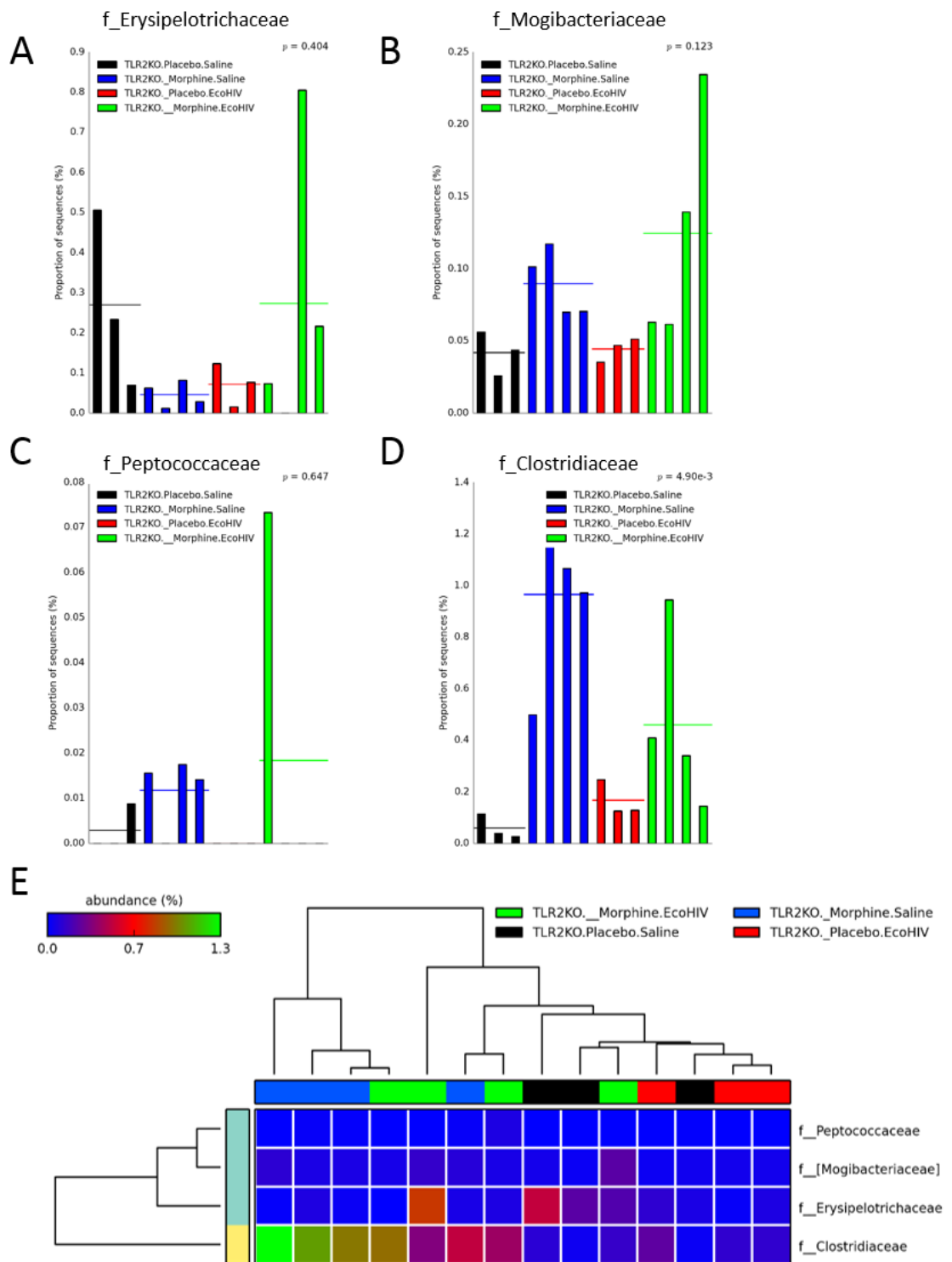
Fig 3. 18 TLR2KO prevents changes in 3 out of 4 families that were significantly changed by morphine and EcoHIV in wildtype

157

Significant families in closed-reference-picked species from TLR2KO animals treated with morphine for six days and/or EcoHIV infection for five days. Erysipelotrichaceae (A), Mogibacteriaceae (B), and Peptococcaceae (C) did not change significantly with Ms-TLR2KO or Eco-TLR2KO mice compared with Pl-TLR2KO. (D) Clostridiaceae did have a significant increase in Ms-TLR2KO and EcoMs-TLR2KO, which was the opposite direct that changes occurred in Ms-WT and EcoMs-WT mice. (E) A heatmap of these four families showed that the clustering was not as distinct as with WT animals, however the changes in Clostridiaceae are likely driving some of the Ms-TLR2KO (blue) and EcoMs-TLR2KO (green) samples to cluster distinctly.
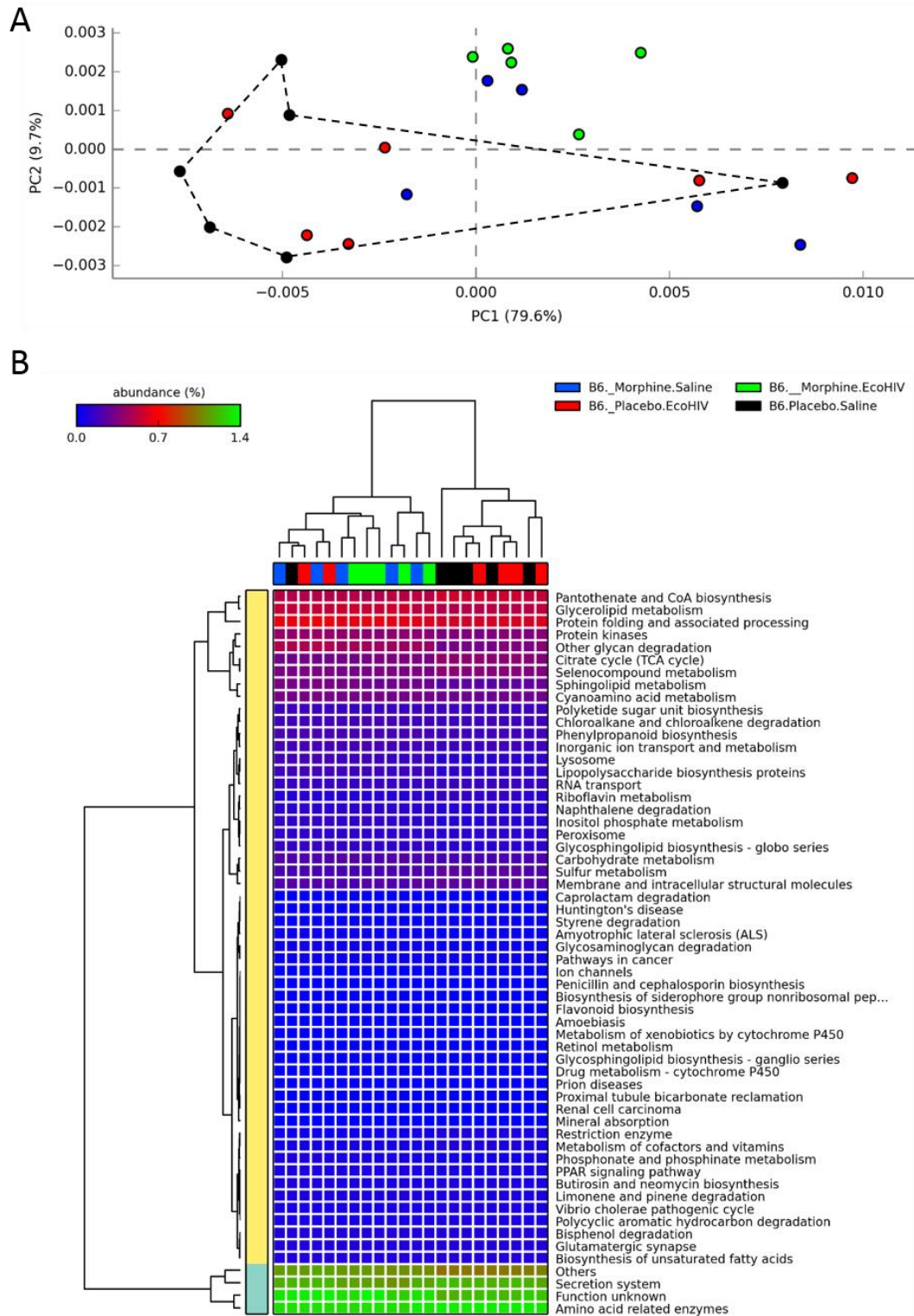
Fig 3. 19 Ms-WT and EcoMs-WT animals have changes in predicted metabolites

Samples of wildtype animals treated with morphine for six days and/or EcoHIV infection for five days were run through PICRUSt analysis. PCoA shows that, excluding one outlier, 5 out of 6 Pl-WT (black, enclosed by black dashed line) and 4 out of 6 Eco-WT (red) cluster in the negative portion of the x-axis while 4 out of 5 Ms-WT (blue) and 5 out of 5 EcoMs-WT (green) cluster in the positive portion of the x-axis. This implies morphine as a common agent of change in the predicted metabolites. (B) Heatmap profile of significantly changed predicted metabolites shows similar clustering with Ms-WT and EcoMs-WT samples distinct aside from one out of six Pl-WT and two out of six Eco-WT.
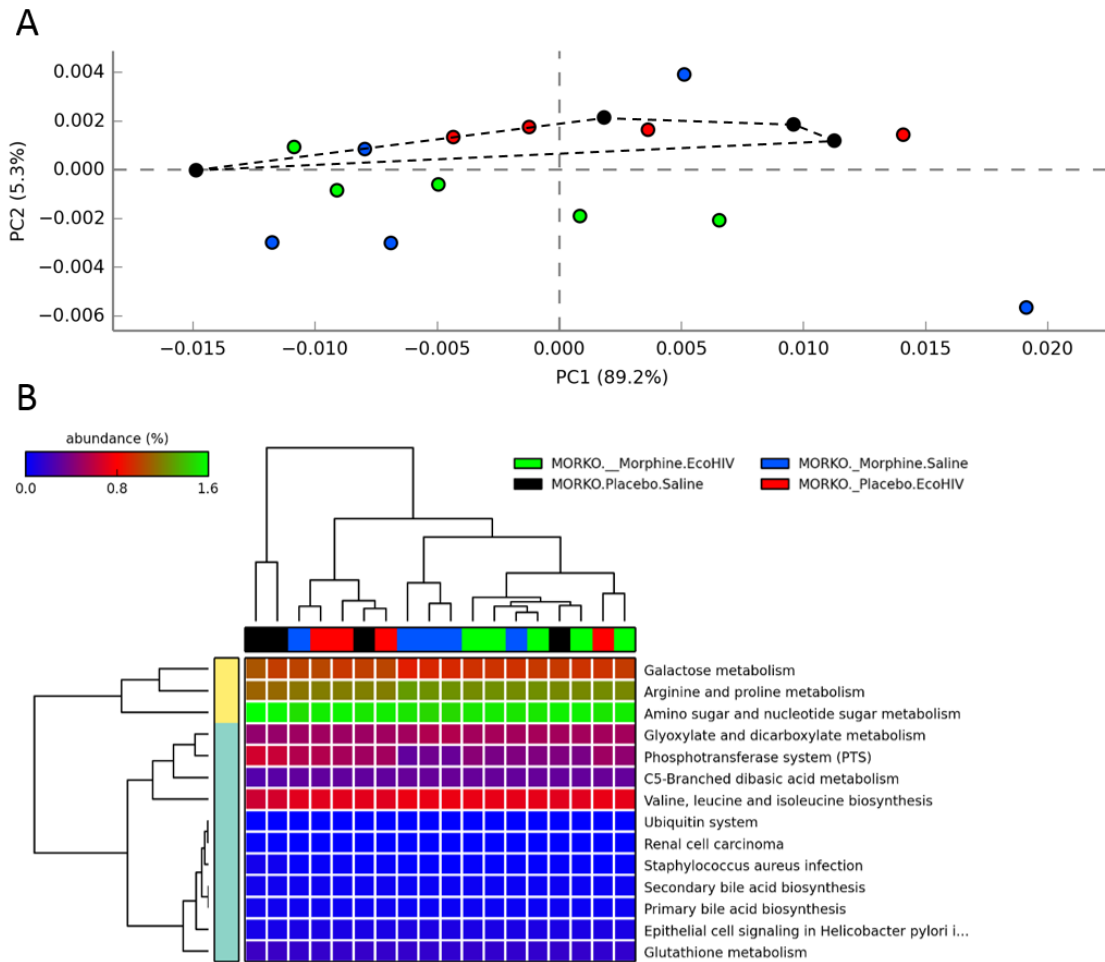
Fig 3. 20 Ms-MORKO animals are protected from morphine-induced changes in predictive metabolites

Samples of MORKO animals treated with morphine for six days and/or EcoHIV infection for five days were run through PICRUSt analysis. PCoA shows that none of the three treatment groups (Ms-MORKO, blue; Eco-MORKO, red; EcoMs-MORKO, green) cluster separately from PI-MORKO (black, enclosed by black dashed line). This is evidence that the shifts in Ms-WT animals are occurring via the mu-opioid receptor. (B) The heatmap profile of significantly changed predicted metabolites, which is quite shorter than WT, shows no clustering of distinct treatment groups aside from two out of four PI-MORKO (black) having their own branch.
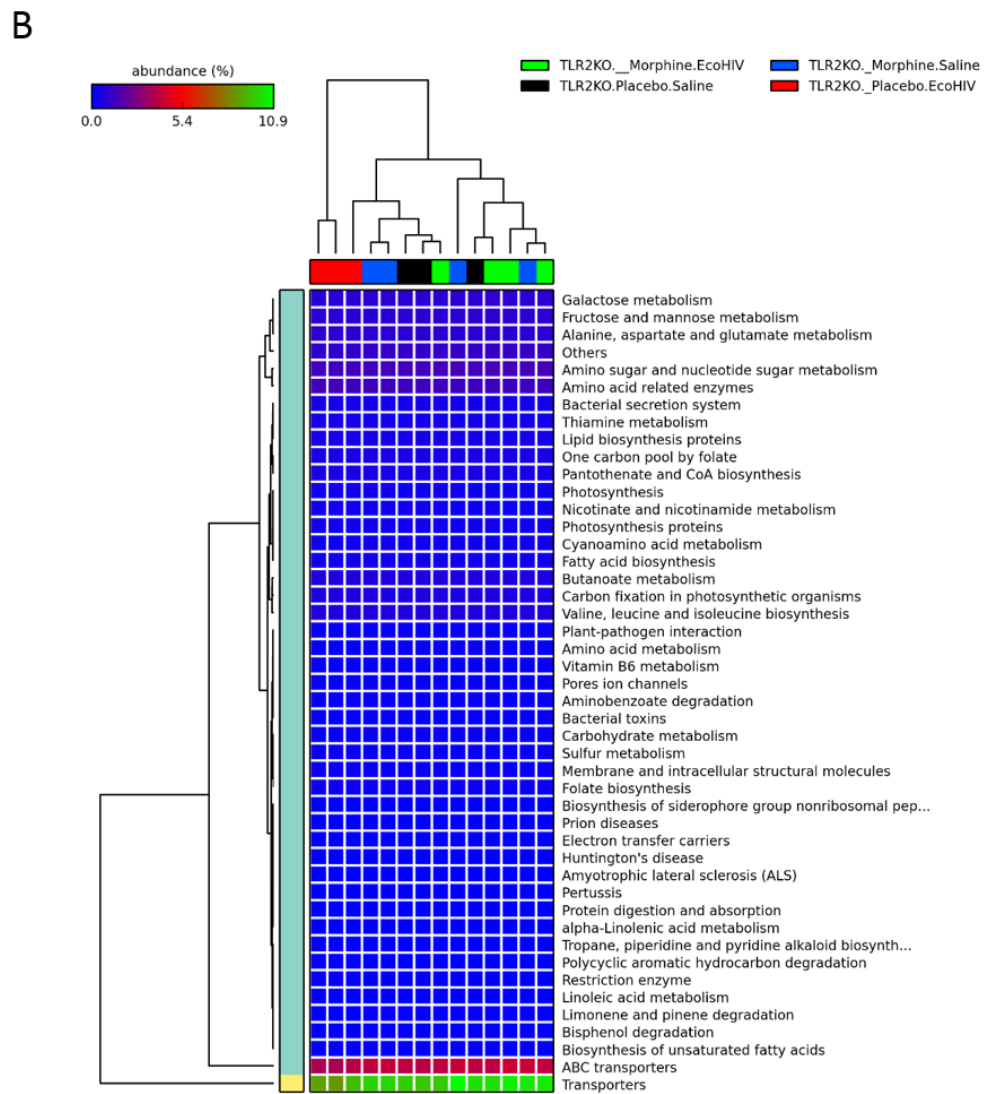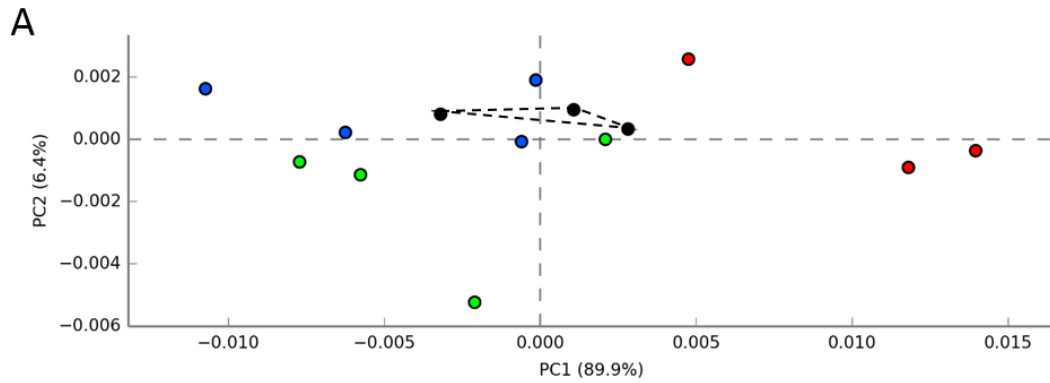
Fig 3. 21 TLR2KO animals are protected from morphine-induced changes in predictive metabolites

Samples of TLR2KO animals treated with morphine for six days and/or EcoHIV infection for five days were run through PICRUSt analysis. PCoA shows that, while the spread of treatment groups (Ms-TLR2KO, blue; Eco-TLR2KO, red; EcoMs-TLR2KO, green) is greater than Pl-TLR2KO (black, enclosed by black dashed line), the populations do not cluster distinctly and have overlap with Pl-TLR2KO. (B) The heatmap profile of significantly changed predicted metabolites shows no clustering of distinct treatment groups aside from two out of three EcoHIV (red) having their own branch.
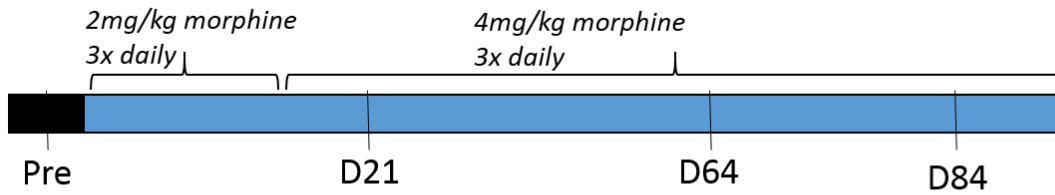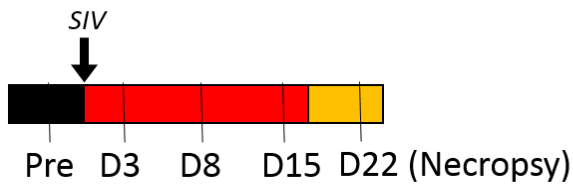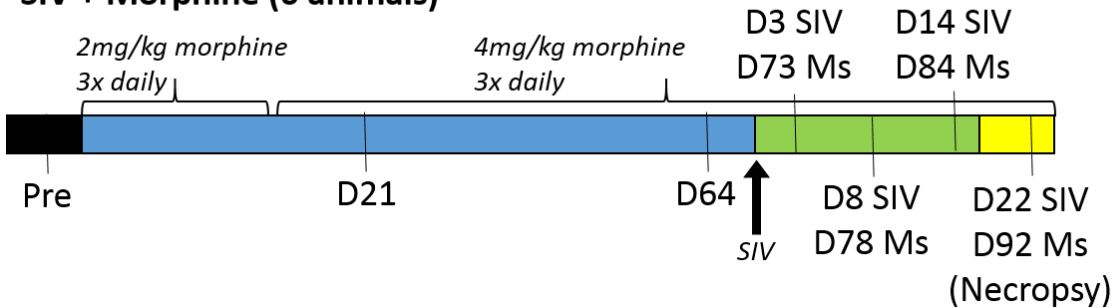
Fig 3. 22 Schematic of nonhuman primate fecal collection points
Pretreatment samples were collected for all 14 animals. Morphine was given at 2mg/kg three times daily for 14 days, when the dose was increased to 4mg/kg three times daily. Animals in SIV+morphine were infected with SIV after being on morphine for 70 days, when the collection timecourse mimicked the SIV sampling

164
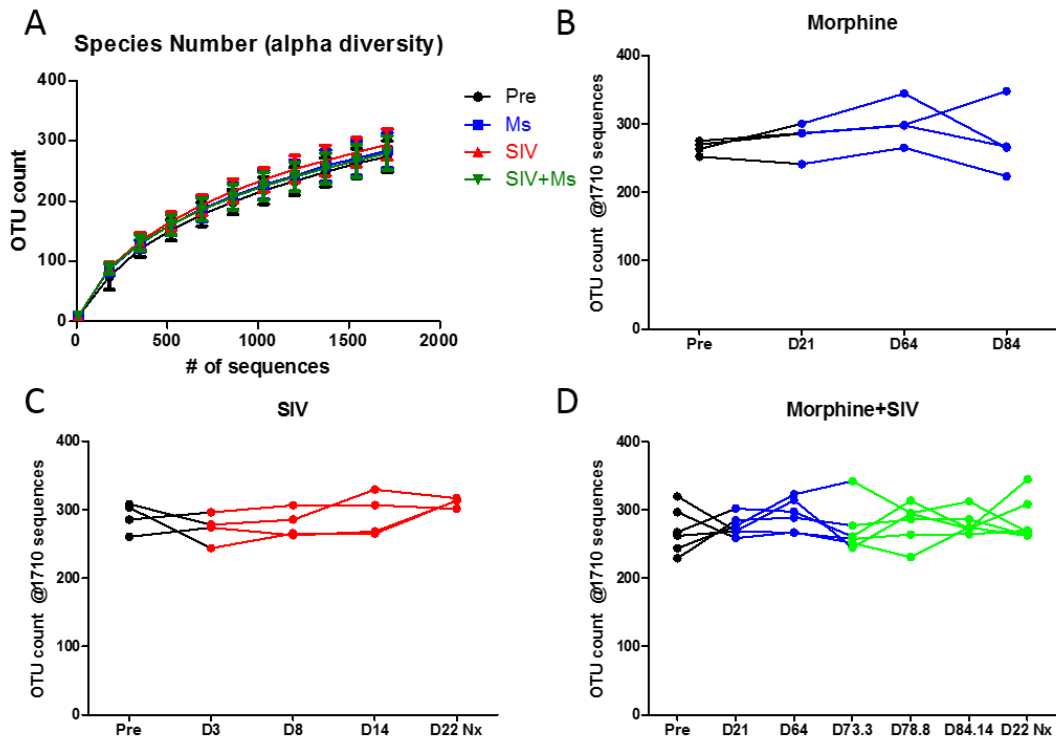
Fig 3. 23 Morphine and/or SIV does not change the number of species over time
The number of species (alpha diversity) was calculated up to 1710 sequences, which was the minimum sequence number in all samples. (A) No difference was observed in species number between treatment groups when all time points were lumped together. At 1710 sequences, there was no change in at any timepoint in Ms-NHP (B), SIV-NHP (C) or SIVMs-NHP (D) treated animals.
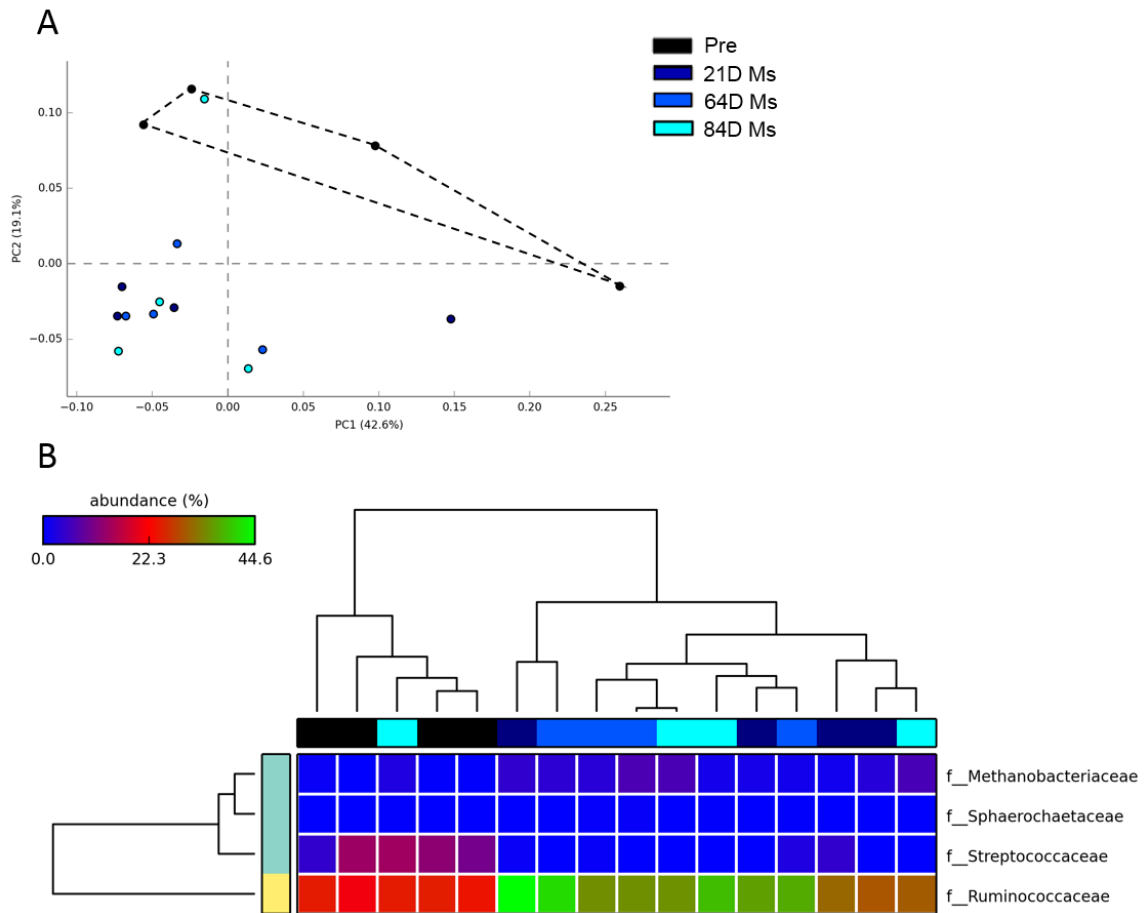
Fig 3. 24 Morphine induces dysbiosis in nonhuman primates which is stable over time
(A) Ms-NHP (various shades of blue) altered the microbial signature of animals from matched Pre-NHP (black) samples at the earliest (21D) time point, which was stable over time. (B) A heatmap of significantly changed families between time points showed that Pre-NHP (black) was distinctly clustered from Ms-NHP samples, aside from one animal at 84D morphine.

166
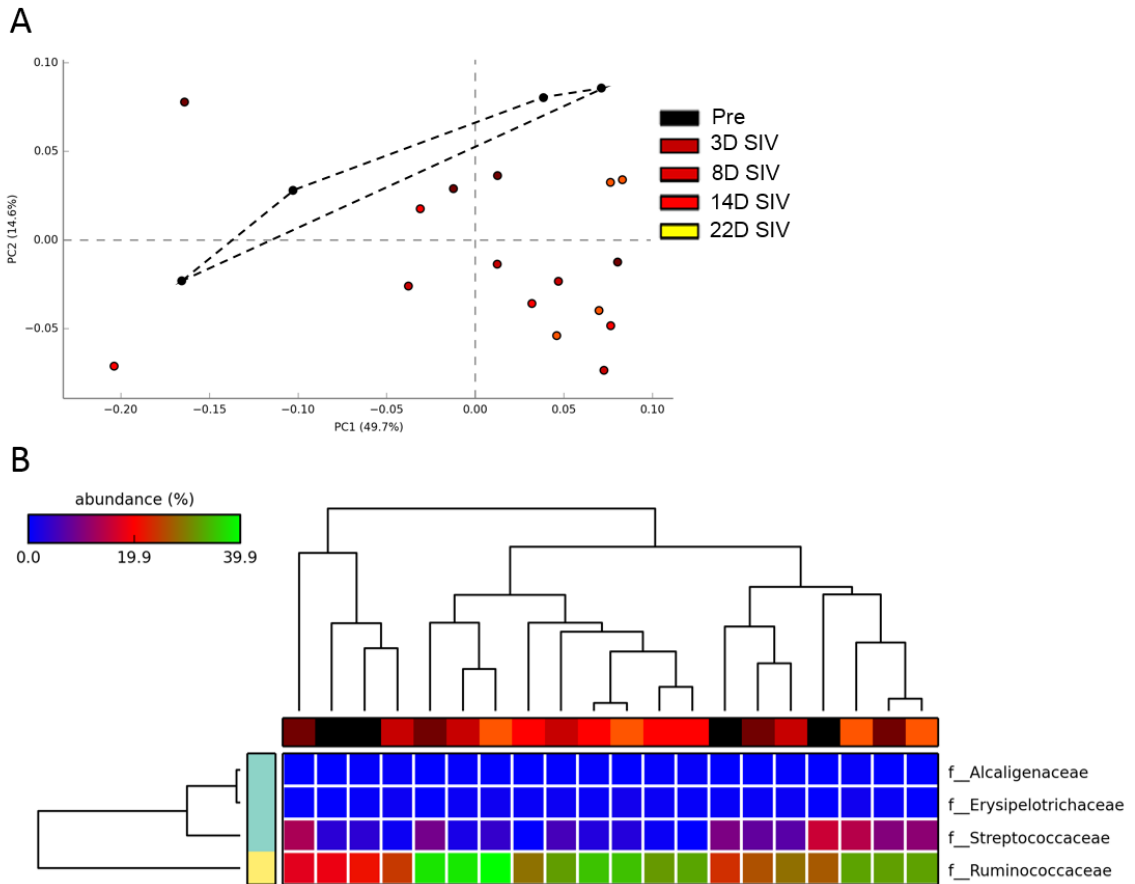
Fig 3. 25 SIV induces dysbiosis in some, but not all, animals
(A) SIV-NHP (various shades of red) altered the microbial signature of animals from matched Pre-NHP (black) samples. However, the earliest (3D, dark red) time point was not changed greatly. (B) A heatmap of significantly changed families between time points showed disparity between Pre-NHP (black) samples. SIV-NHP samples that associated closely with Pre-NHP samples were from the same animal, implying that SIV had no induced dysbiosis at that point. Despite this, a large number of SIV-NHP samples clustered distinctly as a middle branch from Pre-NHP.

167
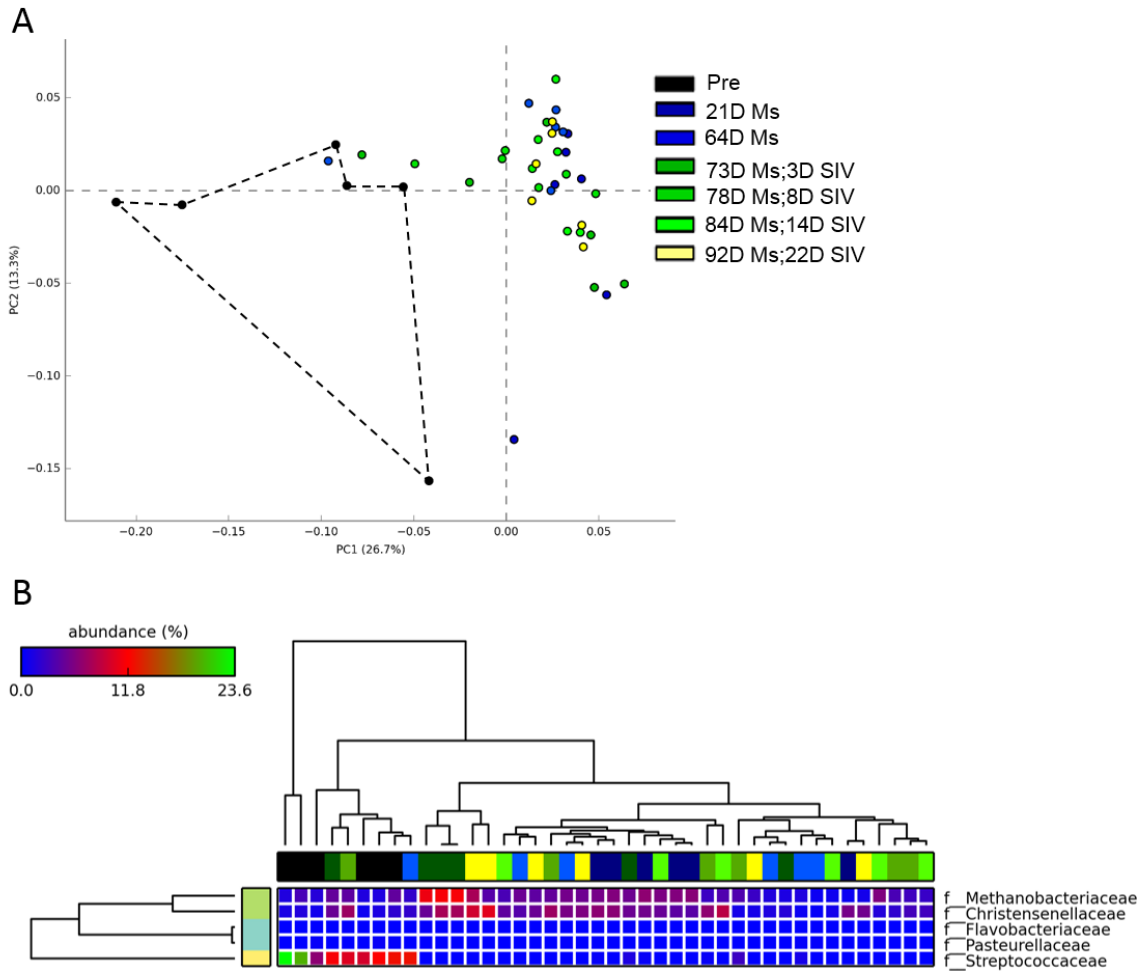
Fig 3. 26 Morphine induces dysbiosis that is not altered further with SIV infection
(A) As with Ms-NHP animals, morphine (various shades of blue) altered the microbial signature of animals from their pretreatment (black) samples at the earliest (21D) time point, which was stable over time even after the animals were infected with SIV (various shades of green). (B) A heatmap of significantly changed families between time points showed that placebo (black) was distinctly from the majority of treatment samples (various shades of blue and green). Treatments (matched Ms-NHP vs SIVMs-NHP) or time points did not cluster distinctly.

168
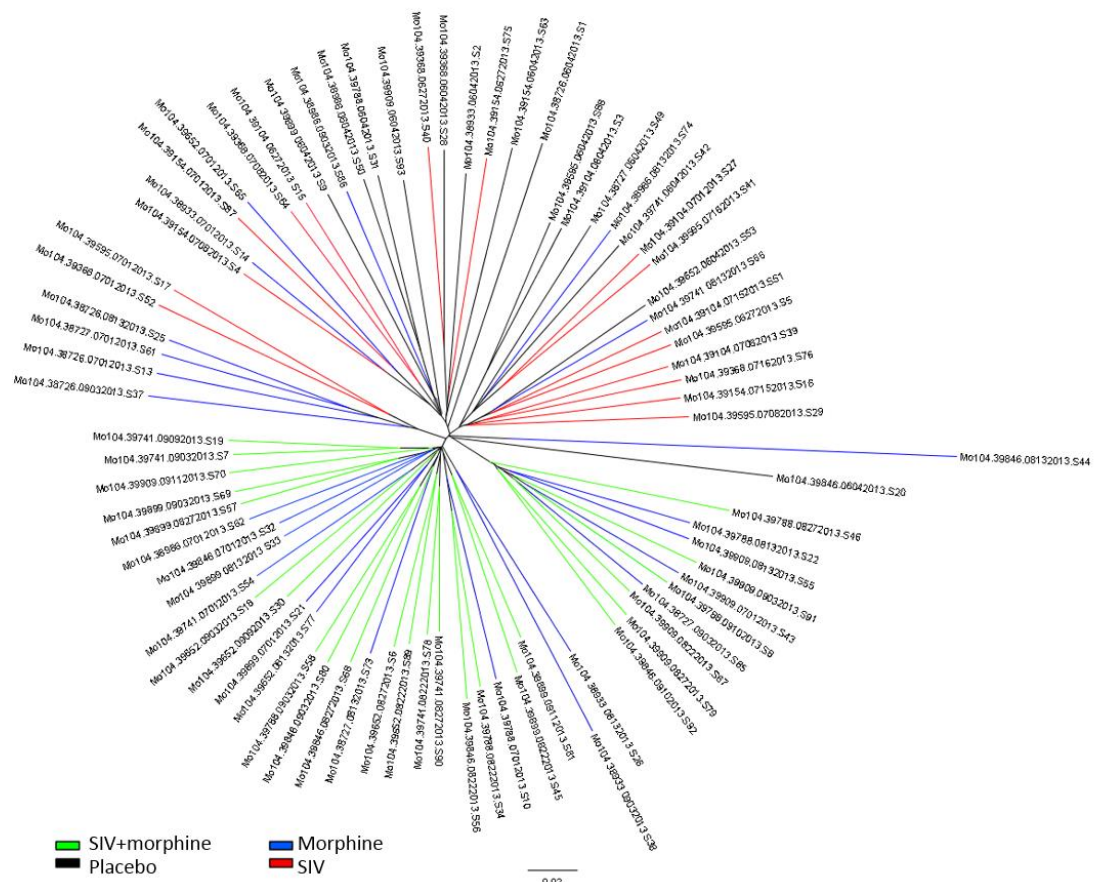
Fig 3. 27 Tree clustering of microbial signature shows Ms-NHP and SIVMs-NHP cluster distinctly from Pre-NHP
Microbial diversity was analyzed as a tree, which clustered samples that were more similar. Treatments were colored independently of time point within the treatment. As expected based on earlier PCoA analysis, Ms-NHP (blue) and SIVMs-NHP (green samples) clustered together and separately from Pre-NHP (black) samples. SIV-NHP (red) samples clustered similarly with Pre-NHP samples, although some nodes were distinct implying that SIV begins to have effects at the later time points that examined.

169

↑Ms-NHP

Phylum	Class	Order	Family	Genus	stat	p value
Bacteroidetes	Bacteroida	Bacteroidales	Paraprevotellaceae	YRC22	0.736	0.042
					0.707	0.034
					0.707	0.034
TM7	TM-7-3	unid.	unid.	unid.	0.707	0.034

Ms-NHP

↓SIVMs-NHP

Phylum	Class	Order	Family	Genus	stat	p value
					0.977	0.003
Firmicutes	Bacilli	Lactobacillales	Streptococcaceae	Streptococcus	0.977	0.003

Pre-NHP

SIVMs-NHP

↓Ms-NHP & SIVMs-NHP

Phylum	Class	Order	Family	Genus	stat	p value
					0.973	0.006
					0.921	0.011
					0.921	0.011
Proteobacteria	Gammaproteobacteria	Pasteurellales	Pasteurellaceae	Aggregatibacter	0.895	0.01

Phylum	Class	Order	Family	Genus	stat	p value
					0.853	0.007
					0.853	0.007
					0.853	0.007
					0.853	0.007
Fibrobacteres	Fibrobacteria	Fibrobacterales	Fibrobacteraceae	Fibrobacter	0.853	0.007
		Aeromonadales	Succinivibrionaceae	Succinivibrio	0.774	0.03
					0.658	0.043
					0.658	0.043
Proteobacteria	Gammaproteobacteria	Enterobacteriales	Enterobacteriaceae	unid.	0.658	0.043

↑SIV-NHP

SIV-NHP

Fig 3. 28 Indicator species between Pre-NHP and terminal collections from Ms-NHP, SIV-NHP, and SIVMs-NHP
Closed-reference-picked species from nonhuman primates at terminal time points only (84D morphine, 22D SIV, 92D morphine/22D SIV) compared with Pre-NHP. Indicators were found in Ms-NHP (blue) and SIV-NHP (red). Taxa common between Pre-NHP and SIV-NHP (overlay of black and red) are taxa that are decreased by morphine. Indicator species analysis of treatment groups revealed a distinct profile of taxa that were associated with SIVMs-NHP (green). Taxa that were associated with Pre-NHP, SIV-NHP, and Ms-NHP (black+red+blue overlay) are decreased in SIVMS-NHP animals only.

170
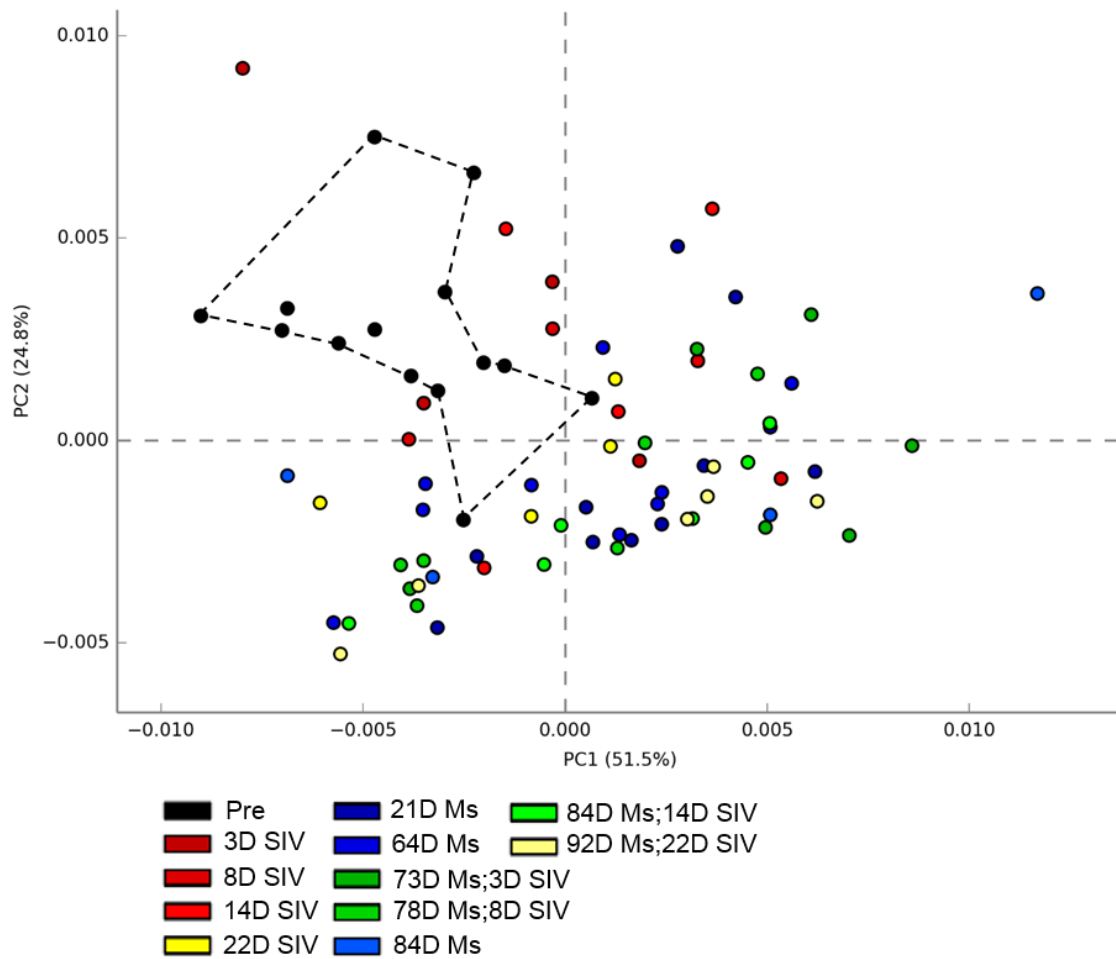
Fig 3. 29 Morphine and/or SIV treatments alter profile of predictive metabolites

Samples of nonhuman primates treated with morphine and/or SIV infection at multiple time points were run through PICRUSt analysis. PCoA shows that Pre-NHP samples (black, enclosed by black dashed line) cluster distinctly from a majority of treated samples (shades of blue, red, or green), which are spread on both the x- and y-axis.

171
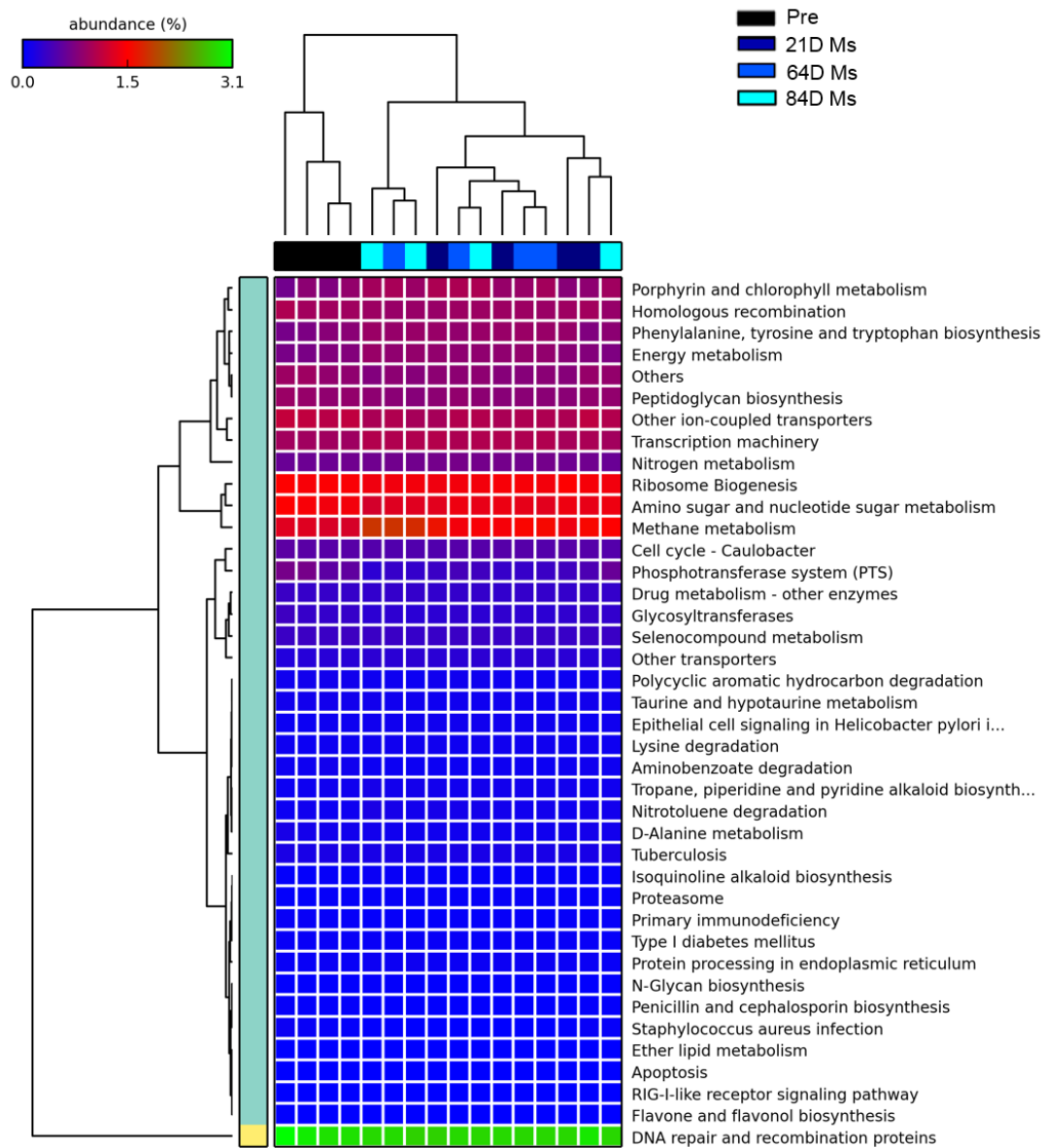
Fig 3. 30 Predicted metabolites of Ms-NHP animals cluster distinctly from Pre-NHP
Heatmap profile of significantly changed predicted metabolites (PICRUSt) shows similar
clustering of Ms-NHP (various shades of blue) samples separately from Pre-NHP, which occurs
independent of collection time (black).
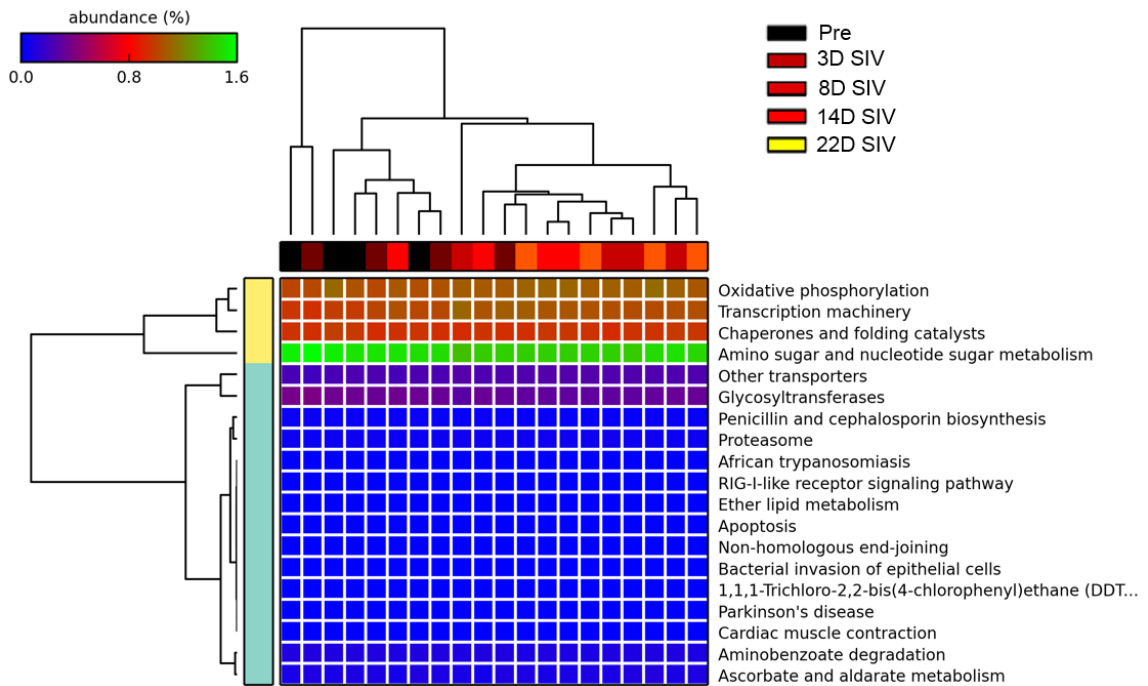
Fig 3. 31 Predicted metabolites of SIV-NHP animals beyond 3D infection cluster distinctly from Pre-NHP
Heatmap profile of significantly changed predicted metabolites (PICRUSt) shows similar clustering of SIV-NHP (various shades of red) samples separately from Pre-NHP (black). This occurs independently of infection time, except 3D SIV-NHP did not cluster distinctly from Pre-NHP, which matches the limited changes observed in microbial signature for this collection.

173
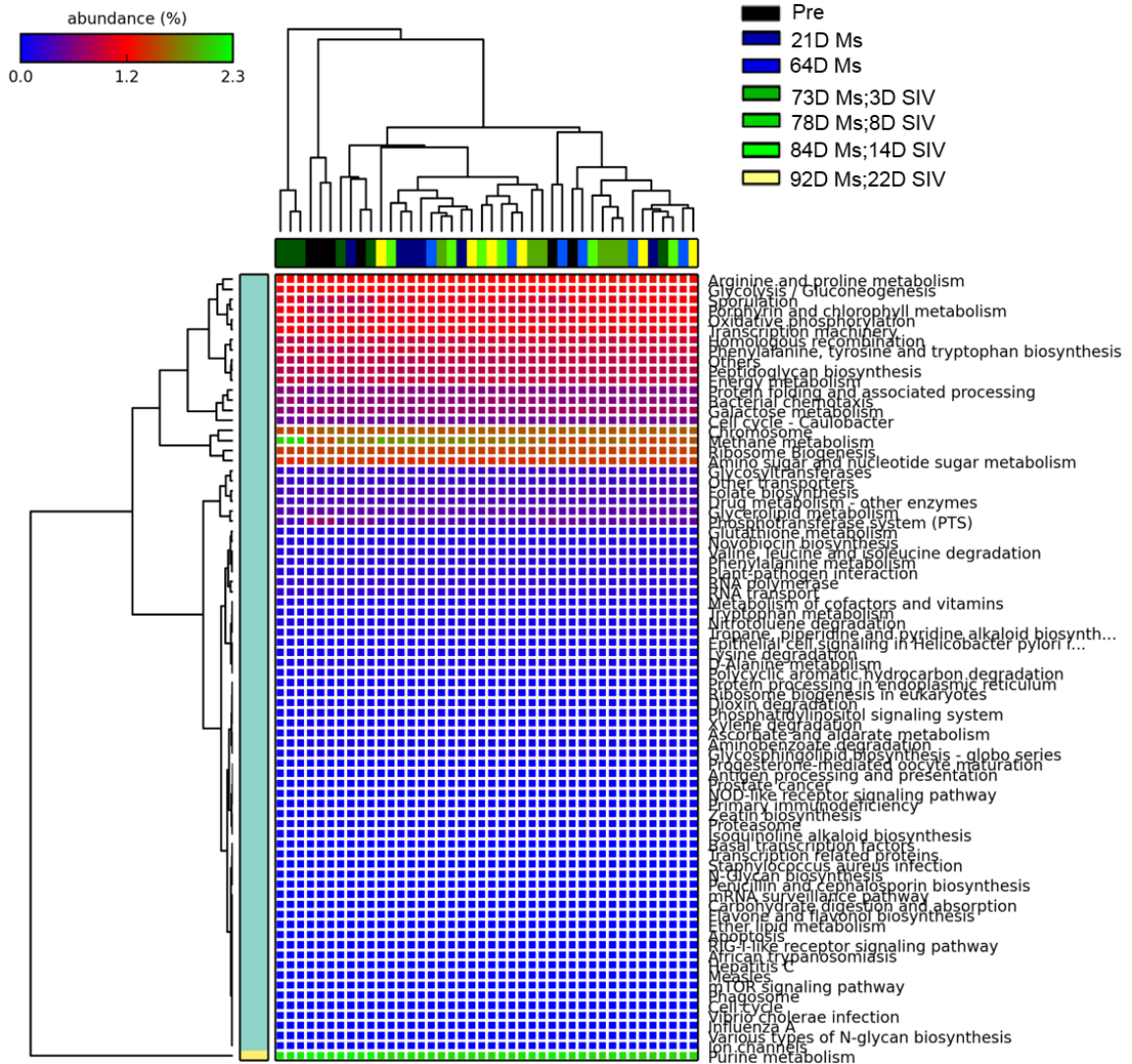
Fig 3. 32 Predicted metabolites of SIVMs-NHP animals cluster distinctly from Pre-NHP
Heatmap profile of significantly changed predicted metabolites (PICRUSt) shows four out of six Pre-NHP samples (black) clustering separately from the majority of treated samples (various shades of blue and green). The other two Pre-NHP samples clustered among the treatment samples but were most closely related to the same animals, which suggests that these animals were more resistant to changes observed in other animals.

174

Chapter 4.   General Discussion

4.1. Conclusions

The present study showed that HIV and opioid drugs interact at early stages of infection to disrupt gut homeostasis. In order to study these interactions, infectious models of HIV, including murine-specific EcoHIV[154] and NHP infected with SIV, was utilized. Bacterial translocation is characteristic of a disruption in gut homeostasis, which was observed in both Ms-WT and Eco-WT animals at 3 days exposure or 2 days post-infection, respectively. When combined in EcoMs-WT, the translocation greatly increased beyond what was observed in Ms-WT and Eco-WT. Translocation has been shown in HIV patients, which is increased in patients who inject opioid drugs, however this has not be studied this early in HIV infection[63,4].

Typically, gut homeostasis is maintained by epithelial and immune cells from the host, as well as commensal bacteria within the lumen of the gut. This study provides evidence that morphine and early HIV infection in combination can negatively impact all three defenses, which act together as a system to protect the host.

Gut morphology was altered in EcoMs-WT animals, which included a disruption of epithelial tight junction protein expression along the lumen of the gut. Tight junctions typically maintain an impermeable barrier to bacteria in the lumen, and disrupting this barrier likely allows bacteria to translocate. Exposure of epithelial cells to HIV protein Tat, in the absence of infection, induced similar

disruption in tight junction function. Additionally, epithelial expression of the innate immune receptors TLR2 and TLR4 was increased by morphine and EcoHIV, which recognize gram positive and gram negative bacterial cell wall products respectively. This increase can lead to inappropriate responses to commensal bacteria and may contribute to microbial dysbiosis.

Immune cells were not decreased in number as they are in later stages of HIV infection, however the function of immune cells was disrupted by both morphine treatment and EcoHIV infection. An increase in inflammatory cytokines was observed systemically in EcoMs-WT mice, likely a response to bacterial translocation. Of particular concern is the reduced capacity of macrophages to phagocytose, which is a mechanism for the host to control bacteria that are able to cross the epithelial barrier. This deficiency, along with the disruption of tight junction proteins, may be the likely reason for bacterial translocation systemically to the liver.

Finally, this study showed that morphine and HIV infection can induce microbial dysbiosis in the large intestine. Morphine induced microbial dysbiosis as early as 3 days in mice and 21 days in NHP. While morphine-induced constipation likely plays a role,[94] activation of the host immune system in response to translocated bacteria also has a negative impact on the gut microbiome. This is clearly illustrated by the use of TLR2 and NSG animals, both of which showed reduced microbial shifts and decreased bacterial translocation.

At the early time points of infection studied, both EcoHIV and SIV models of HIV had relatively few microbial shifts. When infection was combined with morphine, dysbiosis was very similar to morphine alone suggesting that no interaction occurs at this stage of infection.

The results presented in this thesis provide evidence for how HIV and opioids may be interacting at early stages of disease in the gut. Compared to previous studies in HIV patients that typically focus on later stages of infection, utilizing animal models allowed us to examine early HIV pathology in the gut for the first time. Generally, events occurring in early HIV infection are poorly understood, which is unfortunate given that it is an optimal time to intervene and prevent the onset of AIDS. HIV infection is known to disrupt GALT CD4+ T-cells early and consistently, however the trigger for this is unknown.[3] Interestingly, changes were observed in all three of the classical compartments mediating gut homeostasis: epithelial barrier, immune function, and microbial dysbiosis. The models used for HIV infection suggest that HIV alters the gut environment at very early stages of infection. Even if bacteria that translocated to systemic tissues is cleared in HIV infection as observed at 5 days of EcoHIV infection, these studies suggest that inflammation from initial exposure to bacterial translocation is enough to drive pathology in the gut, especially on the host side. Microbial dysbiosis was not observed in this case, which is observed in late stage HIV infection. Rather than being consistent interruption, at early stages of HIV

infection the host may be more susceptible to insults within the gut that leads to a cyclical period of inflammation and recovery, as is observed in IBD. Opioids may worsen this cycle and increase the amount of bacterial translocation and inflammation.

## 4.2.	Clinical Implications

Overall, the present study shows that HIV infection with opioids interrupts gut homeostasis more severely than in HIV alone. The severe disruption of gut homeostasis observed with opioids and models of HIV supports what is observed in the literature as HIV patients who inject opioids have higher levels of bacterial translocation than patients who do not use opioids,[4] which is likely why HIV patients who abuse opioids have a more severe pathogenesis of HIV and develop AIDS much more quickly than nonusers.[157–159]

Several mechanisms have come to light in this study which may propose options for therapeutic interventions to prevent or slow the pathogenesis in the gut. Both TLR2 and TLR4 seem to play an important role in the initial bacterial translocation insult as well as subsequent inflammation. Antagonists to TLR2 and TLR4 may be useful if given orally to patients who abuse opioids to combat the overexpression of these proteins in the epithelium, however dosing will require experimentation as TLR2 and TLR4 signaling is still needed for proper maintenance in the gut, as was observed by the microbial shift in TLR2KO animals. Another interesting therapeutic opportunity is to supplement bile acids

orally, which has been shown to prevent microbial overgrowth and bacterial translocation in an animal model deficient in bile acid production.[207] Finally, oral naloxone may be an interesting treatment option in opioid abusers as it has been shown to inhibit constipation, but not block analgesic (or euphoric) effects[209], which would potentially limit adherence to the drug in this population. These targets, with naloxone and oral bile acids commercially available and TLR2 and TLR4 antagonists being developed, provide translational opportunities that could be moved into the clinics immediately. Unfortunately, many people diagnosed with HIV, especially amongst drug abusers, are still not identified until the disease has already progressed with AIDS. With better public health programs, the drug abusing population can hopefully be targeted to improve access to healthcare and ultimately initiate some of these interventions.

Aside from potential therapeutic interventions, this study adds evidence to the increasing list of systemic alterations induced by opioids. Combined, these findings raise concerns about the use of opioids as analgesics in uninfected populations, but especially with HIV infected individuals. Pain is the most common symptom experienced in clinical patients, occurring almost ubiquitously as a symptom for wounds, surgery, and disease. The findings in this study show shifts in microbiome populations and metabolites within the gut, which could impact the recovery from the underlying ailment of pain. Despite this, opioids are being prescribed at alarmingly high rates, and need to be used judiciously both to

avoid systemic side effects as well as combat potential addiction[213,214]. Aside from the potential use of oral naloxone to block effects of opioid receptor activation in the gut[209], alternate analgesics to opioids are desperately needed to reduce associated side effects, especially in at-risk populations such as HIV infected individuals.

4.3.   Limitations/Future Directions

Murine EcoHIV infection is a useful model for studying HIV effects on the gut in combination with morphine as it recapitulates bacterial translocation and disruption of gut homeostasis that one would expect from data available in previous HIV studies. That said, EcoHIV is limited in that it utilizes different receptor to enter cells (MCAT-1[215]) than HIV (CD4 and CCR5/CXCR4). Thus, entry of EcoHIV may be in different cells, including B-cells being infected as white blood cells have high expression of MCAT-1.[216] Still, CD4+ T-cells and macrophages typically infected by HIV have been shown to be infected by EcoHIV as well.[154] Another issue is that EcoHIV lacks HIV gp120,[154] which is the protein that allows HIV to bind CD4 and enter human cells. Aside from cell entry, gp120 has also been shown to induce negative effects in the gut as a secreted protein.[126] To overcome this, other models may need to be utilized such as humanized mice which can be infected directly with HIV.

Another major limitation of these experiments was the timing of morphine exposure. In the EcoHIV infection model presented in these studies, animals

were pretreated with a 25mg morphine pellet for 24 hr to simulate a drug user becoming infected with HIV. The pellet reaches steady state quickly, and has maximum dosing between 24 and 72 hr, when the dosing is severely diminished beyond 120 hr (5 days) [175]. Bacterial translocation induced by morphine and EcoHIV was observed in animals at 72 hr exposure to morphine but not at 144 hr, which may be a function of morphine levels being nonexistent. Future studies will need to overcome this timing by improving the dosing, likely through using daily injections of morphine.

The goal for these studies was to examine very early HIV infection. With the EcoHIV model, two time points were focused on: 2 days post-infection, where bacterial translocation was observed with EcoHIV and more with EcoHIV+morphine, and 5 days post-infection where no translocation was observed but pathology was expected from the infection- and morphine-induced translocation. A more robust time course of collections would have ideally been performed, and may have allowed us to more accurately map the onset of the disruption of homeostasis. This was especially apparent in the studies examining microbial dysbiosis. Given the difference in host pathology observed between Ms-WT and EcoMs-WT, where EcoMs-WT had higher bacterial translocation and inflammation, microbial dysbiosis was expected to be greater in EcoMs-WT animals. This difference was not observed as Ms-WT and EcoMs-WT clustered together, implying that EcoHIV did not alter the dysbiosis induced

by morphine. The 5 day post-infection collection may have been too early to see microbiome shifts, so future studies should include later time points paired with morphine injections discussed above. Studies with NHP infected with SIV showed small shifts in the microbial composition, especially at 8, 15 and 22 days post-infection. Similar to EcoHIV-infected mice, the dysbiosis from SIV was minor compared with the dysbiosis in morphine-treated animals. While microbial dysbiosis has not been examined using the EcoHIV model, SIV-infection has been shown to induce microbial dysbiosis at later time points (beyond 4 months).[200,201] Thus, later time points in both EcoHIV and SIV infections would be useful for understanding gut homeostasis disruption, especially in microbial dysbiosis.

Microbiome studies in mice focused on changes in the large intestinal fecal content since a preliminary study showed changes induced by morphine in large intestine but not small intestine. However, the preliminary study used animals treated with a 25mg morphine pellet for 6 days, a time associated with probably lower circulating levels of morphine as discussed above, as well as a potential development of tolerance. Changes may occur in the small intestine at earlier exposure times to the morphine pellet, but may have become tolerant by the time examined. In this study, differences were observed between Ms-WT mice examined at 3 days and 6 days exposure to morphine, with 6 days appearing much closer to placebo. Small intestine has fewer total bacteria than

large intestine, and thus may be quicker to revert. In addition to small intestine, it would be interesting to examine adherent bacteria to look for changes with treatment. This study examined fecal content, which collected loose stool pellets from within the large intestine. This approach is good for looking at global changes, however with bacterial translocation the expectation is that bacteria need to adhere and cross the epithelial boundary. Additionally, constipation induced by morphine may allow bacteria greater access to adhere as it is not readily pushed along via fecal transit. However, it is currently unknown whether morphine causes an increase in adherent bacteria. Adherent bacteria can be studied by washing the intestine of fecal content and isolating 16S DNA from tissue samples, which should be examined in future studies.

This study showed a disruption of gut homeostasis by opioids and HIV, but readouts were largely descriptive in nature. To determine underlying mechanisms, future studies will be needed using more discrete readouts. A particularly interesting study would be to look at the role of TLR2 in disruption of gut homeostasis induced by opioids and HIV. The above studies implied that TLR2 plays a key role in this process, as TLR2KO animals had protection from bacterial translocation and microbial dysbiosis induced by morphine. It would be useful to differentiate whether TLR2 on epithelial cells or immune cells was more integral to this process by using adoptive transfer experiments using TLR2KO and WT animals. Previous data suggests that TLR2 on epithelial cells is

184

increased by morphine, which would be validated with the adoptive transfer study.[97] If epithelial cells were truly the target, oral medication with either a mu-opioid receptor antagonist or TLR2 antagonist may be effective in preventing these changes. Another interesting mechanism would be to examine the function of CD4+ helper T-cells within the gut, especially Th17 cells, when morphine and HIV are present. These cells are known to play a key role in maintaining gut homeostasis, especially in HIV infection[217–219]. Th17 being out of balance with Tregs may explain the pathology observed in EcoMs-WT mice, however this needs to be examined.

Combined, future studies including those listed above will utilize the data generated in this study as a baseline for understanding opioid and HIV effects in gut homeostasis. Although the current study has some limitations it also shows for the first time that opioids combine with HIV to induce a disruption of gut homeostasis at very early stages of disease. The combination of opioids with HIV infection results in bacterial translocation that has been shown to drive HIV infection[63], which highlights how opioids may enhance the severity of HIV infection.[157–159]

References

1.   Mathers BM, Degenhardt L, Phillips B, et al. Global epidemiology of injecting drug use and HIV among people who inject drugs: a systematic review. *Lancet*. 2008;372(9651):1733–45. doi:10.1016/S0140-6736(08)61311-2.

2.   Banerjee A, Strazza M, Wigdahl B, Pirrone V, Meucci O, Nonnemacher MR. Role of mu-opioids as cofactors in human immunodeficiency virus type 1 disease progression and neuropathogenesis. *J Neurovirol*. 2011;17(4):291–302. doi:10.1007/s13365-011-0037-2.

3.   Simon V, Ho DD, Abdool Karim Q. HIV/AIDS epidemiology, pathogenesis, prevention, and treatment. *Lancet*. 2006;368(9534):489–504. doi:10.1016/S0140-6736(06)69157-5.HIV/AIDS.

4.   Ancuta P, Kamat A, Kunstman KJ, et al. Microbial translocation is associated with increased monocyte activation and dementia in AIDS patients. *PLoS One*. 2008;3(6):e2516. doi:10.1371/journal.pone.0002516.

5.   Saxena D, Li Y, Yang L, et al. Human microbiome and HIV/AIDS. *Curr HIV/AIDS Rep*. 2012;9(1):44–51. doi:10.1007/s11904-011-0103-7.

6.   Mutlu EA, Keshavarzian A, Losurdo J, et al. A Compositional Look at the Human Gastrointestinal Microbiome and Immune Activation Parameters in HIV Infected Subjects. *PLoS Pathog*. 2014;10(2). Available at: http://dx.plos.org/10.1371/journal.ppat.1003829. Accessed September 20, 2014.

7.   Dillon S, Lee E, Kotter C, Austin G. An altered intestinal mucosal microbiome in HIV-1 infection is associated with mucosal and systemic immune activation and endotoxemia. *Mucosal …*. 2014. Available at: http://www.nature.com/mi/journal/vaop/ncurrent/full/mi2013116a.html. Accessed September 20, 2014.

8.   Blanpain C, Horsley V, Fuchs E. Epithelial stem cells: turning over new leaves. *Cell*. 2007;128(3):445–58. doi:10.1016/j.cell.2007.01.014.

9.   Clevers H. Wnt/beta-catenin signaling in development and disease. *Cell*. 2006;127(3):469–80. doi:10.1016/j.cell.2006.10.018.

10. Bullen TF, Forrest S, Campbell F, et al. Characterization of epithelial cell shedding from human small intestine. *Lab Invest*. 2006;86(10):1052–63. doi:10.1038/labinvest.3700464.

11. Marsh MN. Digestive-absorptive functions of the enterocyte. *Ann R Coll Surg Engl*. 1971;48(6):356–68. Available at: http://www.pubmedcentral.nih.gov/articlerender.fcgi?artid=2387884&tool=pmcentrez&rendertype=abstract. Accessed August 30, 2014.

12. Daniel H. Molecular and integrative physiology of intestinal peptide transport. *Annu Rev Physiol*. 2004;66:361–84. doi:10.1146/annurev.physiol.66.032102.144149.

13. Chabot S, Wagner JS, Farrant S, Neutra MR. TLRs regulate the gatekeeping functions of the intestinal follicle-associated epithelium. *J Immunol*. 2006;176(7):4275–83. Available at: http://www.ncbi.nlm.nih.gov/pubmed/16547265.

14. Turner JR. Intestinal mucosal barrier function in health and disease. *Nat Rev Immunol*. 2009;9(11):799–809. doi:10.1038/nri2653.

15. Abreu MT. Toll-like receptor signalling in the intestinal epithelium: how bacterial recognition shapes intestinal function. *Nat Rev Immunol*. 2010;10(2):131–44. doi:10.1038/nri2707.

16. Anderson JM, Van Itallie CM. Physiology and function of the tight junction. *Cold Spring Harb Perspect Biol*. 2009;1(2):a002584. doi:10.1101/cshperspect.a002584.

17. Pittet MJ, Mempel TR. Regulation of T-cell migration and effector functions: insights from in vivo imaging studies. *Immunol Rev*. 2008;221:107–29. doi:10.1111/j.1600-065X.2008.00584.x.

18. Stevenson BR, Siliciano JD, Mooseker MS, Goodenough DA. Identification of ZO-1: a high molecular weight polypeptide associated with the tight junction (zonula occludens) in a variety of epithelia. *J Cell Biol*. 1986;103(3):755–66. Available at: http://www.pubmedcentral.nih.gov/articlerender.fcgi?artid=2114282&tool=pmcentrez&rendertype=abstract. Accessed September 1, 2014.

19. Furuse M, Hirase T, Itoh M, Nagafuchi A, Yonemura S, Tsukita S. Occludin: a novel integral membrane protein localizing at tight junctions. *J*

187

Cell Biol. 1993;123(6 Pt 2):1777–88. Available at:
http://www.pubmedcentral.nih.gov/articlerender.fcgi?artid=2290891&tool=p
mcentrez&rendertype=abstract. Accessed August 20, 2014.

20. Fanning AS, Jameson BJ, Jesaitis LA, Anderson JM. The tight junction
     protein ZO-1 establishes a link between the transmembrane protein
     occludin and the actin cytoskeleton. *J Biol Chem.* 1998;273(45):29745–53.
     Available at: http://www.ncbi.nlm.nih.gov/pubmed/9792688. Accessed
     August 17, 2014.

21. Yu D, Marchiando AM, Weber CR, et al. MLCK-dependent exchange and
     actin binding region-dependent anchoring of ZO-1 regulate tight junction
     barrier function. *Proc Natl Acad Sci U S A.* 2010;107(18):8237–41.
     doi:10.1073/pnas.0908869107.

22. Marchiando AM, Shen L, Graham WV, et al. The epithelial barrier is
     maintained by in vivo tight junction expansion during pathologic intestinal
     epithelial shedding. *Gastroenterology.* 2011;140(4):1208–1218.e1–2.
     doi:10.1053/j.gastro.2011.01.004.

23. Su L, Shen L, Clayburgh DR, et al. Targeted epithelial tight junction
     dysfunction causes immune activation and contributes to development of
     experimental colitis. *Gastroenterology.* 2009;136(2):551–563.
     doi:10.1053/j.gastro.2008.10.081.

24. Rock FL, Hardiman G, Timans JC, Kastelein RA, Bazan JF. A family of
     human receptors structurally related to Drosophila Toll. *Proc Natl Acad Sci
     U S A.* 1998;95(2):588–93. Available at:
     http://www.pubmedcentral.nih.gov/articlerender.fcgi?artid=18464&tool=pm
     centrez&rendertype=abstract. Accessed September 1, 2014.

25. Leow-Dyke S, Allen C, Denes A, et al. Neuronal Toll-like receptor 4
     signaling induces brain endothelial activation and neutrophil transmigration
     in vitro. *J Neuroinflammation.* 2012;9:230. doi:10.1186/1742-2094-9-230.

26. Fitzner N, Clauberg S, Essmann F, Liebmann J, Kolb-Bachofen V. Human
     skin endothelial cells can express all 10 TLR genes and respond to
     respective ligands. *Clin Vaccine Immunol.* 2008;15(1):138–46.
     doi:10.1128/CVI.00257-07.

27. Mukherji A, Kobiita A, Ye T, Chambon P. Homeostasis in Intestinal
     Epithelium Is Orchestrated by the Circadian Clock and Microbiota Cues

Transduced by TLRs. *Cell*. 2013;153(4):812–27. doi:10.1016/j.cell.2013.04.020.

28. Kondo T, Kawai T, Akira S. Dissecting negative regulation of Toll-like receptor signaling. *Trends Immunol*. 2012;33(9):449–58. doi:10.1016/j.it.2012.05.002.

29. Ortega-Cava CF, Ishihara S, Rumi MAK, et al. Strategic compartmentalization of Toll-like receptor 4 in the mouse gut. *J Immunol*. 2003;170(8):3977–85. doi:10.4049/jimmunol.170.8.3977.

30. Lotz M, Gütle D, Walther S, Ménard S, Bogdan C, Hornef MW. Postnatal acquisition of endotoxin tolerance in intestinal epithelial cells. *J Exp Med*. 2006;203(4):973–84. doi:10.1084/jem.20050625.

31. Cario E, Podolsky DK. Differential alteration in intestinal epithelial cell expression of toll-like receptor 3 (TLR3) and TLR4 in inflammatory bowel disease. *Infect Immun*. 2000;68(12):7010–7. Available at: http://www.pubmedcentral.nih.gov/articlerender.fcgi?artid=97811&tool=pm centrez&rendertype=abstract. Accessed September 2, 2014.

32. Artis D. Epithelial-cell recognition of commensal bacteria and maintenance of immune homeostasis in the gut. *Nat Rev Immunol*. 2008;8(6):411–20. doi:10.1038/nri2316.

33. Nenci A, Becker C, Wullaert A, et al. Epithelial NEMO links innate immunity to chronic intestinal inflammation. *Nature*. 2007;446(7135):557–61. doi:10.1038/nature05698.

34. Zaph C, Troy AE, Taylor BC, et al. Epithelial-cell-intrinsic IKK-beta expression regulates intestinal immune homeostasis. *Nature*. 2007;446(7135):552–6. doi:10.1038/nature05590.

35. Dignass AU, Podolsky DK. Cytokine modulation of intestinal epithelial cell restitution: central role of transforming growth factor beta. *Gastroenterology*. 1993;105(5):1323–32. Available at: http://www.ncbi.nlm.nih.gov/pubmed/8224636. Accessed August 13, 2014.

36. Rescigno M, Urbano M, Valzasina B, et al. Dendritic cells express tight junction proteins and penetrate gut epithelial monolayers to sample bacteria. *Nat Immunol*. 2001;2(4):361–7. doi:10.1038/86373.

37. Chieppa M, Rescigno M. Dynamic imaging of dendritic cell extension into the small bowel lumen in response to epithelial cell TLR engagement. *J ….* 2006. Available at: http://jem.rupress.org/content/203/13/2841.short. Accessed September 7, 2014.

38. Fink LN, Frøkiaer H. Dendritic cells from Peyer's patches and mesenteric lymph nodes differ from spleen dendritic cells in their response to commensal gut bacteria. *Scand J Immunol.* 2008;68(3):270–9. doi:10.1111/j.1365-3083.2008.02136.x.

39. Chirdo FG, Millington OR, Beacock-Sharp H, Mowat AM. Immunomodulatory dendritic cells in intestinal lamina propria. *Eur J Immunol.* 2005;35(6):1831–40. doi:10.1002/eji.200425882.

40. Allers K, Fehr M, Conrad K, et al. Macrophages accumulate in the gut mucosa of untreated HIV-infected patients. *J Infect Dis.* 2014;209(5):739–48. doi:10.1093/infdis/jit547.

41. Genua M, D'Alessio S, Cibella J, et al. The urokinase plasminogen activator receptor (uPAR) controls macrophage phagocytosis in intestinal inflammation. *Gut.* 2014. doi:10.1136/gutjnl-2013-305933.

42. Denning TL, Wang Y, Patel SR, Williams IR, Pulendran B. Lamina propria macrophages and dendritic cells differentially induce regulatory and interleukin 17-producing T cell responses. *Nat Immunol.* 2007;8(10):1086–94. doi:10.1038/ni1511.

43. Van Egmond M, Damen CA, van Spriel AB, Vidarsson G, van Garderen E, van de Winkel JG. IgA and the IgA Fc receptor. *Trends Immunol.* 2001;22(4):205–11. Available at: http://www.ncbi.nlm.nih.gov/pubmed/11274926. Accessed September 7, 2014.

44. Van der Heijden PJ, Stok W, Bianchi AT. Contribution of immunoglobulin-secreting cells in the murine small intestine to the total "background" immunoglobulin production. *Immunology.* 1987;62(4):551–5. Available at: http://www.pubmedcentral.nih.gov/articlerender.fcgi?artid=1454168&tool=pmcentrez&rendertype=abstract. Accessed September 7, 2014.

45. Izcue A, Powrie F. Special regulatory T-cell review: Regulatory T cells and the intestinal tract--patrolling the frontier. *Immunology.* 2008;123(1):6–10. doi:10.1111/j.1365-2567.2007.02778.x.

46.   Blaschitz C, Raffatellu M. Th17 cytokines and the gut mucosal barrier. *J Clin Immunol*. 2010;30(2):196–203. doi:10.1007/s10875-010-9368-7.

47.   Hapfelmeier S, Lawson M, Slack E. Reversible microbial colonization of germ-free mice reveals the dynamics of IgA immune responses. *Science (80-)*. 2010. Available at: http://www.sciencemag.org/content/328/5986/1705.short. Accessed September 11, 2014.

48.   Niess JH, Leithäuser F, Adler G, Reimann J. Commensal gut flora drives the expansion of proinflammatory CD4 T cells in the colonic lamina propria under normal and inflammatory conditions. *J Immunol*. 2008;180(1):559–68. Available at: http://www.ncbi.nlm.nih.gov/pubmed/18097058. Accessed September 11, 2014.

49.   Strauch UG, Obermeier F, Grunwald N, et al. Influence of intestinal bacteria on induction of regulatory T cells: lessons from a transfer model of colitis. *Gut*. 2005;54(11):1546–52. doi:10.1136/gut.2004.059451.

50.   Hooper L V, Wong MH, Thelin A, Hansson L, Falk PG, Gordon JI. Molecular analysis of commensal host-microbial relationships in the intestine. *Science*. 2001;291(5505):881–4. doi:10.1126/science.291.5505.881.

51.   Wells JM, Rossi O, Meijerink M, van Baarlen P. Epithelial crosstalk at the microbiota-mucosal interface. *Proc Natl Acad Sci U S A*. 2011;108 Suppl :4607–14. doi:10.1073/pnas.1000092107.

52.   Woese CR, Fox GE. Phylogenetic structure of the prokaryotic domain: The primary kingdoms. *Proc Natl Acad Sci*. 1977;74(11):5088–5090. doi:10.1073/pnas.74.11.5088.

53.   Bubnoff A von. Next-generation sequencing: the race is on. *Cell*. 2008. Available at: http://www.sciencedirect.com/science/article/pii/S0092867408002766. Accessed September 13, 2014.

54.   Qin J, Li R, Raes J, Arumugam M. A human gut microbial gene catalogue established by metagenomic sequencing. *Nature*. 2010. Available at: http://www.nature.com/nature/journal/v464/n7285/abs/nature08821.html. Accessed September 13, 2014.

55. Yatsunenko T, Rey FE, Manary MJ, et al. Human gut microbiome viewed across age and geography. *Nature*. 2012;486(7402):222–7. doi:10.1038/nature11053.

56. Tremaroli V, Bäckhed F. Functional interactions between the gut microbiota and host metabolism. *Nature*. 2012. Available at: http://www.nature.com/nature/journal/v489/n7415/abs/nature11552.html. Accessed September 22, 2014.

57. Kamada N, Kim Y-G, Sham HP, et al. Regulated virulence controls the ability of a pathogen to compete with the gut microbiota. *Science*. 2012;336(6086):1325–9. doi:10.1126/science.1222195.

58. Pflughoeft KJ, Versalovic J. Human Microbiome in Health and Disease. 2012. Available at: http://www.annualreviews.org/doi/abs/10.1146/annurev-pathol-011811-132421. Accessed September 13, 2014.

59. Kawamoto S, Maruya M, Kato LM, et al. Foxp3+ T Cells Regulate Immunoglobulin A Selection and Facilitate Diversification of Bacterial Species Responsible for Immune Homeostasis. *Immunity*. 2014;41(1):152–65. doi:10.1016/j.immuni.2014.05.016.

60. Hooper L V, Macpherson AJ. Immune adaptations that maintain homeostasis with the intestinal microbiota. *Nat Rev Immunol*. 2010;10(3):159–69. doi:10.1038/nri2710.

61. Hansson G. Role of mucus layers in gut infection and inflammation. *Curr Opin Microbiol*. 2012. Available at: http://www.sciencedirect.com/science/article/pii/S1369527411001858. Accessed September 13, 2014.

62. MacFie J, O'boyle C, Mitchell C. Gut origin of sepsis: a prospective study investigating associations between bacterial translocation, gastric microflora, and septic morbidity. *Gut*. 1999. Available at: http://gut.bmj.com/content/45/2/223.abstract. Accessed September 13, 2014.

63. Brenchley JM, Price D a, Schacker TW, et al. Microbial translocation is a cause of systemic immune activation in chronic HIV infection. *Nat Med*. 2006;12(12):1365–71. doi:10.1038/nm1511.

64. Cani P, Amar J, Iglesias M, Poggi M. Metabolic endotoxemia initiates obesity and insulin resistance. *Diabetes*. 2007. Available at: http://diabetes.diabetesjournals.org/content/56/7/1761.short. Accessed September 13, 2014.

65. Laffineur G, Lescut D, Vincent P, Quandalle P, Wurtz A, Colombel JF. [Bacterial translocation in Crohn disease]. *Gastroentérologie Clin Biol*. 1992;16(10):777–81. Available at: http://europepmc.org/abstract/MED/1478405. Accessed September 13, 2014.

66. Zareie M, Johnson-Henry K, Jury J, Yang P. Probiotics prevent bacterial translocation and improve intestinal barrier function in rats following chronic psychological stress. *Gut*. 2006. Available at: http://gut.bmj.com/content/55/11/1553.short. Accessed September 13, 2014.

67. DEITCH E, MORRISON J. Effect of hemorrhagic shock on bacterial translocation, intestinal morphology, and intestinal permeability in conventional and antibiotic-decontaminated rats. *Crit care …*. 1990. Available at: http://journals.lww.com/ccmjournal/Abstract/1990/05000/Effect_of_hemorrhagic_shock_on_bacterial.14.aspx. Accessed September 13, 2014.

68. Berg R. Bacterial translocation from the gastrointestinal tracts of mice receiving immunosuppressive chemotherapeutic agents. *Curr Microbiol*. 1983. Available at: http://link.springer.com/article/10.1007/BF01577729. Accessed September 13, 2014.

69. Berg R, Wommack E, Deitch E. Immunosuppression and intestinal bacterial overgrowth synergistically promote bacterial translocation. *Arch Surg*. 1988. Available at: http://archsurg.jamanetwork.com/article.aspx?articleid=593555. Accessed September 13, 2014.

70. Neal MD, Leaphart C, Levy R, et al. Enterocyte TLR4 Mediates Phagocytosis and Translocation of Bacteria Across the Intestinal Barrier. *J Immunol*. 2006;176(5):3070–3079. doi:10.4049/jimmunol.176.5.3070.

71. Dandekar S, George MD, Bäumler AJ. Th17 cells, HIV and the gut mucosal barrier. *Curr Opin HIV AIDS*. 2010;5(2):173–8. doi:10.1097/COH.0b013e328335eda3.

72. Eastaff-Leung N, Mabarrack N, Barbour A, Cummins A, Barry S. Foxp3+ regulatory T cells, Th17 effector cells, and cytokine environment in inflammatory bowel disease. *J Clin Immunol*. 2010;30(1):80–9. doi:10.1007/s10875-009-9345-1.

73. Fryer J, Grant D, Jiang J, Metrakos P. Influence of macrophage depletion on bacterial translocation and rejection in small bowel transplantation. …. 1996. Available at: http://journals.lww.com/transplantjournal/Abstract/1996/09150/Influence_of_Macrophage_Depletion_on_Bacterial.2.aspx. Accessed September 13, 2014.

74. Medina-Contreras O, Geem D. CX3CR1 regulates intestinal macrophage homeostasis, bacterial translocation, and colitogenic Th17 responses in mice. *J …*. 2011. Available at: http://www.jci.org/articles/view/59150. Accessed September 13, 2014.

75. Tamboli C, Neut C, Desreumaux P, Colombel J. Dysbiosis in inflammatory bowel disease. *Gut*. 2004. Available at: http://gut.bmj.com/content/53/1/1.1.short. Accessed September 13, 2014.

76. Wu C, Li Z, Xiong D. Relationship between enteric microecologic dysbiosis and bacterial translocation in acute necrotizing pancreatitis. *Group*. 1998. Available at: http://www.wjgnet.com/1007-9327/full/v4/i3/242.htm. Accessed September 13, 2014.

77. Gómez-Hurtado I, Santacruz A, Peiró G. Gut microbiota dysbiosis is associated with inflammation and bacterial translocation in mice with CCl4-induced fibrosis. *PLoS One*. 2011. Available at: http://dx.plos.org/10.1371/journal.pone.0023037.g005. Accessed September 13, 2014.

78. Hilburger ME, Adler MW, Truant a L, et al. Morphine induces sepsis in mice. *J Infect Dis*. 1997;176(1):183–8. Available at: http://www.ncbi.nlm.nih.gov/pubmed/9207365.

79. Roy S, Ninkovic J, Banerjee S, et al. Opioid Drug Abuse and Modulation of Immune Function: Consequences in the Susceptibility to Opportunistic Infections. *J Neuroimmune Pharmacol*. 2011. doi:10.1007/s11481-011-9292-5.

80. Brenchley JM, Schacker TW, Ruff LE, et al. CD4+ T cell depletion during all stages of HIV disease occurs predominantly in the gastrointestinal tract. *J Exp Med.* 2004;200(6):749–59. doi:10.1084/jem.20040874.

81. White A, Birnbaum H. Direct costs of opioid abuse in an insured population in the United States. *J Manag ….* 2005. Available at: http://my.amcp.org/data/jmcp/3.pdf. Accessed August 1, 2014.

82. UNODC. *World Drug Report: The opium/heroin market.*; 2011. Available at: http://www.unodc.org/documents/data-and-analysis/WDR2011/The_opium-heroin_market.pdf. Accessed August 1, 2014.

83. CDC. *National Vital Statistics System: Mortality data.*; 2010. doi:CDC Wonder.

84. Volkow N. *Prescription Drug Abuse: It's Not What the Doctor Ordered*. Orlando, FL; 2012. Available at: http://www.slideshare.net/OPUNITE/nora-volkow-final-edits. Accessed August 1, 2014.

85. White A, Birnbaum H, Schiller M, Tang J, Katz N. Analytic models to identify patients at risk for prescription opioid abuse. *Am J Manag Care.* 2009. Available at: http://www.ajmc.com/publications/issue/2009/2009-12-vol15-n12/ajmc_09dec_white_897to906. Accessed August 1, 2014.

86. Laboratories B. Naltrexone. *Drugs.com.* 2013. Available at: http://www.drugs.com/pro/naltrexone.html. Accessed August 1, 2014.

87. Dole VP. A Medical Treatment for Diacetylmorphine (Heroin) Addiction. *JAMA.* 1965;193(8):646. doi:10.1001/jama.1965.03090080008002.

88. Cerner Multum I. Methadone: Uses, Side Effects & Warnings. *Drugs.com.* 2013. Available at: http://www.drugs.com/methadone.html. Accessed August 1, 2014.

89. Stimmel B, Goldberg J, Cohen M, Rotkopf E. DETOXIFICATION FROM METHADONE MAINTENANCE: RISK FACTORS ASSOCIATED WITH RELAPSE TO NARCOTIC USE. *Ann N Y Acad Sci.* 1978;311(1 Recent Develo):173–180. doi:10.1111/j.1749-6632.1978.tb16774.x.

90. NIH. *Heroin Addiction Fact Sheet.*; 2014. Available at: http://report.nih.gov/nihfactsheets/viewfactsheet.aspx?csid=123. Accessed August 1, 2014.

91. FDA. Postmarket Drug Safety Information for Patients and Providers - SUBUTEX AND SUBOXONE APPROVED TO TREAT OPIATE DEPENDENCE. Available at: http://www.fda.gov/Drugs/DrugSafety/PostmarketDrugSafetyInformationfor PatientsandProviders/ucm191521.htm. Accessed August 1, 2014.

92. Stuckert J. Opioid Dependence and Withdrawal. *Psych Cent.* 2011. Available at: http://psychcentral.com/lib/opioid-dependence-and-withdrawal/0008507. Accessed August 1, 2014.

93. Doyle D, Hanks G, Cherney I, Calman K. *Oxford textbook of palliative medicine.* Oxford University Press; 2004. Available at: http://scholar.google.com/scholar?q=doyle+hanks+cherney+2004&btnG=& hl=en&as_sdt=0,24#1. Accessed August 1, 2014.

94. Zhu L, Liu W, Alkhouri R, et al. Structural changes in the gut microbiome of constipated patients. *Physiol Genomics.* 2014. doi:10.1152/physiolgenomics.00082.2014.

95. Roy S, Charboneau RG, Barke RA. Morphine synergizes with lipopolysaccharide in a chronic endotoxemia model. *J Neuroimmunol.* 1999;95(1-2):107–14. Available at: http://www.ncbi.nlm.nih.gov/pubmed/10229120. Accessed September 16, 2014.

96. Ocasio FM, Jiang Y, House SD, Chang SL. Chronic morphine accelerates the progression of lipopolysaccharide-induced sepsis to septic shock. *J Neuroimmunol.* 2004;149(1-2):90–100. doi:10.1016/j.jneuroim.2003.12.016.

97. Meng J, Yu H, Ma J, et al. Morphine Induces Bacterial Translocation in Mice by Compromising Intestinal Barrier Function in a TLR-Dependent Manner. *PLoS One.* 2013;8(1):e54040. doi:10.1371/journal.pone.0054040.

98. Banerjee S, Meng J, Das S, et al. Morphine induced exacerbation of sepsis is mediated by tempering endotoxin tolerance through modulation of miR-146a. *Sci Rep.* 2013;3:1977. doi:10.1038/srep01977.

99. Breslow JM, Feng P, Meissler JJ, et al. Potentiating effect of morphine on oral Salmonella enterica serovar Typhimurium infection is μ-opioid receptor-dependent. *Microb Pathog.* 2010;49(6):330–5. doi:10.1016/j.micpath.2010.07.006.

196

100. Babrowski T, Holbrook C, Moss J, et al. Pseudomonas aeruginosa virulence expression is directly activated by morphine and is capable of causing lethal gut-derived sepsis in mice during chronic morphine administration. *Ann Surg.* 2012;255(2):386–93. doi:10.1097/SLA.0b013e3182331870.

101. Kaposi's sarcoma and Pneumocystis pneumonia among homosexual men--New York City and California. *MMWR Morb Mortal Wkly Rep.* 1981;30(25):305–8. Available at: http://www.ncbi.nlm.nih.gov/pubmed/6789108. Accessed September 20, 2014.

102. Barre-Sinoussi F, Chermann J, Rey F, et al. Isolation of a T-lymphotropic retrovirus from a patient at risk for acquired immune deficiency syndrome (AIDS). *Science (80-).* 1983;220(4599):868–871. doi:10.1126/science.6189183.

103. Dalgleish A, Beverley P. The CD4 (T4) antigen is an essential component of the receptor for the AIDS retrovirus. 1984. Available at: http://www.nature.com/nature/journal/v312/n5996/abs/312763a0.html. Accessed September 22, 2014.

104. Hirsch V, Olmsted R, Murphey-Corb M. An African primate lentivirus (SIVsmclosely related to HIV-2. 1989. Available at: http://www.nature.com/nature/journal/v339/n6223/abs/339389a0.html. Accessed September 22, 2014.

105. UNAID. *UNAIDS Global Report on the AIDS epidemic.*; 2013. Available at: http://www.unaids.org/en/media/unaids/contentassets/documents/epidemiology/2013/gr2013/UNAIDS_Global_Report_2013_en.pdf. Accessed August 1, 2014.

106. Palmisano L, Vella S. A brief history of antiretroviral therapy of HIV infection : success and challenges. 2011:44–48. doi:10.4415/aNN.

107. Marin B, Thiébaut R, Bucher HC, et al. Non-AIDS-defining deaths and immunodeficiency in the era of combination antiretroviral therapy. *AIDS.* 2009;23(13):1743–53. doi:10.1097/QAD.0b013e32832e9b78.

108. Ratner L, Fisher A, Jagodzinski LL, et al. Complete Nucleotide Sequences of Functional Clones of the AIDS Virus. *AIDS Res Hum Retroviruses.* 1987;3(1):57–69. doi:10.1089/aid.1987.3.57.

109. Pilcher C, Shugars D, Fiscus S. HIV in body fluids during primary HIV infection: implications for pathogenesis, treatment and public health. *Aids*. 2001. Available at: http://journals.lww.com/aidsonline/Abstract/2001/05040/HIV_in_body_fluids _during_primary_HIV_infection_.4.aspx. Accessed September 22, 2014.

110. Bleul CC, Farzan M, Choe H, et al. The lymphocyte chemoattractant SDF-1 is a ligand for LESTR/fusin and blocks HIV-1 entry. *Nature*. 1996;382(6594):829–33. doi:10.1038/382829a0.

111. Brenchley J, Douek D. HIV infection and the gastrointestinal immune system. *Mucosal Immunol*. 2008;1(1):23–30. doi:10.1038/sj.mi.2007.1750001.

112. Yang G-B, Alexander L, Aye P, Alvarez X, Desrosiers RC, Lackner AA. Localization of Productively Infected Cells in the Spleen and Peyer's Patches of Rhesus Macaques During Acute Infection with SIVmac239Δnef-Enhanced Green Fluorescent Protein. *AIDS Res Hum Retroviruses*. 2014;30(8):738–9. doi:10.1089/AID.2014.0160.

113. Veazey RS. Gastrointestinal Tract as a Major Site of CD4+ T Cell Depletion and Viral Replication in SIV Infection. *Science (80-)*. 1998;280(5362):427–431. doi:10.1126/science.280.5362.427.

114. Deeks SG, Kitchen CMR, Liu L, et al. Immune activation set point during early HIV infection predicts subsequent CD4+ T-cell changes independent of viral load. *Blood*. 2004;104(4):942–7. doi:10.1182/blood-2003-09-3333.

115. Zeng M, Southern PJ, Reilly CS, et al. Lymphoid tissue damage in HIV-1 infection depletes naïve T cells and limits T cell reconstitution after antiretroviral therapy. *PLoS Pathog*. 2012;8(1):e1002437. doi:10.1371/journal.ppat.1002437.

116. Douek D. HIV disease progression: immune activation, microbes, and a leaky gut. *Top HIV Med*. 2007;15(4):114–7. Available at: http://www.ncbi.nlm.nih.gov/pubmed/17720995.

117. Cecchinato V, Trindade CJ, Laurence a, et al. Altered balance between Th17 and Th1 cells at mucosal sites predicts AIDS progression in simian immunodeficiency virus-infected macaques. *Mucosal Immunol*. 2008;1(4):279–88. doi:10.1038/mi.2008.14.

118. Brenchley JM, Paiardini M, Knox KS, et al. Differential Th17 CD4 T-cell depletion in pathogenic and nonpathogenic lentiviral infections. *Blood*. 2008;112(7):2826–35. doi:10.1182/blood-2008-05-159301.

119. Peng Q, Wang H, Wang H, et al. Imbalances of gut-homing CD4+ T-cell subsets in HIV-1-infected Chinese patients. *J Acquir Immune Defic Syndr*. 2013;64(1):25–31. doi:10.1097/QAI.0b013e318293a114.

120. Raffatellu M, Santos RL, Verhoeven DE, et al. Simian immunodeficiency virus-induced mucosal interleukin-17 deficiency promotes Salmonella dissemination from the gut. *Nat Med*. 2008;14(4):421–8. doi:10.1038/nm1743.

121. Estes JD, Harris LD, Klatt NR, et al. Damaged intestinal epithelial integrity linked to microbial translocation in pathogenic simian immunodeficiency virus infections. *PLoS Pathog*. 2010;6(8). doi:10.1371/journal.ppat.1001052.

122. Klatt NR, Harris LD, Vinton CL, et al. Compromised gastrointestinal integrity in pigtail macaques is associated with increased microbial translocation, immune activation, and IL-17 production in the absence of SIV infection. *Mucosal Immunol*. 2010;3(4):387–98. doi:10.1038/mi.2010.14.

123. Mahajan SD, Aalinkeel R, Sykes DE, et al. Tight junction regulation by morphine and HIV-1 tat modulates blood-brain barrier permeability. *J Clin Immunol*. 2008;28(5):528–41. doi:10.1007/s10875-008-9208-1.

124. Rom S, Rom I, Passiatore G, et al. CCL8/MCP-2 is a target for mir-146a in HIV-1-infected human microglial cells. *FASEB J*. 2010;24(7):2292–300. doi:10.1096/fj.09-143503.

125. Bai L, Zhang Z, Zhang H, et al. HIV-1 Tat protein alter the tight junction integrity and function of retinal pigment epithelium: an in vitro study. *BMC Infect Dis*. 2008;8:77. doi:10.1186/1471-2334-8-77.

126. Nazli A, Chan O, Dobson-Belaire WN, et al. Exposure to HIV-1 directly impairs mucosal epithelial barrier integrity allowing microbial translocation. *PLoS Pathog*. 2010;6(4):e1000852. doi:10.1371/journal.ppat.1000852.

127. Hofer U, Schlaepfer E, Baenziger S, et al. Inadequate clearance of translocated bacterial products in HIV-infected humanized mice. *PLoS Pathog*. 2010;6(4):e1000867. doi:10.1371/journal.ppat.1000867.

128. Michailidis C, Giannopoulos G, Vigklis V, Armenis K, Tsakris a, Gargalianos P. Impaired phagocytosis among patients infected by the human immunodeficiency virus: implication for a role of highly active anti-retroviral therapy. *Clin Exp Immunol*. 2012;167(3):499–504. doi:10.1111/j.1365-2249.2011.04526.x.

129. Dang AT, Cotton S, Sankaran-Walters S, et al. Evidence of an increased pathogenic footprint in the lingual microbiome of untreated HIV infected patients. *BMC Microbiol*. 2012;12(1):153. doi:10.1186/1471-2180-12-153.

130. Branton WG, Ellestad KK, Maingat F, et al. Brain microbial populations in HIV/AIDS: α-proteobacteria predominate independent of host immune status. Bisser S, ed. *PLoS One*. 2013;8(1):e54673. doi:10.1371/journal.pone.0054673.

131. Perez-Santiago J, Gianella S, Massanella M. Gut Lactobacillales are associated with higher CD4 and less microbial translocation during HIV infection. *AIDS*. 2013:2012. Available at: http://journals.lww.com/aidsonline/Abstract/2013/07310/Gut_Lactobacillales_are_associated_with_higher_CD4.9.aspx. Accessed September 20, 2014.

132. Vujkovic-Cvijin I, Dunham R. Dysbiosis of the gut microbiota is associated with HIV disease progression and tryptophan catabolism. *Sci Transl …*. 2013. Available at: http://stm.sciencemag.org/content/5/193/193ra91.short. Accessed September 20, 2014.

133. Equils O, Salehi KK, Cornataeanu R, et al. Repeated lipopolysaccharide (LPS) exposure inhibits HIV replication in primary human macrophages. *Microbes Infect*. 2006;8(9-10):2469–76. doi:10.1016/j.micinf.2006.06.002.

134. Suzuki M, El-Hage N, Zou S, et al. Fractalkine/CX3CL1 protects striatal neurons from synergistic morphine and HIV-1 Tat-induced dendritic losses and death. *Mol Neurodegener*. 2011;6(1):78. doi:10.1186/1750-1326-6-78.

135. Buscemi L, Ramonet D, Geiger JD. Human immunodeficiency virus type-1 protein Tat induces tumor necrosis factor-alpha-mediated neurotoxicity. *Neurobiol Dis*. 2007;26(3):661–70. doi:10.1016/j.nbd.2007.03.004.

136. Ju SM, Song HY, Lee JA, Lee SJ, Choi SY, Park J. Extracellular HIV-1 Tat up-regulates expression of matrix metalloproteinase-9 via a MAPK-NF-κB dependent pathway in human astrocytes. *Exp Mol Med*. 2009;41(2):86. doi:10.3858/emm.2009.41.2.011.

137. Buonaguro L, Barillari G, Chang HK, et al. Effects of the human immunodeficiency virus type 1 Tat protein on the expression of inflammatory cytokines. *J Virol*. 1992;66(12):7159–67. Available at: http://www.pubmedcentral.nih.gov/articlerender.fcgi?artid=240407&tool=pmcentrez&rendertype=abstract.

138. Gurwell JA, Nath A, Sun Q, et al. Synergistic neurotoxicity of opioids and human immunodeficiency virus-1 Tat protein in striatal neurons in vitro. *Neuroscience*. 2001;102(3):555–563. doi:10.1016/S0306-4522(00)00461-9.

139. Pandrea I, Sodora DL, Silvestri G, Apetrei C. Into the wild: simian immunodeficiency virus (SIV) infection in natural hosts. *Trends Immunol*. 2008;29(9):419–28. doi:10.1016/j.it.2008.05.004.

140. Nishimura Y, Igarashi T, Buckler-White A, et al. Loss of naïve cells accompanies memory CD4+ T-cell depletion during long-term progression to AIDS in Simian immunodeficiency virus-infected macaques. *J Virol*. 2007;81(2):893–902. doi:10.1128/JVI.01635-06.

141. Hartigan-O'Connor DJ, Hirao L a, McCune JM, Dandekar S. Th17 cells and regulatory T cells in elite control over HIV and SIV. *Curr Opin HIV AIDS*. 2011;6(3):221–7. doi:10.1097/COH.0b013e32834577b3.

142. Marchetti G, Tincati C, Silvestri G. Microbial translocation in the pathogenesis of HIV infection and AIDS. *Clin Microbiol Rev*. 2013;26(1):2–18. doi:10.1128/CMR.00050-12.

143. Kopp JB, Klotman ME, Adler SH, et al. Progressive glomerulosclerosis and enhanced renal accumulation of basement membrane components in mice transgenic for human immunodeficiency virus type 1 genes. *Proc Natl Acad Sci*. 1992;89(5):1577–1581. doi:10.1073/pnas.89.5.1577.

144. Fan Y, Wei C, Xiao W, Zhang W, Wang N. Temporal Profile of the Renal Transcriptome of HIV-1 Transgenic Mice during Disease Progression. *PLoS One*. 2014. Available at:

http://dx.plos.org/10.1371/journal.pone.0093019.g014. Accessed September 22, 2014.

145. Prakash O, Teng S, Ali M, et al. The human immunodeficiency virus type 1 Tat protein potentiates zidovudine-induced cellular toxicity in transgenic mice. *Arch Biochem Biophys*. 1997;343(2):173–80. doi:10.1006/abbi.1997.0168.

146. Brady HJ, Abraham DJ, Pennington DJ, Miles CG, Jenkins S, Dzierzak E a. Altered cytokine expression in T lymphocytes from human immunodeficiency virus Tat transgenic mice. *J Virol*. 1995;69(12):7622–9. Available at: http://www.pubmedcentral.nih.gov/articlerender.fcgi?artid=189702&tool=pmcentrez&rendertype=abstract.

147. El-Hage N, Bruce-Keller AJ, Yakovleva T, et al. Morphine exacerbates HIV-1 Tat-induced cytokine production in astrocytes through convergent effects on [Ca(2+)](i), NF-kappaB trafficking and transcription. *PLoS One*. 2008;3(12):e4093. doi:10.1371/journal.pone.0004093.

148. Browning J, Horner J, Pettoello-Mantovani M, et al. Mice transgenic for human CD4 and CCR5 are susceptible to HIV infection. *Proc …*. 1997;94(26):14637–14641. Available at: http://www.pnas.org/content/94/26/14637.short. Accessed September 22, 2014.

149. Sawada S, Gowrishankar K. Disturbed CD4+ T Cell Homeostasis and In Vitro HIV-1 Susceptibility in Transgenic Mice Expressing T Cell Line–tropic HIV-1 Receptors. *… Med*. 1998. Available at: http://jem.rupress.org/content/187/9/1439.abstract. Accessed September 22, 2014.

150. Bieniasz P, Cullen B. Multiple blocks to human immunodeficiency virus type 1 replication in rodent cells. *J Virol*. 2000. Available at: http://jvi.asm.org/content/74/21/9868.short. Accessed September 22, 2014.

151. Mariani R, Rutter G, Harris M. A block to human immunodeficiency virus type 1 assembly in murine cells. *J …*. 2000. Available at: http://jvi.asm.org/content/74/8/3859.short. Accessed September 22, 2014.

152. Denton PW, Garcia JV. Novel humanized murine models for HIV research. *Curr HIV/AIDS Rep*. 2009;6(1):13–9. Available at: http://www.ncbi.nlm.nih.gov/pubmed/19149992.

153. Zhang L, Su L. HIV-1 immunopathogenesis in humanized mouse models. *Cell Mol Immunol*. 2012;(February):237–244. doi:10.1038/cmi.2012.7.

154. Potash MJ, Chao W, Bentsman G, et al. A mouse model for study of systemic HIV-1 infection, antiviral immune responses, and neuroinvasiveness. *Proc Natl Acad Sci U S A*. 2005;102(10):3760–5. doi:10.1073/pnas.0500649102.

155. Albritton L, Tseng L, Scadden D, Cunningham J. A putative murine ecotropic retrovirus receptor gene encodes a multiple membrane-spanning protein and confers susceptibility to virus infection. *Cell*. 1989. Available at: http://www.sciencedirect.com/science/article/pii/0092867489901347. Accessed September 22, 2014.

156. Mathers BM, Degenhardt L, Ali H, et al. HIV prevention, treatment, and care services for people who inject drugs: a systematic review of global, regional, and national coverage. *Lancet*. 2010;375(9719):1014–28. doi:10.1016/S0140-6736(10)60232-2.

157. Kapadia F, Vlahov D, Donahoe RM, Friedland G. The role of substance abuse in HIV disease progression: reconciling differences from laboratory and epidemiologic investigations. *Clin Infect Dis*. 2005;41(7):1027. Available at: http://cid.oxfordjournals.org/content/41/7/1027.short. Accessed September 26, 2011.

158. Rivera-Amill V, Silverstein PS, Noel RJ, Kumar S, Kumar A. Morphine and rapid disease progression in nonhuman primate model of AIDS: inverse correlation between disease progression and virus evolution. *J Neuroimmune Pharmacol*. 2010;5(1):122–32. doi:10.1007/s11481-009-9184-0.

159. Byrd D a, Fellows RP, Morgello S, et al. Neurocognitive impact of substance use in HIV infection. *J Acquir Immune Defic Syndr*. 2011;58(2):154–62. doi:10.1097/QAI.0b013e318229ba41.

160. MacArthur GJ, Minozzi S, Martin N, et al. Opiate substitution treatment and HIV transmission in people who inject drugs: systematic review and meta-analysis. *BMJ*. 2012;345(oct03_3):e5945. doi:10.1136/bmj.e5945.

161. Ho W, Guo C, Yuan C. Methylnaltrexone antagonizes opioid-mediated enhancement of HIV infection of human blood mononuclear phagocytes. *J Pharmacol …*. 2003. Available at: http://jpet.aspetjournals.org/content/307/3/1158.short. Accessed September 22, 2014.

162. Anthony IC, Arango J-C, Stephens B, Simmonds P, Bell JE. The effects of illicit drugs on the HIV infected brain. *Front Biosci*. 2008;13:1294–307. Available at: http://www.ncbi.nlm.nih.gov/pubmed/17981630. Accessed September 22, 2014.

163. Bell JE, Arango J-C, Anthony IC. Neurobiology of multiple insults: HIV-1-associated brain disorders in those who use illicit drugs. *J Neuroimmune Pharmacol*. 2006;1(2):182–91. doi:10.1007/s11481-006-9018-2.

164. Bell JE, Brettle RP, Chiswick a, Simmonds P. HIV encephalitis, proviral load and dementia in drug users and homosexuals with AIDS. Effect of neocortical involvement. *Brain*. 1998;121 (Pt 1:2043–52. Available at: http://www.ncbi.nlm.nih.gov/pubmed/9827765.

165. Bokhari SM, Yao H, Bethel-Brown C, et al. Morphine enhances Tat-induced activation in murine microglia. *J Neurovirol*. 2009;15(3):219–28. doi:10.1080/13550280902913628.

166. Cornwell WD, Lewis MG, Fan X, Rappaport J, Rogers TJ. Effect of chronic morphine administration on circulating T cell population dynamics in rhesus macaques. *J Neuroimmunol*. 2013;265(1-2):43–50. doi:10.1016/j.jneuroim.2013.09.013.

167. Beyrer C, Malinowska-Sempruch K, Kamarulzaman A, Kazatchkine M, Sidibe M, Strathdee S a. Time to act: a call for comprehensive responses to HIV in people who use drugs. *Lancet*. 2010;376(9740):551–63. doi:10.1016/S0140-6736(10)60928-2.

168. Donahoe RM, Vlahov D. Opiates as potential cofactors in progression of HIV-1 infections to AIDS. *J Neuroimmunol*. 1998;83(1-2):77–87. Available at: http://www.ncbi.nlm.nih.gov/pubmed/9610676.

169. Wolfe D, Carrieri MP, Shepard D. Treatment and care for injecting drug users with HIV infection: a review of barriers and ways forward. *Lancet*. 2010;376(9738):355–66. doi:10.1016/S0140-6736(10)60832-X.

170. Kedia S, Sell M, Relyea G. Mono-versus polydrug abuse patterns among publicly funded clients. *Subst Abuse Treat Prev Policy*. 2007;9:1–9. doi:10.1186/1747-597X-2-Received.

171. Pandrea I V, Gautam R, Ribeiro RM, et al. Acute loss of intestinal CD4+ T cells is not predictive of simian immunodeficiency virus virulence. *J …*. 2007. Available at: http://www.jimmunol.org/content/179/5/3035.short. Accessed June 24, 2013.

172. Gordon S, Klatt N, Bosinger S, et al. Severe depletion of mucosal CD4+ T cells in AIDS-free simian immunodeficiency virus-infected sooty mangabeys. *J Immunol*. 2007. Available at: http://www.jimmunol.org/content/179/5/3026.short. Accessed September 3, 2014.

173. Shultz LD, Brehm MA, Garcia-Martinez JV, Greiner DL. Humanized mice for immune system investigation: progress, promise and challenges. *Nat Rev Immunol*. 2012;12(11):786–98. doi:10.1038/nri3311.

174. Prakash O, Teng S, Ali M, et al. The human immunodeficiency virus type 1 Tat protein potentiates zidovudine-induced cellular toxicity in transgenic mice. *Arch Biochem Biophys*. 1997;343(2):173–80. doi:10.1006/abbi.1997.0168.

175. Fischer SJ, Arguello a a, Charlton JJ, Fuller DC, Zachariou V, Eisch a J. Morphine blood levels, dependence, and regulation of hippocampal subgranular zone proliferation rely on administration paradigm. *Neuroscience*. 2008;151(4):1217–24. doi:10.1016/j.neuroscience.2007.11.035.

176. Denning TL, Wang Y, Patel SR, Williams IR, Pulendran B. Lamina propria macrophages and dendritic cells differentially induce regulatory and interleukin 17-producing T cell responses. *Nat Immunol*. 2007;8(10):1086–94. doi:10.1038/ni1511.

177. Kelschenbach JL, Saini M, Hadas E, et al. Mice Chronically Infected with Chimeric HIV Resist Peripheral and Brain Superinfection: A Model of Protective Immunity to HIV. *J Neuroimmune Pharmacol*. 2011. doi:10.1007/s11481-011-9316-1.

178. He H, Sharer LR, Chao W, et al. Enhanced human immunodeficiency virus Type 1 expression and neuropathogenesis in knockout mice lacking Type I

interferon responses. *J Neuropathol Exp Neurol*. 2014;73(1):59–71. doi:10.1097/NEN.0000000000000026.

179. Feldman GJ, Mullin JM, Ryan MP. Occludin: structure, function and regulation. *Adv Drug Deliv Rev*. 2005;57(6):883–917. doi:10.1016/j.addr.2005.01.009.

180. Clarke TB, Francella N, Huegel A, Weiser JN. Invasive Bacterial Pathogens Exploit TLR-Mediated Downregulation of Tight Junction Components to Facilitate Translocation across the Epithelium. *Cell Host Microbe*. 2011;9(5):404–414. Available at: http://www.sciencedirect.com/science/article/pii/S193131281100134X. Accessed December 7, 2011.

181. Bjarnason I, Sharpstone DR, Francis N, et al. Intestinal inflammation, ileal structure and function in HIV. *AIDS*. 1996;10(12):1385–91. Available at: http://www.ncbi.nlm.nih.gov/pubmed/8902068. Accessed September 27, 2014.

182. Chu C, Zhu J, Dagda R. Beclin 1-independent pathway of damage-induced mitophagy and autophagic stress. *Autophagy*. 2007. Available at: http://www.landesbioscience.com/journals/autophagy/ChuAUTO3-6.pdf. Accessed September 27, 2014.

183. Tarnawski A, Stachura J, Durbin T, Sarfeh IJ, Gergely H. Increased expression of epidermal growth factor receptor during gastric ulcer healing in rats. *Gastroenterology*. 1992;102(2):695–8. Available at: http://europepmc.org/abstract/MED/1732139. Accessed September 27, 2014.

184. Pahar B, Lackner A a, Veazey RS. Intestinal double-positive CD4+CD8+ T cells are highly activated memory cells with an increased capacity to produce cytokines. *Eur J Immunol*. 2006;36(3):583–92. doi:10.1002/eji.200535520.

185. Tubaro E, Avico U, Santiangeli C. Morphine and methadone impact on human phagocytic physiology. *Int J ….* 1985. Available at: http://www.sciencedirect.com/science/article/pii/0192056185900499. Accessed September 27, 2014.

186. Rojavin M, Szabo I, Bussiere J, Rogers T. Morphine treatment in vitro or in vivo decreases phagocytic functions of murine macrophages. *Life Sci*.

1993. Available at:
http://www.sciencedirect.com/science/article/pii/002432059390122J.
Accessed September 27, 2014.

187. Ninković J, Roy S. Morphine decreases bacterial phagocytosis by inhibiting actin polymerization through cAMP-, Rac-1-, and p38 MAPK-dependent mechanisms. *Am J Pathol*. 2012;180(3):1068–79. doi:10.1016/j.ajpath.2011.11.034.

188. Faust N, Varas F, Kelly LM, Heck S, Graf T. Insertion of enhanced green fluorescent protein into the lysozyme gene creates mice with green fluorescent granulocytes and macrophages. *Blood*. 2000;96(2):719–26. Available at: http://www.ncbi.nlm.nih.gov/pubmed/10887140.

189. Peeters T, Vantrappen G. The Paneth cell: a source of intestinal lysozyme. *Gut*. 1975. Available at: http://gut.bmj.com/content/16/7/553.abstract. Accessed September 27, 2014.

190. Bokhari SM, Hegde R, Callen S, et al. Morphine Potentiates Neuropathogenesis of SIV Infection in Rhesus Macaques. *J Neuroimmune Pharmacol*. 2011:1–14. Available at: http://www.springerlink.com/index/H2K2873240R38004.pdf. Accessed September 26, 2011.

191. Hollenbach R, Sagar D, Khan ZK, et al. Effect of morphine and SIV on dendritic cell trafficking into the central nervous system of rhesus macaques. *J Neurovirol*. 2014;20(2):175–83. doi:10.1007/s13365-013-0182-x.

192. Spikes L, Dalvi P, Tawfik O, et al. Enhanced pulmonary arteriopathy in simian immunodeficiency virus-infected macaques exposed to morphine. *Am J Respir Crit Care Med*. 2012;185(11):1235–43. doi:10.1164/rccm.201110-1909OC.

193. Rivera I, García Y, Gangwani MR, et al. Identification and molecular characterization of SIV Vpr R50G mutation associated with long term survival in SIV-infected morphine dependent and control macaques. *Virology*. 2013;446(1-2):144–51. doi:10.1016/j.virol.2013.07.027.

194. Nowroozalizadeh S, Månsson F, da Silva Z, et al. Microbial translocation correlates with the severity of both HIV-1 and HIV-2 infections. *J Infect Dis*. 2010;201(8):1150–4. doi:10.1086/651430.

195. Gordon SN, Cervasi B, Odorizzi P, et al. Disruption of intestinal CD4+ T cell homeostasis is a key marker of systemic CD4+ T cell activation in HIV-infected individuals. *J Immunol*. 2010;185(9):5169–79. doi:10.4049/jimmunol.1001801.

196. Hauser KF, El-Hage N, Stiene-Martin A, et al. HIV-1 neuropathogenesis: glial mechanisms revealed through substance abuse. *J Neurochem*. 2007;100(3):567–86. doi:10.1111/j.1471-4159.2006.04227.x.

197. Hinkin CH, Hardy DJ, Mason KI, et al. Medication adherence in HIV-infected adults: effect of patient age, cognitive status, and substance abuse. *AIDS*. 2004;18 Suppl 1:S19–25. Available at: http://www.pubmedcentral.nih.gov/articlerender.fcgi?artid=2886736&tool=pmcentrez&rendertype=abstract. Accessed June 25, 2014.

198. Khoruts A, Dicksved J, Jansson JK, Sadowsky MJ. Changes in the Composition of the Human Fecal Microbiome After Bacteriotherapy for Recurrent. *J Clin Gastroenterol*. 2010;44(5):354–360.

199. Nell S, Suerbaum S, Josenhans C. The impact of the microbiota on the pathogenesis of IBD: lessons from mouse infection models. *Nat Rev Microbiol*. 2010;8(8):564–77. doi:10.1038/nrmicro2403.

200. Moeller AH, Shilts M, Li Y, et al. SIV-induced instability of the chimpanzee gut microbiome. *Cell Host Microbe*. 2013;14(3):340–5. doi:10.1016/j.chom.2013.08.005.

201. McKenna P, Hoffmann C, Minkah N, et al. The macaque gut microbiome in health, lentiviral infection, and chronic enterocolitis. *PLoS Pathog*. 2008;4(2):e20. doi:10.1371/journal.ppat.0040020.

202. Langille MGI, Zaneveld J, Caporaso JG, et al. Predictive functional profiling of microbial communities using 16S rRNA marker gene sequences. *Nat …*. 2013;31(9):814–21. doi:10.1038/nbt.2676.

203. Parks DH, Tyson GW, Hugenholtz P, Beiko RG. STAMP: Statistical analysis of taxonomic and functional profiles. *Bioinformatics*. 2014;30(21):3123–3124. doi:10.1093/bioinformatics/btu494.

204. Cáceres M De, Legendre P. Associations between species and groups of sites: indices and statistical inference. *Ecology*. 2009;90(12):3566–3574. doi:10.1890/08-1823.1.

205. Hofmann AF, Eckmann L. How bile acids confer gut mucosal protection against bacteria. *Proc Natl Acad Sci U S A*. 2006;103(12):4333–4. doi:10.1073/pnas.0600780103.

206. Boesjes M, Brufau G. Metabolic effects of bile acids in the gut in health and disease. *Curr Med Chem*. 2014;21(24):2822–9. Available at: http://www.ncbi.nlm.nih.gov/pubmed/24606522. Accessed September 23, 2014.

207. Lorenzo-Zúñiga V, Bartoli R. Oral bile acids reduce bacterial overgrowth, bacterial translocation, and endotoxemia in cirrhotic rats. …. 2003. Available at: http://onlinelibrary.wiley.com/doi/10.1053/jhep.2003.50116/abstract. Accessed October 24, 2014.

208. Oberst F. Studies on the fate of morphine. *J Pharmacol Exp …*. 1942. Available at: http://jpet.aspetjournals.org/content/74/1/37.short. Accessed October 30, 2014.

209. Meissner W, Schmidt U, Hartmann M, Kath R, Reinhart K. Oral naloxone reverses opioid-associated constipation. *Pain*. 2000;84(1):105–109. doi:10.1016/S0304-3959(99)00185-2.

210. Feng P, Truant AL, Meissler JJ, Gaughan JP, Adler MW, Eisenstein TK. Morphine withdrawal lowers host defense to enteric bacteria: spontaneous sepsis and increased sensitivity to oral Salmonella enterica serovar Typhimurium infection. *Infect Immun*. 2006;74(9):5221–6. doi:10.1128/IAI.00208-06.

211. Russell WR, Hoyles L, Flint HJ, Dumas M-E. Colonic bacterial metabolites and human health. *Curr Opin Microbiol*. 2013;16(3):246–54. doi:10.1016/j.mib.2013.07.002.

212. Asselin C, Gendron F-P. Shuttling of information between the mucosal and luminal environment drives intestinal homeostasis. *FEBS Lett*. 2014. doi:10.1016/j.febslet.2014.02.049.

213. Compton W, Volkow N. Major increases in opioid analgesic abuse in the United States: concerns and strategies. *Drug Alcohol Depend*. 2006. Available at: http://www.sciencedirect.com/science/article/pii/S0376871605001821. Accessed December 3, 2014.

214. Kuehn BM. Opioid prescriptions soar: increase in legitimate use as well as abuse. *JAMA*. 2007;297(3):249–51. doi:10.1001/jama.297.3.249.

215. Lee S, Zhao Y, Anderson WF. Receptor-Mediated Moloney Murine Leukemia Virus Entry Can Occur Independently of the Clathrin-Coated-Pit-Mediated Endocytic Pathway. *J Virol*. 1999;73(7):5994–6005. Available at: http://jvi.asm.org/content/73/7/5994.full. Accessed November 9, 2014.

216. Perkins CP, Mar V, Shutter JR, et al. Anemia and perinatal death result from loss of the murine ecotropic retrovirus receptor mCAT-1. *Genes Dev*. 1997;11(7):914–925. doi:10.1101/gad.11.7.914.

217. Ancuta P, Monteiro P, Sekaly R-P. Th17 lineage commitment and HIV-1 pathogenesis. *Curr Opin HIV AIDS*. 2010;5(2):158–65. doi:10.1097/COH.0b013e3283364733.

218. Hunt PWPW. Th17, gut, and HIV: therapeutic implications. *Curr Opin HIV AIDS*. 2010;5(2):189. doi:10.1097/COH.0b013e32833647d9.Th17.

219. Kanwar B, Favre D, McCune JM. Th17 and regulatory T cells: implications for AIDS pathogenesis. *Curr Opin HIV AIDS*. 2010;5(2):151. doi:10.1097/COH.0b013e328335c0c1.Th17.